ABSTRACT

Title of dissertation: TRANSFORMATIONS OF TASK-DEPENDENT PLASTICITY FROM A1 TO HIGHER-ORDER AUDITORY CORTEX

Diego E. Elgueda, Doctor of Philosophy, 2016

Dissertation directed by: Professor Shihab Shamma, Department of Electrical and Computer Engineering

Everyday, humans and animals navigate complex acoustic environments, where multiple sound sources overlap. Somehow, they effortlessly perform an acoustic scene analysis and extract relevant signals from background noise. Constant updating of the behavioral relevance of ambient sounds requires the representation and integration of incoming acoustical information with internal representations such as behavioral goals, expectations and memories of previous sound-meaning associations. Rapid plasticity of auditory representations may contribute to our ability to attend and focus on relevant sounds. In order to better understand how auditory representations are transformed in the brain to incorporate behavioral contextual information, we explored task-dependent plasticity in neural responses recorded at four levels of the auditory cortical processing hierarchy of ferrets: the primary auditory cortex (A1), two higher-order auditory areas (dorsal PEG and ventral-anterior PEG) and dorso-lateral frontal cortex. In one study we explored the laminar profile of rapid-task related plasticity in A1 and found that plasticity occurred at all depths,

but was greatest in supragranular layers. This result suggests that rapid task-related plasticity in A1 derives primarily from intracortical modulation of neural selectivity. In two other studies we explored task-dependent plasticity in two higher-order areas of the ferret auditory cortex that may correspond to belt (secondary) and parabelt (tertiary) auditory areas. We found that representations of behaviorally-relevant sounds are progressively enhanced during performance of auditory tasks. These selective enhancement effects became progressively larger as you ascend the auditory cortical hierarchy. We also observed neuronal responses to non-auditory, task-related information (reward timing, expectations) in the parabelt area that were very similar to responses previously described in frontal cortex. These results suggests that auditory representations in the brain are transformed from the more veridical spectrotemporal information encoded in earlier auditory stages to a more abstract representation encoding sound behavioral meaning in higher-order auditory areas and dorso-lateral frontal cortex.

TRANSFORMATIONS OF TASK-DEPENDENT PLASTICITY FROM A1 TO HIGHER-ORDER AUDITORY CORTEX

by

Diego E. Elgueda González

Dissertation submitted to the Faculty of the Graduate School of the
University of Maryland, College Park in partial fulfillment
of the requirements for the degree of
Doctor of Philosophy
2016

Advisory Committee:
Professor Shihab A. Shamma, Chair/Advisor
Dr. Jonathan B. Fritz, Co-Advisor
Professor Catherine E. Carr
Professor Daniel A. Butts
Professor Robert J. Dooling

Preface

The present thesis work is composed of three studies performed in the Neural Systems Lab under Dr. Shihab A. Shamma and Jonathan B. Fritz supervision. To date, one publication resulted from the work presented in Chapter 4:

Atiani, S.*, David, S. V.*, Elgueda, D., Locastro, M., Radtke-Schuller, S., Shamma, S. A., Fritz, J. B. **(2014)**.
Emergent selectivity for task-relevant stimuli in higher-order auditory cortex.
Neuron, 82(2), 486499. doi:10.1016/j.neuron.2014.02.029

Two publications are currently being prepared from data presented in Chapters 3 and 5:

Francis N. A.*, Elgueda D.*, Englitz B., Fritz J. B., Shamma S.A. The Laminar Profile of Rapid Task-Dependent Plasticity in Primary Auditory Cortex.

Elgueda D., Duque, D., Trzcinski, N. K., David, S. V., Radtke-Schuller S., Shamma S. A., Fritz J. B. Top-down Attentional Modulation of Responses in Ferret Higher Order Auditory Cortex.

* : *co-first authors*

Foreword

Results presented in Chapter 4 have been previously published:

Atiani, S., David, S. V., Elgueda, D., Locastro, M., Radtke-Schuller, S., Shamma, S. A., and Fritz, J. B. (2014). **Emergent selectivity for task-relevant stimuli in higher-order auditory cortex.** Neuron 82, 486499. doi:10.1016/j.neuron.2014.02.029.

The contribution of Mr. Elgueda González on this jointly-authored publication was substantial, and he was advised by the dissertation committee and dissertation director to include its results in chapter 4.

Dedication

To my parents, for supporting me in every desicion I've ever taken. To my wife María Teresa, for her unconditional and resolute support.

Acknowledgments

I wish to thank my advisors Shihab Shamma and Jonathan Fritz for giving me the fantastic oportunity to work in such an amazing topic. I will always cherish the learning experience of working in such a stimulating place.

I also owe my gratitude to my advisory Ph.D. committee, Professors Catherine Carr, Daniel Butts and Robert Dooling for sharing their knowledge and invaluable time with me, your helpful comments have strengthened every aspect of my research work during these five years of research. I also grateful to every person in the Neuroscience and Cognitive Science program at the University of Maryland for their helpful advice and for making every step in these years as a graduate student so fruitful. Special thanks to Pam Komarek and Ricardo Araneda, for always being available for advice and help.

I'm also very thankful to all the people at the Neural Systems Laboratory, who made these years far from home an enjoyable learning experience. Special thanks to Bernhard Englitz, Stephen David, Pingbo Yin, Daniel Duque, Nikolas Francis, Kai Lu, Natalie Trzcinski for all the invaluable discussions and help I got from you all. Thanks to Dani Duque for teaching me how to play hattrick.

I wish to thank to my great friends in Chile and the rest of the world that despite being so far were always present for sharing those conversations I love so

much. Nobody has better friends than I do. You are way too many to mention in these pages you'll probably never read. I'm also grateful to those new friends I met in Maryland that were my family away from home: Rodrigo and Fares, Felipe and Maca, Dani and Cris, Pepe and Montse, Jose Cabezas, Beatriz and Cristian and Pablo and Alejandra. Special thanks to Olivia Cordero for receiving me in my first home away from Chile and for being so incredibly kind and generous with me and my wife.

I also very grateful to Drs. Luis Robles and Paul Delano for their friendship and for encouraging me to engage in science. I will always cherish the years I spent working with them, their advices and the great opportunities in life that became available for being part of their lab.

My greatest thanks go to my dear parents, I owe you everything, and all I want to achieve in life is to make you proud. The hardest part of being far from home was to be far from you both and from my dear brothers.

Finally, I owe the greatest gratitute to my loved wife. You are the bravest person I know and you inspire me every day. We achieved this together.

Table of Contents

List of Figures

List of Abbreviations

A1	Primary auditory cortex
AAF	Anterior auditory field
ADF	Anterior dorsal field
AEG	Anterior ectosylvian gyrus
ANOVA	Analysis of variance
AVF	Anterior ventral field
BF	Best frequency
CN	Cochlear nucleus
CSD	Current source density
dlFC	dorsolateral frontal cortex
dPEG	Dorsal posterior ectosylvian gyrus
SOC	Superior olivary complex
HG	High gamma frequency range of the local field potential
IC	Inferior colliculus
LFP	Local field potential
MEG	Medial ectosylvian gyrus
MGB	Medial geniculate body
MU	Multi-unit
n.s.	Not significant
PEG	Posterior ectosylvian gyrus
PFC	Pre-frontal cortex
PSF	Posterior suprasylvian field
PSS	Pseudosylvian sulcus
PSSC	Pseudo-sylvian sulcal cortex
PSTH	Peristimulus time histogram
PPF	Posterior pseudosylvian field
rSC	Spike count correlation, or Noise correlation
SEM	Standard error of the mean
SNR	Signal-to-noise ratio
SPL	Sound pressure level
SSS	Suprasylvian sulcus
STRF	Spectro-temporal receptive field
TORC	Temporally-orthogonal ripple combination
V1	Primary visual cortex
MT	Middle temporal area
V4	Visual area V4
vaPEG	Ventral anterior posterior ectosylvian gyrus
VP	Ventral posterior field
VPc	Caudal VP
VPr	Rostral VP
VPv	Ventral VP

Chapter 1: Introduction

1.1 Sensory representations

In order for animals to be able to understand and explore their surroundings and interact with their environment and socialize with other individuals, the brain must be able to generate internal representations of the physical world in which the animal is immersed, and generate predictions about the future. This fascinating ability of the nervous system is critical for survival, because it allows animals to continuously scan the current environment and also predict future likely events and assess whether any given combination of sensory inputs are coming from sources that pose a threat for their integrity or if it has the potential of being advantageous. This evaluation of the continuous stream of incoming sensory information is crucial to allow animals to shape their behavior in order to enhance their environmental fitness by, for example, enhancing their nutrition, reproductive performance, or lowering the risk of predation.

The impressive active process that we call perception results from a succession of events starting from the faithful transduction of physical properties of sensory stimuli into neural code and its subsequent transformation into increasingly more

complex and meaningful internal representations that integrate information from multiple sensory systems, memory and internal expectations and goals. Understanding how sensory representations are sequentially transformed in the brain remains as one of the most fascinating questions in neuroscience.

1.2 Organization and function of the auditory system of mammals

The auditory system captures vibrations propagating in the medium the animals are immersed in, either the atmosphere or water, and interprets the incoming acoustic information through a complex process of neural computation to perform acoustic scene segregation. One of the most conspicuous organizational features of the auditory system is tonotopy, which is the spatial arrangement of neuronal responsiveness depending on the frequency of stimulation. This tonotopy can be found as early as in the mechanical response of the basilar membrane of the organ of Corti in the cochlea, where traveling vibrations reach a maximum peak depending on the frequency of stimulation and location along the length of the cochlea (Robles & Ruggero, 2001). This way, the cochlea performs the first decomposition of the incoming acoustical stimulation into its spectral components (Figure 1.1).

Inner hair cells of the organ of Corti transduce these mechanical vibrations into bioelectrical membrane potentials that are later propagated through afferent fibers of the auditory nerve; the signals produced in the cochlea reach auditory cortex through an intricate ascending pathway with many processing stations before

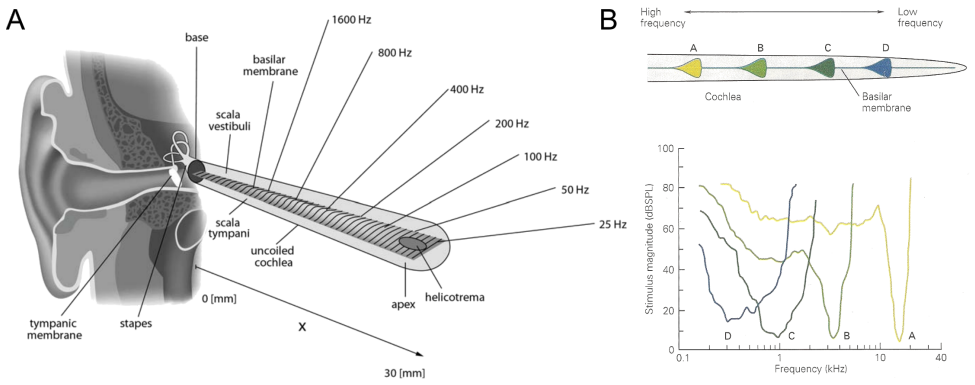

Figure 1.1: **Tonotopy in the cochlea** originates in the mechanical response of the basilar membrane **A**: Depiction of approximate best frequencies along the length of the basilar membrane. **B**. This tonotopy activate frequency selective populations of hair cells in the organ of Corti, which display sharp tuning curves. Hair cells in the cochlear base respond maximally to high frequencies, while hair cells at the apex to low frequencies. Adapted from Hudspeth (2000); Kern et al. (2008)

reaching the auditory cortex (Malmierca, 2003; Pickles, 2012). Cochlear afferents join the vestibulo-cochlear nerve and enter the cochlear nucleus (CN), the first processing stage in the ascending auditory pathway. Auditory afferents arriving CN innervate several cell types in the three subdivisions of the CN, which code for different sound attributes (Cant & Benson, 2003). Then, CN outputs constitute ascending parallel processing pathways that reach the superior olivary complex (SOC), nucleus of the lateral lemniscus and the inferior colliculi (IC). The IC is usually regarded as an obligatory stage in the ascending auditory pathway were most parallel pathways converge, although some projections from CN have been reported to reach auditory thalamus directly (Malmierca et al., 2002). IC outputs reach the medial geniculate body (MGB), the auditory thalamus, and auditory cortex receives inputs from MGB (Figure 1.2).

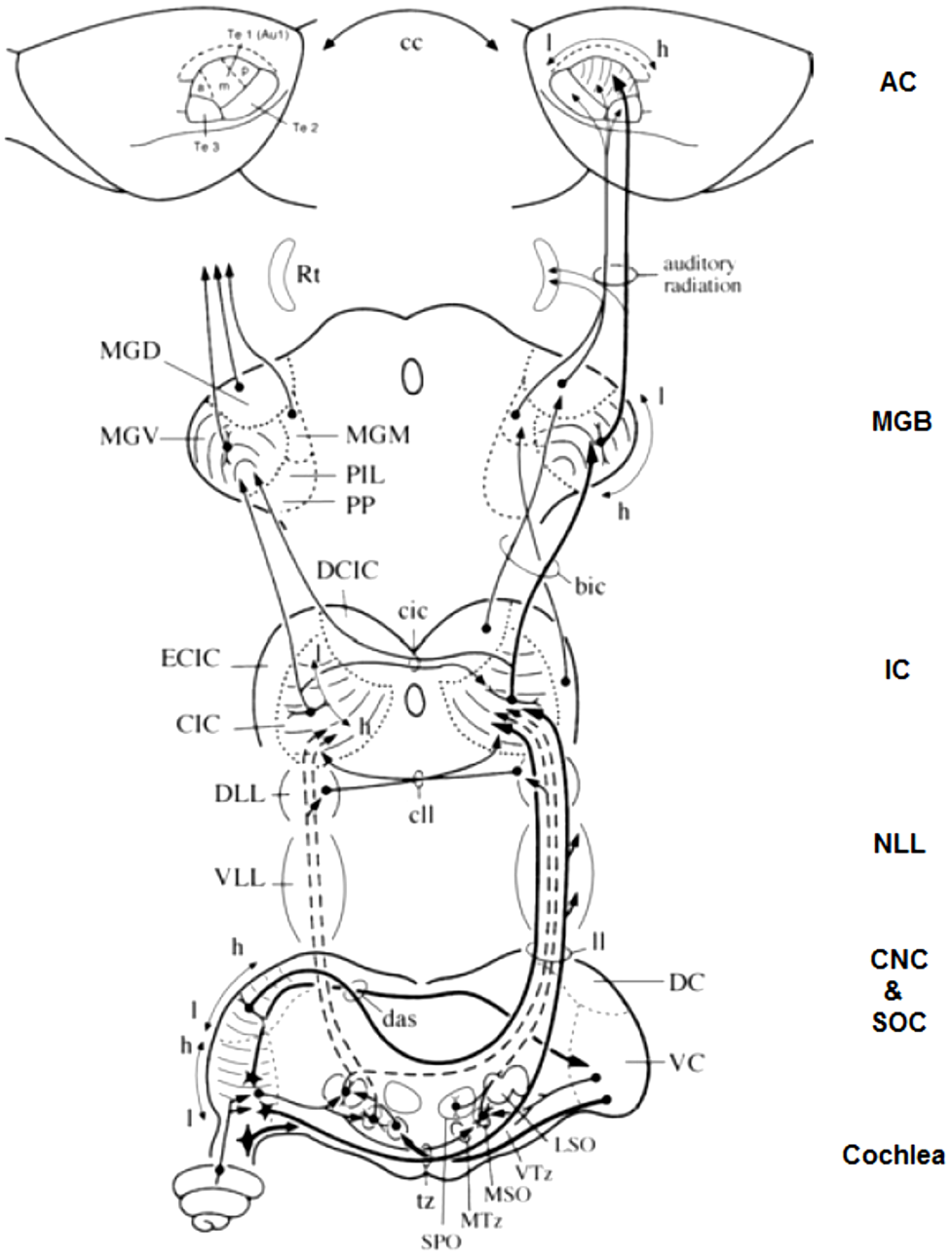

Figure 1.2: **Ascending auditory pathways.** Adapted from Malmierca (2003)

The auditory cortex is composed of at least one primary -or core- field, whose inputs originate from the ventral MGB, and several surrounding non-primary auditory fields, commonly known as belt and parabelt, that receive inputs from auditory core areas and non-lemniscal areas of MGB (Hackett, 2011). Belt areas constitute an obligatory second stage after auditory core areas, and parabelt a third stage after belt. These non-primary areas are considered to be at a higher processing level than core auditory areas, and their role is still not yet completely understood.

In parallel to the intricate ascending projections providing the auditory cortex with sensory information, the auditory system displays a conspicuous descending pathway reaching all subcortical nuclei (Coomes Peterson & Schofield, 2007; Malmierca, 2003; Schofield, 2009; Schofield & Cant, 1999). This anatomical evidence, along with physiological studies (León et al., 2012; Lomber & Malhotra, 2008), strongly suggest that the auditory system does not only send information upstream, but also takes into account top-down influences from higher center into lower stages through efferent projections emerging from the cortex, IC and the olivocochlear system in the SOC.

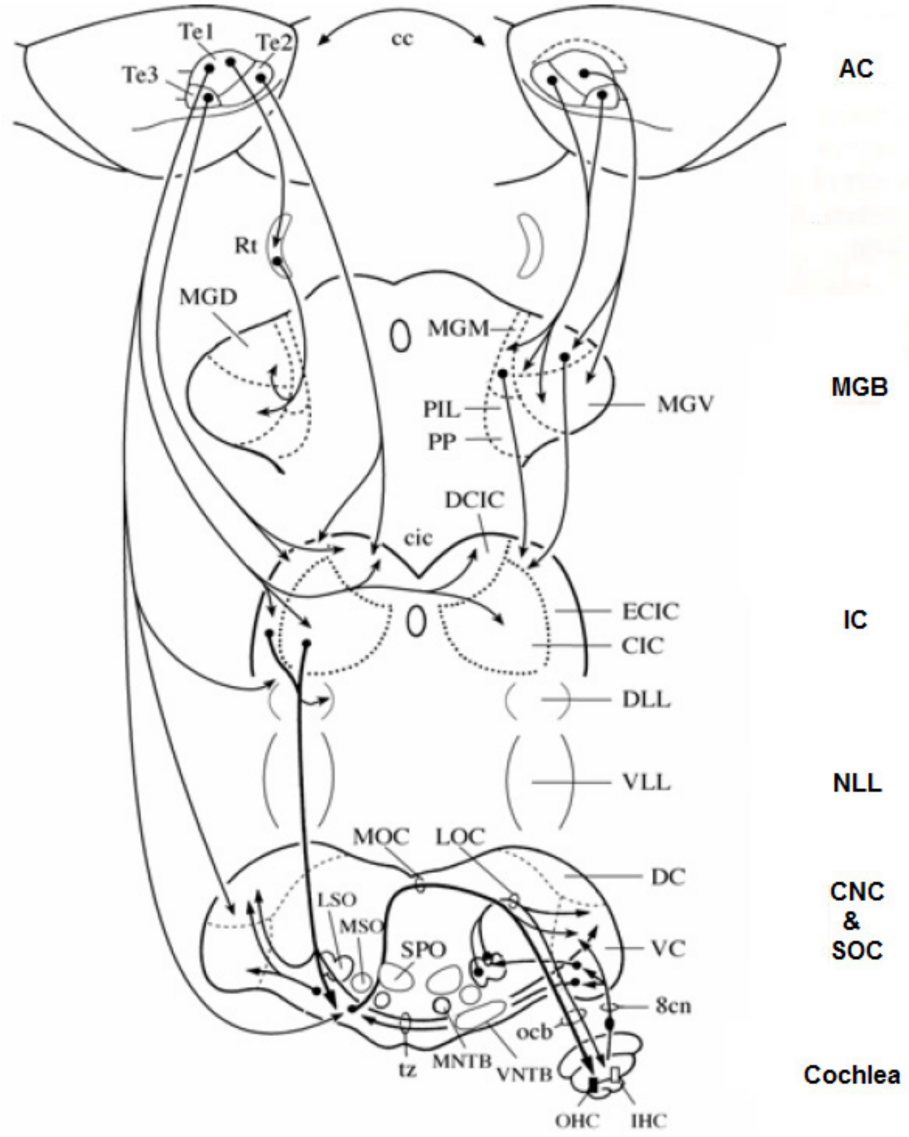

Figure 1.3: **Descending projections of the auditory system.** Adapted from Malmierca (2003)

1.3 Representations in the Auditory System

Despite the fact that the ears are constantly bombarded by airborne vibrations propagating from multiple sources, the brain is able to recognize the multiple auditory objects composing the auditory scene, and can concentrate its processing on the sounds that are more relevant at a given time.

This remarkable achievement requires tolerant and identity-preserving representations of auditory objects (Bizley & Cohen, 2013; DiCarlo & Cox, 2007; Sharpee et al., 2011), and their integration with information coming from other sources (e.g. memories and information from other sensory modalities) in order to allow a constant evaluation of the importance of the perceived sounds depending on the environmental and behavioral context. Then, attention focuses the processing on those components of relevant sounds, while filtering out those that are not relevant in the current context.

In the auditory system, as well as in other sensory modalities, this problem is thought to be solved through the formation of neural representations of stimuli features that hierarchically converge at successive stages of processing. Early representations converge into higher processing levels in order to create more complex representations of the represented stimuli. At the level of a single neuron, these representations encode some region of the sensory space, its receptive field. In the case of auditory neurons, the receptive field is defined as the spectro-temporal pat-

tern that evokes a maximal response from a neuron, that is its spectro-temporal receptive field (STRF).

Auditory objects might emerge by the grouping of sound representations based on their temporal relations. In this binding process, attention is thought to be essential, as it might have a role in enhancing the salience of relevant stimuli component representations as well as their temporal coherence (Shamma et al., 2011). How attention influences neural representations along the sensory processing hierarchy is still not well understood, but it has been shown to have a profound influence.

1.4 Hierarchical functional organization of sensory neocortex

Perhaps the most studied sensory processing hierarchy is that of the visual system of primates and cats. Starting from striate cortex (primary visual cortex, V1), at least two functionally specialized processing pathways emerge: an occipitotemporal or ventral stream, specialized for object recognition (often called the 'what' pathway), and an occipitoparietal or dorsal pathway ('where' pathway), crucial for perception of spatial relationships among objects and visually-oriented motor responses (Mishkin et al., 1983; Ungerleider & Haxby, 1994). Both processing streams have been shown to be anatomically and functionally linked to distinct domains in the frontal lobes that code information related to stimulus identity and location (Wilson et al., 1993), where spatial and non-spatial information is later integrated (Rao et al., 1997).

These feedforward processing hierarchies display response selectivities of increasing complexity and larger receptive fields as one analyzes consecutively higher-order areas. For example, neurons in V1 possess small receptive fields and are sensitive to simple bar-shaped luminance contrasts of specific orientations and their motion in one preferred direction across its receptive field, while some neurons at higher levels of the dorsal stream (middle temporal area or MT) show responses to motion of more complex patterns across bigger areas of the retina, and neurons in higher-order areas of the ventral stream, like area V4 and inferior temporal cortex, are selective to colors and more complex shapes (Hubel & Wiesel, 1959; Movshon et al., 1985; Zeki & Shipp, 1988), and even showing selectivity to faces and hands (Desimone et al., 1984; Tsao et al., 2003, 2006, 2008), in receptive fields much larger than those of V1 neurons.

Despite being a widely influential framework in visual neuroscience, later evidence has challenged the dual stream hypothesis independence of dorsal and ventral streams by finding considerable interaction between object identification and location in both processing streams, such as representation of shapes (Durand et al., 2007; Konen & Kastner, 2008; Lehky & Sereno, 2007; Sereno & Maunsell, 1998; Sereno et al., 2002) and influence of color (Wannig et al., 2007) in the dorsal stream and modulation by motion in the ventral stream (Ferrera et al., 1994). This suggests that information from both processing streams might be integrated even at relatively early stages in both pathways, which might partly account for the presence

of neurons in the prefrontal cortex (PFC) that display sensibility to both stimulus identity and location (Rainer et al., 1998; Rao et al., 1997).

A hierarchical processing scheme has also been proposed for the auditory cortex, based on neuroanatomical data (Hackett, 2011). Auditory cortex has been defined as the areas in the cerebral cortex that receive significant thalamic inputs from the medial geniculate body (MGB). A group of areas with this description have been described in the temporal lobe of several mammals, and the most studied auditory cortices are those of non-human primates and cats.

Functionally and anatomically, auditory cortex is composed of several adjoining areas (Figure 1.4. Those areas that receive inputs mainly from the ventral division of the MGB (lemniscal pathway) are considered primary areas, or core, and display a tonotopic organization in which neurons are spatially arranged by the sound frequency to which they show maximum responses (their best frequency or BF). Similarly to V1 retinotopy, A1 neurons have receptive fields restricted to a small area of the sensory epithelium, and the topography of BFs in core auditory areas resembles that found on the basilar membrane of the cochlea. Several other non-primary areas, usually denominated and grouped as belt and parabelt, are located around the core and receive inputs mainly from the medial and dorsal divisions of the MGB, which correspond to the non-lemniscal auditory pathway. In many species studied, the core is composed of more than one area, each presenting a tonotopic gradient. Core areas project to contralateral core and ipsilaterally almost

exclusively to their adjacent belt areas, with which it makes reciprocal connections. Auditory belt areas receive distinct thalamic inputs from the non-tonotopic, non-lemniscal pathway and directly from core areas, making belt a second stage in the auditory cortical processing hierarchy. Belt areas have been shown to display tonotopic gradients as well (Bizley et al., 2005; Rauschecker et al., 1995; Romanski et al., 1999a). The parabelt areas are adjacent to the belt, but not to the core areas, and receive connections from the belt areas, while sending projections to belt, core and to other areas of the cerebral cortex. The parabelt areas do not receive inputs from the core areas, so parabelt constitutes a third distinct stage in cortical auditory processing (Hackett, 2011; Hackett et al., 2014; Kaas & Hackett, 2000; Recanzone & Cohen, 2010).

The auditory tuning properties of non-core areas are still a matter of debate, and are far less well understood than those of non-primary visual areas. It has been reported that, generally, while core responds reliably to tones and broadband stimuli, non-core areas respond best to more complex sounds like bandpassed noise or conspecific vocalizations (Poremba et al., 2004; Rauschecker et al., 1995; Recanzone, 2008; Tian et al., 2001). In humans, several functional magnetic resonance imaging studies have shown activation by sounds of increasing complexity along successive stages of the cortical auditory hierarchy (Humphries et al., 2014; Obleser et al., 2007; Okada et al., 2010; Wessinger et al., 2001). Parabelt areas studies on passive tuning properties has been sparse. Nonetheless, a recent study performed in awake macaque monkeys has suggested that parabelt can respond robustly to

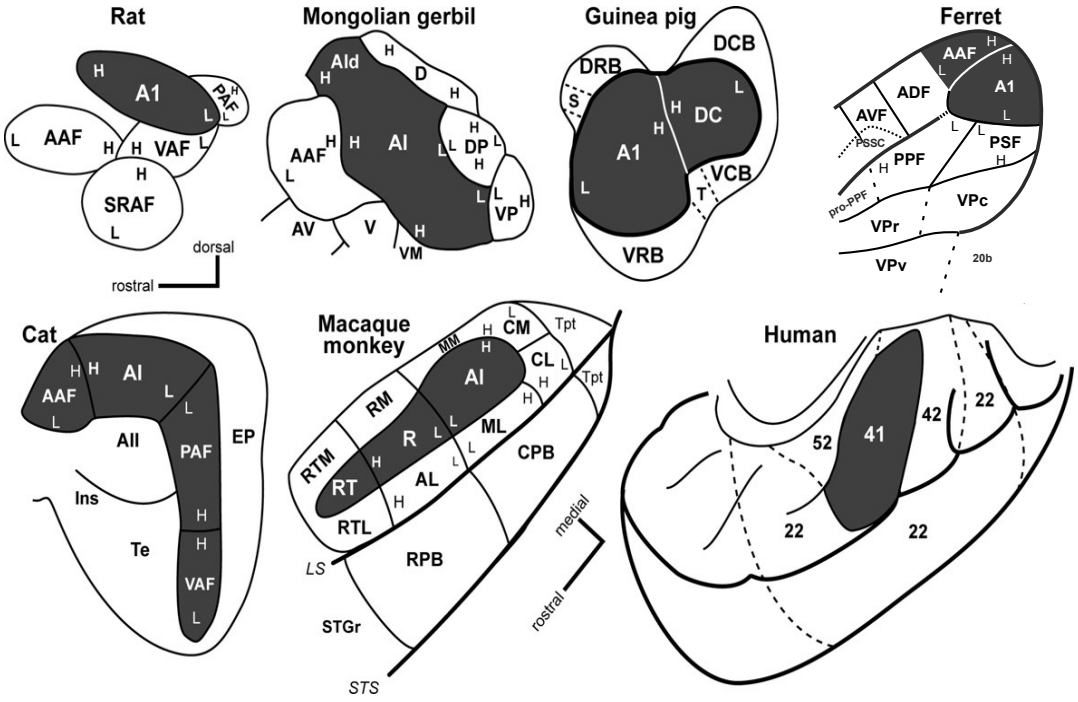

Figure 1.4: **Auditory areas in auditory cortices of seven mammalian species.** Primary (core) areas are shaded in dark color. Belt and parabelt (non-primary) areas are white. Tonotopic gradients are indicated by high (H) and low (L) frequencies. Adapted from Hackett (2011). Ferret auditory cortex redrawn from Atiani et al. (2014).

tones as well as bandpassed noise, and also suggests that a tonotopic gradient might exist in parabelt as well as in belt and core (Kajikawa et al., 2015). Yet, no clear evidence exists yet about which stimulus features these higher-order auditory areas are preferentially processing, and given the larger amount of subcortical processing stages in the auditory than in the visual system, in which much auditory feature processing takes place, it has been proposed that auditory cortical areas might be coding more complex computations (such as the representation of auditory objects) instead of more basic stimulus features as is the case of visual cortical areas (King & Nelken, 2009).

The auditory cortex is reciprocally connected with higher-order association areas of the cerebral cortex in the parietal and frontal lobes (Figure 1.5), which are involved in attentional and executive functions (Hackett, 2011). Hackett (2011) has grouped these areas beyond auditory cortex under the term 'auditory-related areas'. Since these connections overlap with those involved in visual 'what' and 'where' pathways, a similar ventral and dorsal parallel processing scheme has been proposed for the auditory flow of information (Kaas & Hackett, 2000; Rauschecker & Tian, 2000; Romanski et al., 1999a,c). This dual-pathway theory, while still controversial, has gathered some physiological evidence of spatial and non-spatial division of labor in monkeys (Tian et al., 2001), cats (Lomber & Malhotra, 2008) and humans (Ahveninen et al., 2013; Arnott et al., 2004; Du et al., 2013).

It has been found, in primates, that most reciprocal connections between the

frontal lobe and auditory cortex are concentrated in non-core, higher-order auditory areas as belt, parabelt and rostral superior temporal gyrus (STG), being in general, more numerous in parabelt and STG, less in belt areas and absent in A1 (Hackett et al., 1998b; Medalla & Barbas, 2014; Plakke & Romanski, 2014; Romanski et al., 1999a). Preliminary results of frontal-auditory cortex connectivity in the ferret suggests a similar trend (Radtke-Schuller et al., 2011), in which connections between dorsolateral frontal cortex (dlFC) and auditory cortex were more abundant in putative belt and parabelt areas (ventral-anterior areas of the posterior ectosylvian gyrus, PEG; pseudosylvian sulcus cortex, PSSC; and ventroposterior field, VP) and were absent in core areas (A1 and anterior auditory field, AAF). This connectivity pattern has been found to be different in rodents such as the mongolian gerbil (Budinger & Scheich, 2009), where A1 is broadly connected with frontal cortex among other areas, and in the mouse, where projections from motor areas have been described to contact A1 (Nelson et al., 2013; Schneider & Mooney, 2015).

1.5 Influence of attention on neural representations

Since sensory systems are constantly receiving a stream of stimulation coming from diverse sources, the brain must be able to focus its limited processing resources towards relevant stimuli. Attention is the cognitive process of concentrating the limited cognitive resources into a restricted amount of information coming from the sensory world or from internal representations. Attention can rise from bottom-

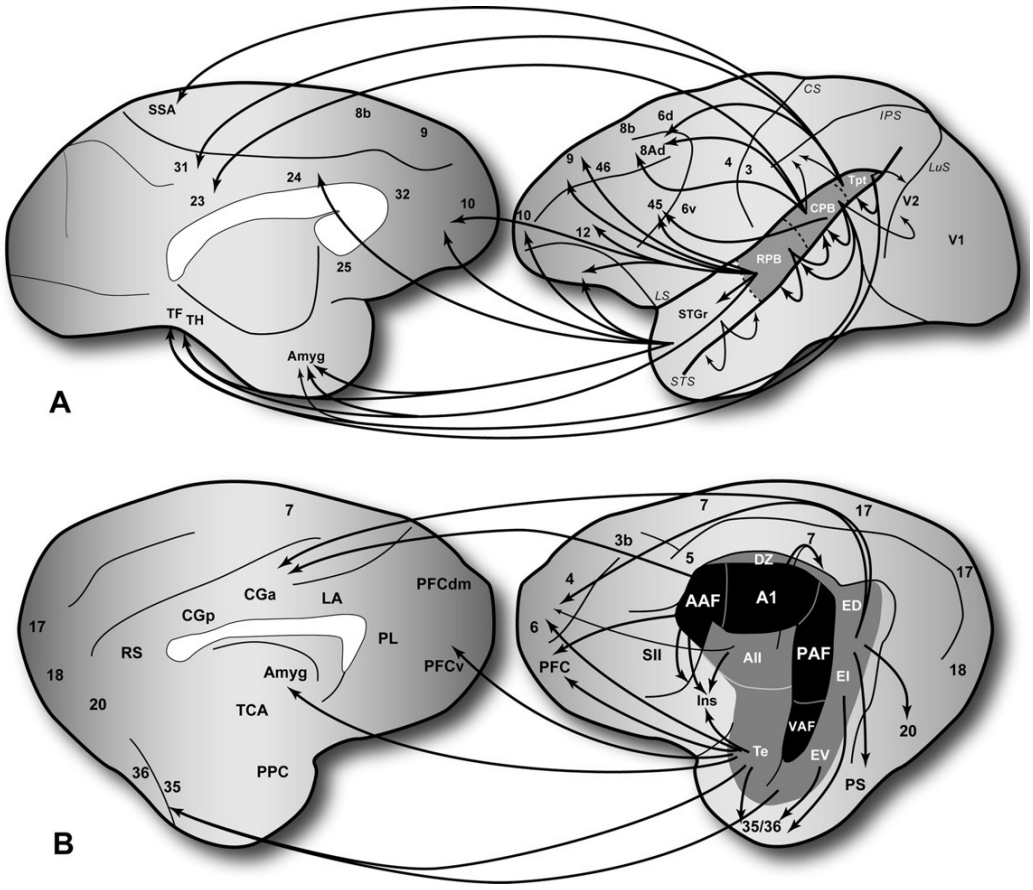

Figure 1.5: **Interconnection of auditory cortex with auditory-related areas** in the temporal, parietal, occipital and frontal lobes in left hemispheres of the macaque monkey (**A**) and cat (**B**). From Hackett (2011)

up and top-down processes. Bottom-up attention emerges when a salient stimuli captures one's attention. Top-down attention results from voluntarily attending to a specific stimuli (Matlin, 2012). This is achieved by searching for stimulus features that are known or guessed based on information gained by previous experience.

The effects of attention on sensory representations have been studied at multiple levels in the visual processing hierarchy and the general finding is that attentional modulatory effects become greater at higher cortical levels (Kastner & Pinsk, 2004; Maunsell & Treue, 2006) for both spatial, feature and even semantic category attention (Kim & Kastner, 2013), usually enhancing responses to the attended feature and suppressing that to unattended features or distractors (Störmer & Alvarez, 2014) and sometimes reshaping center-surround receptive field structure of neurons (Anton-Erxleben et al., 2009). Many of the attentional effects have been ascribed not only to increased responses, but also to a decrease in interneuronal noise correlations, which increases the signal-to-noise ratio and enhances the coding of relevant stimuli (Cohen & Maunsell, 2009). However, not all neurons in visual cortical areas show attentional effects and this may be the result of tuned normalization (Ni et al., 2012). Visual attention may involve coordinated oscillations between different cortical areas involved in processing the spatial location or feature being attended, and visual areas may interact through different oscillatory frequency channels for feedforward and feedback (Bastos et al., 2014; Bosman et al., 2012). The complementary interaction of bottom-up and top-down attention has also been studied in the visual system (McMains & Kastner, 2011). Subcortical structures such as the

pulvinar nucleus of the thalamus may also play a role in this coordination (Saalmann et al., 2012; Zhou et al., 2016). Advances in research on the role of attention in the visual system can help direct studies of top-down task-related attention in the auditory system.

The vast connectivity of auditory cortical fields with cortical areas associated with the attentional network (Petersen & Posner, 2012), as well as the prominent network of descending connections along the auditory pathways (Figure 1.3), have motivated several studies on how attention can modulate auditory representations throughout the auditory system.

Attention has been shown to affect auditory responses at several processing stages of the auditory system, even at the auditory periphery. Visual attention has been shown to reduce the sensitivity of the auditory receptor, the cochlea (Delano et al., 2007; Hernandez-Peon et al., 1956; Oatman, 1971), presumably through activation of the medial olivocochlear efferent system (Elgueda et al., 2011). At higher stages, as auditory cortex and midbrain, the general finding is that attention relatively enhances the representation of attended sounds. Fritz et al. (2003) recorded single unit responses from ferret A1 while animals were engaged in a task in which they had to attend to a series of broadband sounds and detect the occurrence of a pure-tone. They found that attention can trigger rapid plasticity in spectrotemporal receptive fields (STRFs) that were facilitatory towards detection of the target tone frequency. These adaptive goal-oriented changes triggered by attention in A1

receptive fields have been confirmed in several other studies in the ferret (David et al., 2012; Fritz et al., 2007, 2005), and recently, have also been shown to occur in the inferior colliculus (Slee & David, 2015).

The changes caused by attention in auditory receptive fields indicate that the brain can alter its sensory representations of the world depending on the animal's current behavioral goals and the behavioral meaning of salient sound objects. In this light, Fritz et al. (2010) found responses in ferret dlFC that were selective to target sounds and were gated by behavior. These responses invariantly coded for sound meaning (warning in an avoidance task), and did not encode acoustical properties (like amplitude or frequency). Some cells in dlFC encoded target whether in an auditory or parallel visual task. Moreover, in simultaneous local field potential (LFP) recordings from A1 and dlFC, behavior-related changes were found in LFP interareal spectral coherence when animals were engaged in auditory tasks, suggesting that there is an interaction between these two areas during behavior (Fritz et al., 2010). This evidence, along with anatomical data, indicate that areas in the frontal lobe might indeed be a source of top-down influences in auditory representations. However, the differential topography of connections with frontal cortex in the auditory fields raises the question whether plasticity of representations can be influenced differently at the different auditory cortical stages. This question is further emphasized by the general finding in the visual system that attention modulatory effects become greater (Kastner & Pinsk, 2004; Maunsell & Treue, 2006) and occur earlier (Buffalo et al., 2010) at higher visual cortical levels. Also, a similar hierarchical

build up of neural correlates of perceptual judgments has been described in the somatosensory system (de Lafuente & Romo, 2006), where increasing proportions of neurons in higher-order areas correctly predicted behavioral responses of monkeys performing a tactile detection task.

As one of the most important and exciting questions in neuroscience is how and where internal higher-order representations (coded in areas such as dlFC) integrates with early sensory information, making abstract task-relevant stimulus representations emerge in sensory systems, the present dissertation work expands on previous research done in our lab by describing how top-down influences change sound representations in two higher-order stages whithin the cortical hierarchy of ferret auditory cortex as well as in the different laminae of A1.

Chapter 3 addresses the question of how task-related plasticity of receptive fields in A1 is defined in the different cortical laminae. Technical limitations in previous experiments from our lab don't allow to determine what cortical layers are involved in task-related plasticity. In this study we recorded multi-unit activity and local field potentials using electrodes in a linear array, which allow to estimate the relative depth of each electrode relative to the cortical layers. The results reported are important in order to better understand the cortical circuitry involved in task-related plasticity of STRFs in A1.

In order to explore how behaviorally-relevant sounds are represented in higher-

order areas of the auditory cortex, we recorded in belt and parabelt areas in the Posterior Ectosylvian Gyrus (PEG). Results from belt areas in the dorsal PEG (dPEG) are reported in chapter 4. In chapter 5 we studied neural responses in a collection of cortical areas (collectively labeled as ventral anterior PEG, vaPEG) that has been shown, preliminarily (Radtke-Schuller et al., 2011) to be the main center of reciprocal connections between auditory cortex and dlFC in the ferret. Recent evidence on cortico-cortical connectivity (Bizley et al., 2015), as well as it tuning properties, are consistent with the hypothesis that vaPEG constitute a parabelt area in the auditory cortex of the ferret. The results presented in chapter 5 suggest that this cortical area might be an important stage in the auditory processing circuit, where higher-order auditory information gets integrated with abstract task-related information. Descending connections from belt and parabelt to core auditory areas might account for top-down effects reported previously in A1 receptive fields.

Chapter 2: Methods

All experimental procedures were approved by the University of Maryland Animal Care and Use Committee and conformed to standards specified by the National Institutes of Health.

2.1 Training and behavioral tasks

The A1 laminar study (Chapter 3) includes data from 2 animals, which were also used in the vaPEG study (Chapter 5). Chapter 4 includes data from dPEG recordings performed in 8 animals and Chapter 5 presents data from vaPEG recordings from 4 animals, one of such was also recorded simultaneously from vaPEG and dlFC. In Chapters 4 and 5 some data from previous studies in A1 and dlFC done in our lab (David et al., 2012; Fritz et al., 2003, 2010) was reanalyzed and presented for comparison (A1 n= 4 animals, dlFC n = 5 animals). The total number of animals used among the three studies was 18.

All animals used in the three studies, as well from earlier studies in A1 and dlFC were female descented, neutered, adult ferrets (*Mustela putorius furo*).

Animals were trained in two go/no-go auditory tasks (Figure 2.1): a tone detection (Fritz et al., 2003) and click rate discrimination, using a conditioned avoidance procedure (Heffner & Heffner, 1995). Chapters 3 and 4 present data exclusively for tone detection task, while Chapter 5 reports data from both tasks. The total number of animals trained in the tone detection task was 18, of which 4 were trained in both tone detection and click rate discrimination tasks.

In both tasks, ferrets can freely lick water flowing continuously from a spout during presentation of a variable number of reference sounds (1−6) until they hear a warning target sound. Animals have learned to briefly stop licking after target offset (for a minimum of 400 ms) in order to avoid a mild shock in the tail (in the head-fixed condition) or tongue (in the freely-moving training condition before headpost implant surgery).

In the tone-detection task, reference stimuli are 1−2 s broad-band TORCs (temporally-orthogonal ripple combinations) and target stimuli correspond to 1−2 s single-frequency tones. In the click rate discrimination task, stimuli are composed of 1.25 s long TORCs followed by a 0.75 s long click train (2 s total stimulus duration). Reference and target stimuli differed in the presentation rate of the click train, meaning that ferrets have to discriminate between low (4−24 Hz) and a high (18−40 Hz) click rates. Half of the ferrets (n=2/4) were trained with low-rate references and high-rate targets, while the other half were trained with high-rate references and low-rate targets. Both tone frequency and click train rates varied

between experiments, but are held fixed during a single behavioral block of 39 trials. Inter-stimulus intervals in both tasks have a duration of 1.2−1.6 s. During electrophysiological recordings, the identical task stimulus set is presented before and after behavior, while the animal passively listens (i.e. not engaged in the task).

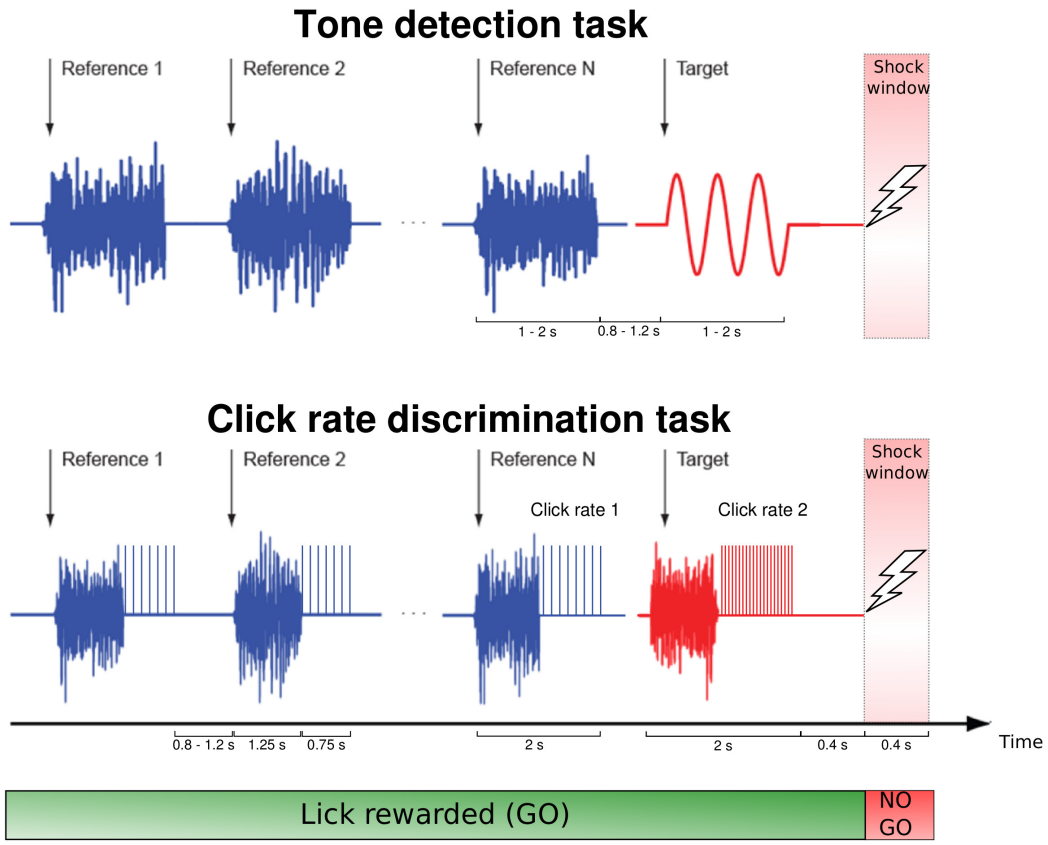

Figure 2.1: **Tone detection and Click rate discrimination conditioned avoidance task paradigms.**

2.2 Surgery

Initially, animals were trained in a freely-moving setting until they reach a consistent and acceptable performance, that is, achieving $> 80\%$ hit rate accuracy and $< 20\%$ false alarm rate for a discrimination rate > 0.65 (Fritz et al., 2003, 2010) in at least two consecutive training sessions. In order to secure stable electrophysiological recordings, ferrets were surgically implanted with a stainless steel headpost that is attached to the parietal bones suture in the midline. The bone cement (Zimmer) implant securing the headpost allows to keep open craniotomies well protected from the environment in between recording sessions.

Ferrets were anesthetized with a combination of Ketamine (35 mg/Kg IM) and Dexmedetomidine (0.03 mg/Kg SC) for induction, and deep levels of anesthesia were maintained with $1-2\%$ Isoflurane throughout the surgery. Animals were also medicated with atropine sulphate (0.05 mg/kg SC) to control salivation and to increase heart and respiratory rates. During surgery, ECG, pulse and blood oxygenation were monitored, and rectal temperature was maintained at $\sim 38°$C. Using sterile procedure, the skull was surgically exposed by making a midline incision in the scalp and by dissecting both temporal muscles. The headpost was secured in the skull with titanium screws and polycarboxylate cement (Durelon), and then areas surrounding frontal and auditory cortices are covered with bone cement (Zimmer), leaving small ($\sim 2-3$ square mm) cavities for easy access to auditory and frontal cortex in both hemispheres. Following surgery, antibiotics (Cefazolin, 25 mg/Kg SC)

and analgesics (Dexamethasone 2 mg/Kg SC and Flunixin meglumine 0.3 mg/Kg SC) are administered.

Animals were allowed to recover for ~ 2 weeks prior to be habituated to head restraint in a customized Lucite horizontal cylindrical holder for a period of $\sim\ 1-2$ weeks, and then retrained to reach acceptable levels of task performance.
Before recording sessions, small craniotomies were made over auditory or frontal cortex and, in simultaneous recording experiments, ipsilateral auditory and frontal cortex. Cavities of the head cap implant containing the craniotomies were kept sealed in between experiments with silicone ear impression material (Examix NDS) and were cleaned and treated with topical antiseptic drugs (Povidone-iodine) and antibiotics (cefazolin or enrofloxacin, $\sim$0.2 ml) at least once per week. The skin surrounding the implant was cleaned 3 times per week with warm saline, and treated with povidone-iodine and sulfadiazine cream ointment.

2.3 Structure of recording sessions

Recording sessions had duration of $4-8$ hours, with a typical experiment duration of 7 hours. After securing the animal in a lucite holder, the head was held fix by securing the headposts implanted in the skull to a steel bar afixed to the holder. After cleaning the surface of the craniotomy, electrodes were advanced until spontaneous neural activity was seen in all or most recording channels. This process

usually takes $1-3$ hours.

Later, $1-3$ sets of neurons at different electrode penetration depths were tested in passive and active conditions. Passive tuning properties were measured from responses to tones, TORCs and click trains. Measuring passive tuning properties from these stimuli usually took $20-45$ minutes with each neuron set.

After assessing the passive tuning properties of the neurons isolated at each penetration depth, animals were presented with passive and active iterations of the auditory tasks. Each iteration was composed of 40 trials. The minimal sequence used in each task was composed of 40 trials of passive presentation of the task sounds, where the animals were not given any water or punishment and quietly listened to task sounds, followed by an equal number of trials in the behavior condition, where animals received water reward and were required to report the presence of target sounds by refraining from licking water after target presentation. After 40 trials in the active condition, 40-80 trials of passive task sounds (post-passive) were presented to measure recovery of neural responses. Each task sequence (pre-passive - active - post-passive) lasted $30-60$ minutes. After testing the neurons at hand in the passive and active conditions, electrodes were advanced $150-200$ μm in order to find a new set of neurons. A typical recording session lasted for 7 hours in which 2 electrode penetration depths were tested in passive and active conditions. After recordings, electrodes were slowly withdrawn from the brain and the craniotomy was cleaned with saline and treated with topical antibiotics (cefazolin or enrofloxacin).

Craniotomies were then sealed using ear impression silicone (Examix).

2.4 Electrophysiological recording procedures

Training and neurophysiological recording experiments were conducted in a double-walled sound attenuating chamber (IAC). High impedance (1.26 MΩ at 1 kHz) tungsten electrodes (FHC) were used for extracellular neurophysiological recordings and elgiloy electrodes (FHC or Microprobes) for iron deposit markings. Electrodes were arranged in a 4-electrode square array and separated by 0.5 mm from their nearest neighbor. In each recording session, four electrodes per recording area (four in auditory and four in frontal cortex) were independently advanced through the duramater into cerebral cortex using an Alpha-Omega EPS drive system. Electrodes were advanced until good spike isolation was found in the majority of the electrodes. Data acquisition was performed with an Alpha-Omega AlphaLab data acquisition system, signals recorded at 25,000 samples/s and amplified 15,000 X. Laminar recordings from primary auditory cortex were performed using a 24 electrode linear array (Plexon U-Probe) with 75 μm between electrode contacts and impedances between $275 - 1500$ kΩ at 1 kHz, using Plexon and TBSI 1X headstages, amplified with Plexon preamplifiers and acquired using MANTA, an open source data acquisition suite written for MATLAB (Englitz et al., 2013).

Single units (usually one or two per electrode) were isolated by k-means clus-

tering using custom software written in MATLAB. Sound stimuli, behavioral operation, on-line analysis and recording triggering are controlled with customized open source software (Behavioral Auditory PHYsiology, BAPHY).

2.5 Localization of auditory fields and recording sites

The location of A1 was first determined by relative distance to external cranial landmarks. In female ferrets, A1 is usually found close to an area 16 mm anterior to the occipital midline crest and 12 mm lateral to the skull midline. During first recording sessions for each animal, small craniotomies were directed towards A1 using these coordinates, and then its location confirmed by analyzing the tuning properties of the recorded cells in response to 100 ms tone pips of random frequencies spanning 8 octaves, presented at intervals of 1 s. Also, 3 s temporally orthogonal ripple combinations (TORCs) were used to compute spectro-temporal receptive fields (STRFs). A1 neurons are know to present sharp tuning to pure tones and clear single-peak, short latency STRFs. Determination of neuronal best frequencies allowed us to confirm the location of A1 based on its characteristic tonotopic organization of high to low frequency gradient in a dorsal-ventral direction (Bizley et al., 2005; Shamma et al., 1993). Then, by ventrally expanding the existing craniotomy it is possible to have access to non-primary auditory areas in the Posterior Ectosylvian Gyrus (PEG, Bizley et al., 2005; Pallas & Sur, 1993). Two subfields in the dorsal PEG (dPEG), Posterior Pseudosylvian Field (PPF) and Posterior Suprasyl-

vian Field (PSF), display a reversal in the tonotopic map, sharing a low frequency area with A1 and displaying higher frequency regions more ventrally. Both fields are also separated by a low frequency border, meaning that PSF displays a low to high frequency tonotopic gradient in a antero-dorsal to postero-ventral direction, while PPF displays low frequencies postero-dorsally and high frequencies antero-ventrally (Bizley et al., 2005). Neurons in these areas display broader tuning, longer latencies and longer sustained responses than A1 (see results in Chapters 4 and 5), and its STRFs display more complex patterns of excitatory and inhibitory subfields, with more numerous, longer and less compact excitatory and inhibitory subfields in both the spectral and temporal axis (Atiani et al., 2014, Chapter 4). The location of dPEG recordings was then confirmed by checking the tuning properties of its neurons and its location relative to the tonotopic map.

Ventral Anterior PEG (vaPEG) recordings were located in a region ventral and anterior to dPEG. We describe as vaPEG the Ventral Posterior field (VP), posterior bank of the Pseudosylvian sulcal cortex (PSSC) and an area anterior and ventral to PPF that has been named as pro-PPF (Atiani et al., 2014). We determined vaPEG to be in the vicinity of 2 mm ventral and 2-3 mm anterior to the low frequency border region between A1 and dPEG. Neurons in vaPEG display longer latencies, broader tuning and longer sustained responses than dPEG and A1 (see results in Chapter 5). Also, many times, responses of vaPEG neurons to pure tones and TORCs were inhibitory. To our knowledge, no previous study has explored the response properties to passive stimulation in auditory areas ventral to dPEG fields

PPF and PSF of the ferret.

Careful measurements of the location of the electrode array relative to 2 reference marks placed in the dental cement surrounding the craniotomy and to a mark at the center of the headpost, were recorded for later reconstruction of electrode penetration sites in the surface. 9 electrolytic lesions were placed in the 8 animals used for dPEG recordings (Chapter 4). Electrolytic lesions were done by passing a small current ($8-11$ μA) for $30-90$ seconds through a $\sim$1 MΩ tungsten electrode. In the 4 animals used in the vaPEG study (Chapter 5), small iron deposits were placed in vaPEG for posterior confirmation of recording locations. Iron deposits were made by passing a small current (10 μA) for 5 minutes using elgiloy electrodes. Although these iron deposits can be visualized in-vivo using structural magnetic resonance imaging, we were unable to do so because of the stainless steel bone screws used to secure the implant in the skull. The location of the iron deposits was determined post-mortem by using prussian-blue staining.

2.6 Stimuli

All acoustical stimuli were presented at 70 dB SPL, with the exception of tones used for multi-level tuning assessment. Sounds were digitally generated at 40 kHz with custom-made MATLAB functions and National Instruments A/D hardware (PCI-6052E) and presented with a free-field speaker at 30 cm from the animal's

head.

Tones (5 ms onset and offset ramps) were used as target stimuli in the tone detection task and, previous to any behavioral testing, to assess frequency tuning by using tone pips of random frequencies. Clicks in the click-rate discrimination task and at passive testing out of behavioral context were composed of 0.01 s square pulses of alternating polarity.

Temporally-orthogonal ripple combinations (TORCs) were used as task distractor (reference) sounds and also for computation of STRFs in and out of task context. TORCs were randomly chosen from a set of 30 TORCs. Each TORC was composed of 5-octave wide broadband noise with a dynamic spectrotemporal profile product of the superposition of the envelopes of six temporally orthogonal ripples. Ripples composing the TORCs have a linear sinusoidal spectral profile with peaks at 1.2 cycles per octave. The envelope of these ripples drifts temporally up or down down the logarithmic frequency axis at a constant velocity ($4 - 48$ or $4 - 24$ Hz). The 5 octave spectrum of TORCs can be varied in several ranges and were chosen to span the best frequencies of the neurons currently recorded.

2.7 Data analysis

Basic tuning properties were determined by analyzing the responses to random frequency tones spanning $6-8$ octaves (11 tones per octave), usually ranging from 125 Hz to 32 kHz at $65-70$ dB SPL. A Gaussian function was fit to the mean firing rate during a window of 100 ms after tone onset. Best frequency was determined to be the mean of the Gaussian curve, and tuning spectral bandwidth was measured as its width in octaves at half-height. Tones presented had a duration of 100 ms and were presented at 1 s intervals. Response latency was measured from the peri-stimulus time histogram (PSTH) binned at 1 ms and computed from the responses to all pure frequency tones by measuring the time from tone onset to the peak spike rate in a 100 ms window.

TORCs were also presented to compute spectro-temporal receptive fields (STRFs) by means of reverse correlation (Klein et al., 2000) between each time-varying neural response (i.e., spikes, multi-unit activity or LFP high-gamma or current source density) and the spectrogram of the TORCs presented during experiments. Positve STRF values indicate time and frequency components of TORCs correlated with increased neural responses (i.e., an excitatory field), while negative values indicate components correlated with decreased responses (i.e., an inhibitory field). The reliability of responses to TORCs, and the quality of resulting STRFs, was measured by calculating a signal-to-noise ratio (SNR) that corresponds to the trial-by-trial phase locking to the set of TORCs. Only responses with SNR values equal or higher

than 0.2 were used. Response duration was measured as the width at half-height of the STRF positively rectified and averaged over frequency. Since STRFs varied in their complexity among auditory areas, with clear excitatory/inhibitory fields over a restricted spectrotemporal range in A1, and more complex STRF shapes in higher-order auditory areas, we measured a STRF sparseness index as the ratio of peak magnitude to the average amplitude over all spectrotemporal bins. For this, in STRF responses with SNR values ≥ 0.2, we measured the peak value among all STRF spectrotemporal bins and divided it by the mean standard deviation of the remaining bins. Higher sparseness values are usually associated with sharply tuned STRFs that concentrate maximum magnitudes over a few contiguous bins. Since A1 STRFs have more spectro-temporal coefficients closer to zero (smaller standard deviations), and clear tuning peaks, A1 sparseness indexes were greater than those computed from higher-order auditory neurons. Significance of differences of tuning parameters between areas was assessed using Kruskal-Wallis one-way analysis of variance after testing for normality with Lilliefors test.

Before averaging STRFs across electrodes in the laminar probe data (results in Chapter 3) we aligned each STRF so that the frequency bin containing the target was in the center of the frequency axis. Since the majority of power in target-aligned STRFs occurred within $\pm$ 0.5 octaves from the target frequency, we constrained our STRF analysis to that frequency range.

Single-unit neural responses to task stimuli were measured by computing

PSTHs by binning spike times at $25 - 50$ ms and obtaining the mean and SEM of the spike rates obtained over all reference and target sound classes. Units were considered auditory-responsive neurons when there were at least 2 bins significantly modulated from baseline in the PSTH in response to any (reference or target) sound ($p<0.05$, t-test, Bonferroni corrected). Significance of behavioral effects within cells was measured by performing either a jackknifed t-test (Chapter 4) or a Wilcoxon signed rank test with Bonferroni correction (Chapter 5) between passive and active PSTHs of each sound class (reference or target). Neural responses were considered to be significantly modulated by behavior if there were at least 2 consecutive significant ($p<0.05$) PSTH bins within the response to any sound class between passive and active conditions.

Normalized average PSTHs were computed by subtracting the baseline firing rate (that obtained in the silence period preceding sounds) and then dividing the PSTHs by the magnitude of the maximum modulation. Mean PSTH and SEM were computed by a jack-knifing procedure. For comparison of mean normalized PSTHs between different areas it became important to account for the large number of neurons in dlFC that display suppressive responses to target sounds (Fritz et al., 2010) by changing the sign of responses that had a maximum absolute value below spontaneous activity.

Target enhancement within a condition (passive or active) was measured as the difference between mean PSTH response to target minus the mean PSTH re-

sponse to reference, measured from the normalized PSTH after sound onset in a 1 s window. Overall enhancement of target response relative to reference response was measured by calculating a target enhancement index. This was computed as the difference of task-related changes in target responses (target active minus target passive) minus task-related changes in reference responses. Values greater than 0 were obtained with relative enhancement of target responses during behavior, even when the responses to both sound classes were suppressed. Responses in the silence period after target offset were analyzed in a 700 ms time window starting 100 ms after target offset. Comparison with responses during the target were done against a time window 700 ms before target offset.

The local field potential (LFP) was obtained by low-pass filtering the acquired signal at 200 Hz. A hardware notch filter at 60 Hz was applied online, and later the data was pre-processed by resampling the data at 600 Hz, applying a 50 Hz low-pass butterworth filter and substracting the mean. Spectral coherence between LFP signals recorded simultaneously from dlFC and vaPEG was computed using all possible vaPEG/dlFC electrode pairs with a multi-tapered method (Chronux functions available at http://chronux.org). Significance between passive and active conditions were assessed through t-test and Bonferroni correction ($p<0.01$). Granger causality in the frequency domain was also computed between vaPEG and dlFC LFP recordings, by using the same set of electrode pairs used for the spectral coherence estimation. Multi-tapered Fourier coefficients and Granger causality were computed using the Fieldtrip MATLAB toolbox (Oostenveld et al., 2011).

In A1 laminar recordings it was necessary to align the recordings to a common depth reference. In order to align all penetrations to the same depth, LFP responses to 100 ms tones were measured during the passive condition to find a common marker of depth. The marker was found for each penetration by first identifying the electrode with the shortest LFP response latency, then finding its LFP waveform correlation coefficient with the LFP waveforms on all other electrodes in the same electrode penetration. The border between the first neighboring electrode pair with positive and negative correlation coefficients defined the superficial vs. middle-deep layer border, most likely corresponding to supragranular layers II/III and granular/infragranular layers IV-VI, respectively. Laminar profiles were averaged across penetrations by aligning to this border.

Multi-unit (MU) spikes were extracted on each electrode by band-pass filtering the raw signal between 300 and 6,000 Hz, then isolating spikes by peak detection (4 standard deviations threshold). On the same electrodes used to extract MUs, we also extracted local field potentials (LFPs). High-gamma (HG) LFPs were extracted by filtering the raw signal between 80-300 Hz, then taking the magnitude of the filtered signals Hilbert transform, and finally low-pass filtering below 70 Hz. Current source densities (CSDs) were derived by low-pass filtering the raw signal below 80 Hz, then computing the second derivative approximation (Pettersen et al., 2006) of the low-pass filtered LFP across the linear array.

Chapter 3: The laminar profile of rapid task-dependent platicity in core auditory cortex

3.1 Introduction

The auditory cortex, as well as all mammalian sensory neocortex, is a complex structure anatomically organized in six horizontal layers or laminae, that differ in cell density, diversity of cell types and connectivity. Functionally, it is organized in vertical radial columns of cells linked synaptically across the laminae, that share functionality and similar stimulus feature affinity, extending from white matter to cortical surface (Mountcastle, 1997). The laminar cortical layout is an effective way to organize input and output neuron relationships, as every layer receives and sends projections from/to diverse areas.

Sensory processing in the cortical column is achieved through an anatomical and functional circuitry that is usually thought to be archetypal among all modalities. The basic cortical circuit is usually idealized as a canonical cortical circuit (Douglas & Martin, 2004), that consists in feedforward excitatory input from thalamus arriving to the granular layer, layer IV (Huang & Winer, 2000). From there,

information proceeds largely serially to superficial (supragranular) layers II-III and then to infragranular (V-VI) layers, from where efferences emerge to project to subcortical and cortical destinations. Despite being an influential theory that describes the main flow of information in the cortical column, it can be misleading, as it greatly oversimplifies a seemingly more complex system. For example, there is evidence showing that neurons in layers V and VI of rat somatosensory cortex can be directly excited by thalamic inputs that do not contact granular layer IV (Constantinople & Bruno, 2013), or more recent evidence showing that direct connectivity between layers IV and V exists and can activate inhibitory interneurons in deep layers, by-passing superficial layers II and III (Pluta et al., 2015).

In auditory cortex, supragranular laminae I to III have been shown to mediate lateral inter-columnar communication (Wallace et al., 1991), as well as interareal connectivity between auditory cortex, auditory-related areas and association areas in the frontal lobe (Barbas et al., 2005; Kaas & Hackett, 2000; Rouiller et al., 1991). Thus, the supragranular intracortical network may provide a pathway for top-down signals from the frontal lobe to influence auditory cortex responsiveness in favor of behaviorally meaningful sounds.

Attention has been shown to cause changes in auditory representations in primary auditory cortex (A1) that are thought to facilitate perception of behaviorally meaningful sounds (Bakin & Weinberger, 1990; Fritz et al., 2003; Ohl & Scheich, 1996; Polley et al., 2006). Rapid task-dependent plasticity is a form of plasticity

in which short-term refinement of neuron tuning occurs within seconds or minutes during the performance of detection or discrimination of auditory targets (Atiani et al., 2009; David et al., 2012; Fritz et al., 2003, 2007). These changes, basically, modulate the filter properties of neurons to better capture acoustic features of foreground stimuli by producing facilitative changes in spectrotemporal receptive fields (STRF) that enhance the representation of foreground acoustical features while suppressing those of background sound features. These studies were based on extracellular recordings done with single electrodes, where these were advanced into the cortex until neural activity was found, and thus, although sampling of units was done across the depth of A1 (Atiani et al., 2009; David et al., 2012; Fritz et al., 2003, 2007), there was no information available about the precise laminar location of the recordings. Hence, the present study was undertaken to clarify the cortical mechanisms involved in rapid task-dependent plasticity and its laminar profile by using more adequate linear electrodes (Figure 3.1) and signal processing techniques to allow the estimation of relative position of recording electrodes in the cortical layers.

Converging lines of evidence from anatomical (Barbas et al., 2005; Kaas & Hackett, 2000; Rouiller et al., 1991; Wallace et al., 1991) and neurophysiological (Guo et al., 2013) studies suggest that rapid task-related plasticity in A1 may be greatest in supragranular laminae. In a recent study by Guo and collaborators (2013), current source density (CSD) analysis of A1 local field potentials (LFPs) measured after auditory training on a single frequency tone detection task revealed, in recordings sites with best frequency (BF) near the target frequency, enhanced

auditory target-evoked CSD current sinks in layers II/III, and no change in thalamorecipient layer IV. Additionally, they did not find any change in CSD responses in recording sites with BFs far from the target frequency, suggesting that training-induced plasticity was selective to cortical areas near the target representation and was caused by changes in intracortical pathways connecting the area of target representation with nearby cortical areas.

In this study we measured rapid task-related plasticity based on the analysis of multi-unit (MU) spiking activity, CSD computed from LFP and high-frequency LFP. The LFP is a continuous broad-band signal that can be recorded from within brain tissue with extracellular microelectrodes, that represents the compound synaptic and spiking activity of many neurons and their synaptic inputs within a volume of brain tissue that can span several millimeters (Kajikawa & Schroeder, 2011). CSDs, computed as the second derivative of LFP signals, are believed to measure transmembrane currents related to spiking activity (Buzsáki et al., 2012; Kajikawa & Schroeder, 2011) and correspond to responses from a spatial extent that is more restricted to that from LFP signal (i.e. it measures a more local phenomenon than LFP). High-frequency LFP, also called high-gamma (HG) LFP, is the oscillatory LFP signal above 80 Hz, and it's considered to measure synchronous activity from many neurons, and it's an even more local estimation of activity, similarly to the analysis of multi-unit spiking activity. We sought to measure rapid task-dependent plasticity in MU, CSD and HG signals in two ferrets trained in a tone detection task (Fritz et al., 2003; Heffner & Heffner, 1995) based on a conditioned avoidance

regime (See Chapter 2). Our study hypotheses are: (1) rapid task-dependent plasticity measured in MU spiking activity should be similar in HG and CSDs, and (2), consistent with anatomical and electrophysiological evidence, plasticity should be greatest in supragranular laminae.

To test these hypotheses, we recorded MU and LFP signals along A1 cortical columns using a 24 channel linear electrode array (Plexon U-probe, Figure 3.1 A). Using signal processing techniques, we depth-registered each recording electrode in order to align all probe penetrations to the same cortical depth. LFP responses to 100 ms tones were measured during the passive condition to find a common marker of depth (figure 3.1 B). The marker was found for each penetration by first identifying the electrode with shortest LFP response latency and then by finding its LFP waveform correlation coefficient with the LFP waveforms on all other electrodes in the same probe penetration. The first neighboring electrode pair with positive and negative correlation coefficients defined the border between superficial and middle-deep layers, most likely corresponding to supragranular layers II/III and granular/infragranular layers IV/VI, respectively (Huang & Winer, 2000; Kajikawa & Schroeder, 2011; Linden & Schreiner, 2003). Laminar profiles were later averaged across penetrations by aligning to this border.

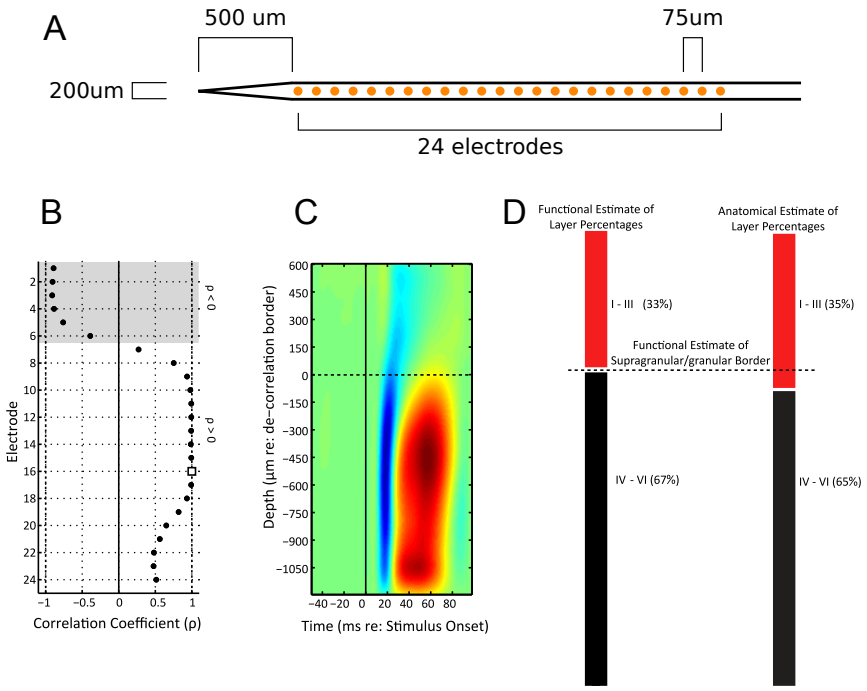

Figure 3.1: **Electrode depth-registration. A:** schematics of the linear array probe used in laminar recordings. 24 electrodes were spaced by 75 μm and spanned a total distance of 1.8 mm. **B:** example from one probe penetration to show the method used to estimate the border between superficial and middle-deep layers, defined as the depth of LFP phase reversal. LFP responses to 100 ms tones were used to find a common marker of depth across penetrations. The marker was found for each penetration by first identifying the electrode with the shortest LFP response latency (marked with a white square), then finding its LFP waveform correlation coefficient with the LFP waveforms on all other electrodes in the same penetration. The border between the first neighboring electrode pair with positive and negative correlation coefficients defined the border between superficial and middle-deep layers. **C:** Grand-average LFP laminar profile in response to 100 ms tones, after depth-registration of all penetrations. **D:** Similarity between our functional estimate of A1 depth percentages for superficial (33%) vs. middle-deep (67%) layers, and the known anatomy in ferrets: 35% for layers I-III and 65% for layers IV-VI (S. Radtke-Schuller, personal communication).

3.2 Results

We recorded MU, CSD and HG responses during presentation of task sound stimuli with animals engaged in the task (active behavior) and passively listening before and after behavior. Animals were trained to refrain from licking water from a spout upon presentation of a target tone that occurred after a random number (1-6) of reference TORC stimuli (see Chapter 2, section 2.5).

3.2.1 Laminar profile of target enhancement

During task performance, we found that average MU, HG and CSD target tone responses were enhanced relative to reference (TORC) responses, and this enhancement occurred mostly in the superficial layers, while mild suppression of target responses occurred in the middle-deep layers (Figure 3.2, panels a, b, d, e, g, h). Reference responses tended to be reduced in both, superficial and middle-deep layers. These changes suggest that A1 enhances its ability to capture the task target by enhancing responses to foreground while suppressing background. The laminar profile of relative enhancement of target responses can be better estimated as a measure of plasticity by calculating the fractional change from passive to active responses to both reference and targets and then displaying the difference between target and reference task-dependent change (Figure 3.2, panels b, e and h). The grand average computed from MU spiking activity, HG and CSD displays little or no plasticity in the middle-deep layers, but considerable target enhancement in the superficial layers.

To quantify the magnitude of plasticity we computed a target enhancement index by taking the maximum difference between target and reference task-dependent change for each electrode. The average target enhancement index measured from MU activity, HG and CSD, was significantly greater for the superficial than middle-deep layers (Figure 3.2, panels c, f and i) and the cumulative distribution functions show that the target enhancement index was greater for most individual recordings. The grand-average target enhancement indexes for superficial vs. middle-deep layers were, MU: 0.48 vs. 0.09 ($p<0.001$), HG: 0.52 vs. 0.19 ($p<0.001$), and CSD: 0.23 vs. 0.18 ($p<0.05$).

3.2.2 Laminar profile of spectrotemporal receptive field plasticity

Rapid task-dependent plasticity has been previously described in A1 through the analysis of STRFs computed from both single-unit and MU spiking activity (Atiani et al., 2009; David et al., 2012; Fritz et al., 2003, 2007). Here, we extend that analysis by computing the average STRF for superficial and middle-deep layers (figure 3.3, panels a, d and g) through reverse correlation between MU, HG and CSD responses to reference TORC stimuli and TORC spectrograms. STRFs computed from reference TORC stimuli allow to predict how neurons change their filter properties relative to the target frequency, and to estimate the magnitude of the response to target tones. Previous to average the resulting STRFs we aligned all

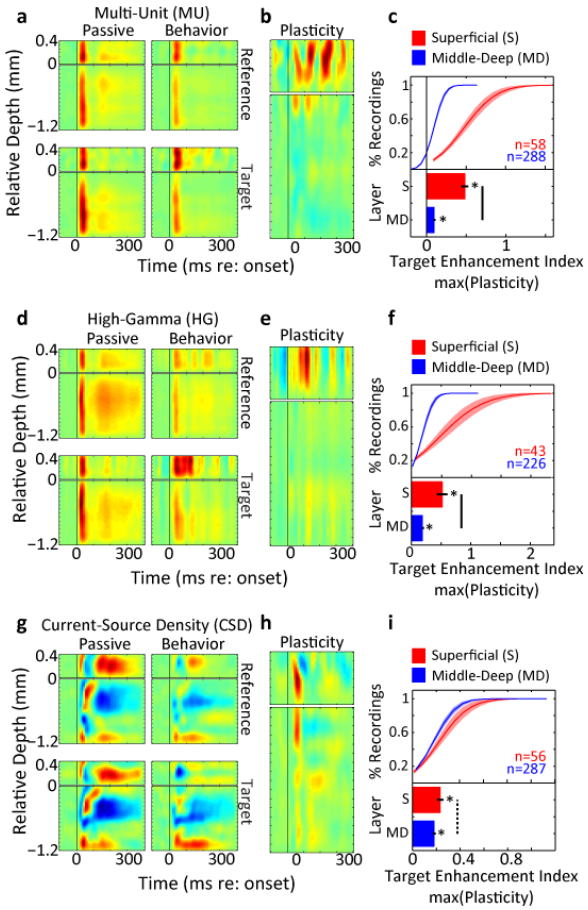

Figure 3.2: **Laminar profiles of stimulus responses in primary auditory cortex (A1).** The top, middle and bottom rows show the data for multi-units (MU), high-gamma (HG) band of the LFP and current source densities (CSDs), respectively. **A, D, G:** Grand-average laminar profiles of responses to reference TORC (top row) and target tones (bottom row) in passive (left column) and behavior (right column) conditions. Depth is relative to the estimated border between superficial and middle-deep layers. For MU and HG, red indicates excitatory auditory responses; for CSDs, red indicate a current source (passive outward flow of ions to the extracellular medium) and blue indicates a current sink (inward active flow of ions caused by synaptic activity). **B, E, H:** laminar profile of rapid task-dependent plasticity on the same depth axis as A, D and G, measured as difference between target and reference response change. Green indicates no task-dependent change, red indicates positive target enhancement during task performance. **C, F, I:** estimates of cumulative distribution functions (top) and grand-averages (bottom) of target enhancement indexes for all electrodes in superficial (red) and middle-deep (blue) layers. Error bars and shades = 1 SEM. Stars indicate significant averages ($p<0.001$, one-sample t-test). Solid and dotted bars indicate significant ($p<0.001$ and $p<0.05$, respectively, bootstrapped t-test) average differences between layers.

STRFs to the target frequency bin.

In order to be able to quantify the magnitude of task-dependent STRF changes, we measured STRF plasticity (figure 3.3, panels b, e and h) by calculating the within-layer fractional change between STRFs from passive to active behavior conditions. We found enhancements at the target frequency in STRF from superficial and middle deep layers, but changes were greater in superficial layers. Changes in superficial layers were mostly due to decreases in inhibitory subfields in STRFs. We measured a STRF target enhancement index calculated as the maximum STRF change at the target frequency bin. Similarly to our results in task-related plasticity in MU, HG and CSD responses, we found greater STRF target enhancements in superficial than in middle-deep layers, in average and for most recordings (Figure 3.3, panels c, f and i). The grand-average STRF target enhancement indexes for superficial vs. middle-deep layers were, MU: 0.6 vs. 0.27 ($p<0.001$), HG: 0.46 vs. 0.28 ($p<0.01$) and CSD: 0.26 vs. 0.18 ($p<0.01$).

3.2.3 Persistence of rapid task-dependent plasticity

Previous studies in rapid task-related plasticity in A1 (Fritz et al., 2003) and in the frontal cortex (Fritz et al., 2010) have shown that some neurons can display persistent target enhancements (in their receptive fields or responses) that are maintained for minutes and even hours after behavior. In order to examine a differential

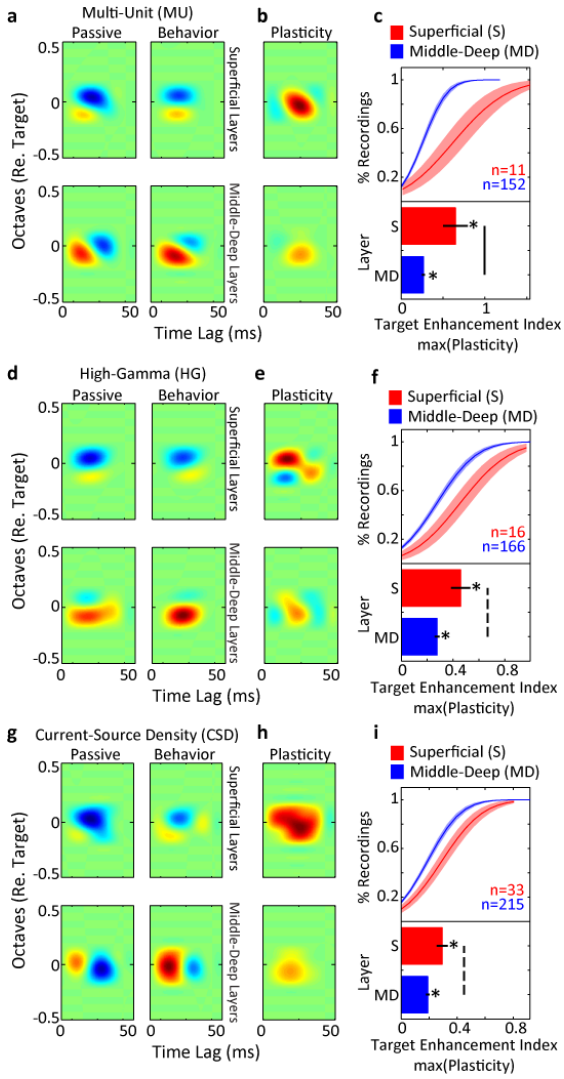

Figure 3.3: **Laminar profiles of spectrotemporal receptive fields (STRFs) in A1.** The top, middle and bottom rows show STRF data computed from MU, HG and CSD responses, respectively. **A, D, G:** grand-average STRF for superficial layers (top row) and middle-deep layers (bottom row), in passive (left column) and active behavior (right column) conditions. Green indicates no change in response, Red and blue indicate excitatory and inhibitory subfields, respectively. **B, E, H:** STRF plasticity in superficial (top row) and middle-deep (bottom row) layers, measured as the fractional change from passive to active behavior conditions. Red indicates target enhancement during task performance. **C, F, I:** STRF target enhancement index cumulative distribution functions (top row) and grand-average (bottom row) for all electrodes in superficial (red) and middle-deep (blue) layers. Error bars and shading show 1 SEM. Stars indicate significance averages ($p<0.001$). Solid and dashed lines indicate significant ($p<0.001$ and $p<0.01$, respectively) average differences between superficial and middle-deep layers.

persistence of task-dependent target enhancements across the cortical laminae, we compared the responses obtained in the passive condition before (pre-passive) vs. after (post-passive) task engagement. We measured the persistence in a similar way as the target enhancement index, by calculating the fraction change from pre-passive to post-passive condition. To put it into the context of task-dependent target enhancement, we plotted these ratios together with target enhancement indexes (Figure 3.4). We compared persistence of plasticity in MU, HG and CSD responses and in STRFs computed from these signals. We found that rapid task-dependent plasticity often persisted after behavior, but did not exceed the magnitude of behavior-related target enhancement.

3.3 Discussion

This study explored how rapid task-related plasticity is distributed in the layers of the cortex, a missing piece of information that might contribute to understand how the cortical circuitry contributes in enhancing the perception of task-relevant sound features. Previous neurophysiological studies using single electrodes did not gather laminar information and, given the larger somatic volume and higher spontaneous firing rates of infragranular relative to supragranular layers, it is possible that single-electrode recordings are biased towards infragranular layers (Petersen & Crochet, 2013).

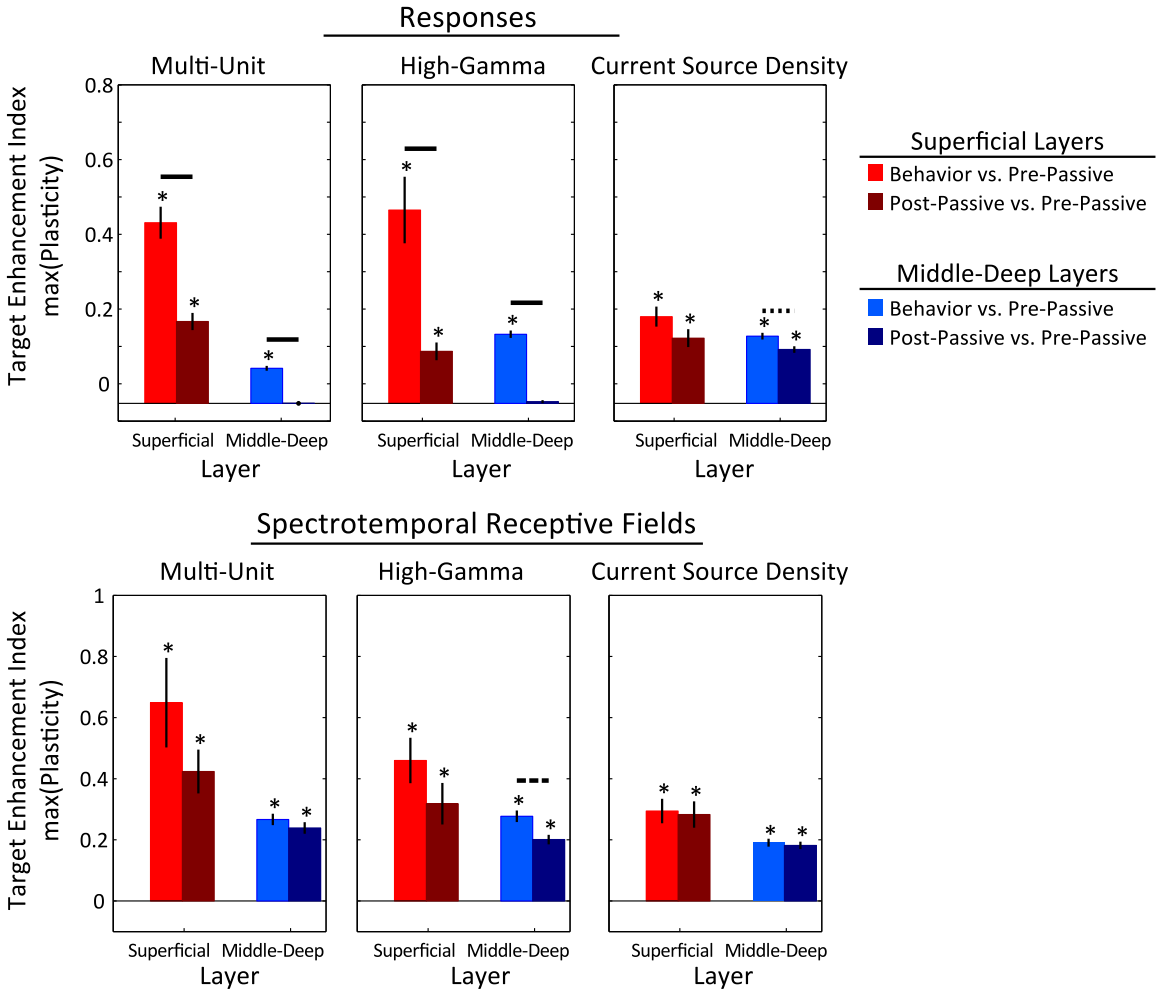

Figure 3.4: **Persistence of rapid task-related plasticity in superficial and middle-deep layers.** Previous studies have shown that rapid task-related plasticity can persist for minutes to hours after behavior. We measured persistence of target enhancement in passive runs of the tone detection paradigm after completion of the active behavior task (post-passive), which normally lasts 9 10.8 minutes. Persistence was quantified the same way as the target enhancement index, but by comparing the passive state after (Post-Passive) vs. before (Pre-Passive) the task. We found that target enhancement often persisted after task performance (stars indicate $p<0.001$), but was always less than during the task. This indicates that plasticity may have required several more minutes to completely decay. Error bars show 1 standard error of the mean. Solid, dashed and dotted lines indicate significant decay of rTDP ($p<0.001$, $p<0.01$, $p<0.05$, respectively).

We found that target enhancement during rapid task-dependent plasticity is present in all layers of A1, it is greatest in superficial layers, and occurs across the gradient of spatial scales measured by CSD, HG and MU responses. Within a column, superficial layers II-III receive inputs from thalamocortical layer IV and from cortico-cortical projections. The projections of the superficial layers are within-columnar outputs to infragranular layers as well as extra-columnar cortico-cortical projections to A1 and other auditory fields (Bizley et al., 2015; Happel et al., 2010; Petersen & Crochet, 2013). The dominance of target enhancement in superficial layers suggests that rapid task-dependent plasticity in A1 derives primarily from intracortical modulation of neural selectivity for behaviorally meaningful sounds.

A recent study also found that long-term experience-dependent plasticity causes enhancement of target evoked current sinks in layers II-III, but not in thalamocortical layer IV (Guo et al., 2013). They argued that, based on evidence of pharmacological alteration of thalamo-cortical circuits (Happel et al., 2010; Intskirveli & Metherate, 2012; Kaur et al., 2004; Kawai et al., 2007), the absence of change in the earliest current sink corresponding to layer IV, along with enhanced current sinks in layers II-III, suggests that this form of long-term plasticity is mainly the result of intracortical processing and not a product of subcortical enhancement of target representations. This raises the question as to whether task-related plasticity recently observed in inferior colliculus is the result of descending cortical projections (Slee & David, 2015).

We also found that the greatest target enhancement measured by CSDs in superficial layers arose from an increase in the magnitude of the target-evoked CSD current sink between $\sim 40-100$ ms (blue in figure 3.2, panel g). Together with Guo et al. (2013), these findings suggest that intracortical modulation of A1 auditory processing is important not only for establishing long-term experience-dependent plasticity, but also for the short-term effects of rapid task-dependent plasticity that arise only during auditory attention. However, since we found task-dependent changes in responses from all cortical laminae, we cannot rule out the influence of subcortical auditory areas (thalamus, inferior colliculus) or neuromotor centers (cholinergic nucleus basalis, noradrenergic locus coeruleus, dopaminergic ventral tegmental area) on plasticity. In fact, a recent paper described rapid task-dependent plasticity of STRFs in the inferior colliculi of ferrets (Slee & David, 2015), that were of similar magnitude but tended to be more suppressive to what was originally described in ferret A1 using the same task (David et al., 2012).

It is important to note, that target enhancement was greater in MUs and HG than in CSDs. Since CSD current sinks represent input to the local network (Buzsáki et al., 2012; Pettersen et al., 2006), and spike metrics such as MUs and HG represent local network output, it may be that intracortical input to A1 initiates or maintains rapid task-dependent plasticity, which is then amplified by local neural populations. Future studies measuring laminar profiles simultaneously across A1 and higher-order cortex, as well as functional and anatomical connectivity studies between auditory and auditory-related cortical areas will help to clarify the network

dynamics of rapid task-dependent plasticity during auditory tasks.

Chapter 4: Task-related plasticity in secondary auditory cortex of the ferret

4.1 Introduction

The auditory cortex of mammals is formed by a collection of areas that are grouped into primary or non-primary depending primarily on their patterns of corticothalamic and corticocortical connectivity (Hackett, 2011; Winer & Lee, 2007). The afferent connectivity between primary (or core) and secondary/tertiary (or belt/parabelt, respectively) auditory areas, as well as the ascending information flow within auditory cortex, has been proposed to be largely serial (Hackett, 2011). This description of a hierarchy of auditory cortical areas, while robust in its neuroanatomy grounds, has not been clearly elucidated functionally, mainly because of the difficulty in characterizing feature selectivity in auditory areas beyond primary auditory cortex (Sharpee et al., 2011).

Studying the auditory cortical hierarchy in a behavioral context might help our understanding on the role the diverse auditory fields have in perception. Studies in the visual system have suggested a differential influence of attention on the vi-

sual processing hierarchy, where attentional modulatory effects on neural responses become greater at higher levels (Kastner & Pinsk, 2004; Maunsell & Cook, 2002; Maunsell & Treue, 2006). Our lab has previously described the influence of attention on two stages of the auditory cortical processing chain, primary auditory cortex (A1, Fritz et al. (2003)) and dorso-lateral frontal cortex (dlFC, Fritz et al. (2010)). Findings in A1 reveal that auditory neurons are able to swiftly refine their spectro-temporal receptive fields (STRFs) to better capture target sounds in a tone detection task. This reshaping of neural filter properties has been shown to enhance the contrast between task-relevant stimulus classes (David et al., 2012) and depend on task difficulty and behavioral performance (Atiani et al., 2009). In contrast, dlFC responses are thought to represent more abstract representations of task-relevant stimuli identity and meaning along with other task events, internal goals and expectations (Miller & Cohen, 2001). In an auditory task, neurons in dlFC do not encode stimulus feature attributes such as frequency, but encode primarily the stimulus behavioral meaning (such as warning sound) by displaying strong task-dependent modulations on their responses during active behavior (Fritz et al., 2010). These behaviorally-gated responses might provide top-down signals that bias responses in A1 and induce rapid task-related changes in STRFs observed in A1 neurons.

The aim of this study was to explore whether auditory representations in belt auditory areas are intermediate between more acoustically-literal A1 and abstract dlFC auditory representations. We recorded in two tonotopic secondary auditory

fields of the ferret in the dorsal posterior ectosylvian gyrus (dPEG). These areas, the Posterior Pseudosylvian Field (PPF) and the Posterior Suprasylvian Field (PSF) were previously described in their passive physiological properties (Bizley et al., 2005) and their corticocortical connectivity (Bizley et al., 2015). These areas lie ventrally adjacent to A1 and present a reversed tonotopical gradients, sharing a low frequency border with A1. PPF and PSF have been shown to be reciprocally connected with A1 and project to higher-order parabelt auditory cortical areas (see Chapter 5) in ventral PEG and PSSC (Bizley et al., 2015; Pallas & Sur, 1993).

We measured behaviorally-driven plasticity in dPEG responses from ferrets performing a tone detection task in which animals learned to report the presence of a target tone after a sequence of reference TORCs (see methods in Chapter 2). Using the same task paradigm used in our lab previous studies of rapid task-related plasticity in A1 and dlFC allowed us to compare dPEG responses with A1 and dlFC task-related response changes.

We found that neurons in dPEG display task-related plasticity by enhancing their responses upon detection of a target tone, and that these modulations in target responses have larger magnitude than A1, but lower than dlFC target enhancements. These results suggest that dPEG lies at an intermediate stage between A1 and dlFC; while presenting robust passive responses to sounds, these present longer latencies and broader tuning properties, but also stronger attentional modulations than A1.

4.2 Results

We measured rapid task-dependent plasticity on single-units from ferret belt auditory areas PPF and PSF of ferrets in both, a passive listening state (N= 1,156, 8 animals) and during active behavior state (N=260, 7 animals). Ferrets that were recorded in the active state were trained in a tone detection task, where they were allowed to lick water from a spout while listening to series of reference noises (either broadband TORCs or bandpassed noise bursts) and learned to report detection of a target tone by avoid licking during a period of 400 ms after the target (see Chapter 2 for details).

We found no significant differences in passive tuning properties and behavioral-driven changes in both PPF and PSF, therefore we grouped PPF and PSF data together into a single dPEG data set. We compared dPEG neural responses with data from A1 single-unit recordings during presentation of the same stimulus set (N=2,448, 20 animals) and the same auditory task paradigm (N=283, 10 animals), as well as with neural data collected from dlFC during the same auditory discrimination behavior (N=534, 5 animals). Data from A1 and dlFC was collected for previously published studies (David et al., 2012; Fritz et al., 2003, 2005), and was reanalyzed for the present study.

4.2.1 Location of auditory recordings in ferret belt areas

Initial recordings in each animal were aimed at finding A1 tonotopic gradient, which is arranged dorso-ventrally form high to low frequencies (Bizley et al., 2005). Immediately ventral to A1, the two fields of the dPEG (PPF and PSF) are found. These fields are characterized by a dorsal common low frequency border with A1 and by sharing a common low frequency area roughly running dorso-ventrally and perpendicular to the A1/dPEG border, which separates PPF (rostral field) and PSF (caudal field). Both PPF and PSF exhibit a rough tonotopic organization from low to high frequencies in rostro-ventral (PPF) and postero-ventral (PSF) directions. After finding A1 tonotopic gradient, we continued recording ventrally to find the frequency reversal between A1 and dPEG, which coincided with a graded transition in the response properties of neurons, with generally longer latencies and sustained responses, broader tone frequency tuning and weaker phase-locking to TORC rippled noise. Determination of A1 and PPF/PSF tonotopic maps allowed us to place electrolytic marks in areal borders of multiple hemispheres, which were later confirmed histologically post-mortem (Figure 4.1).

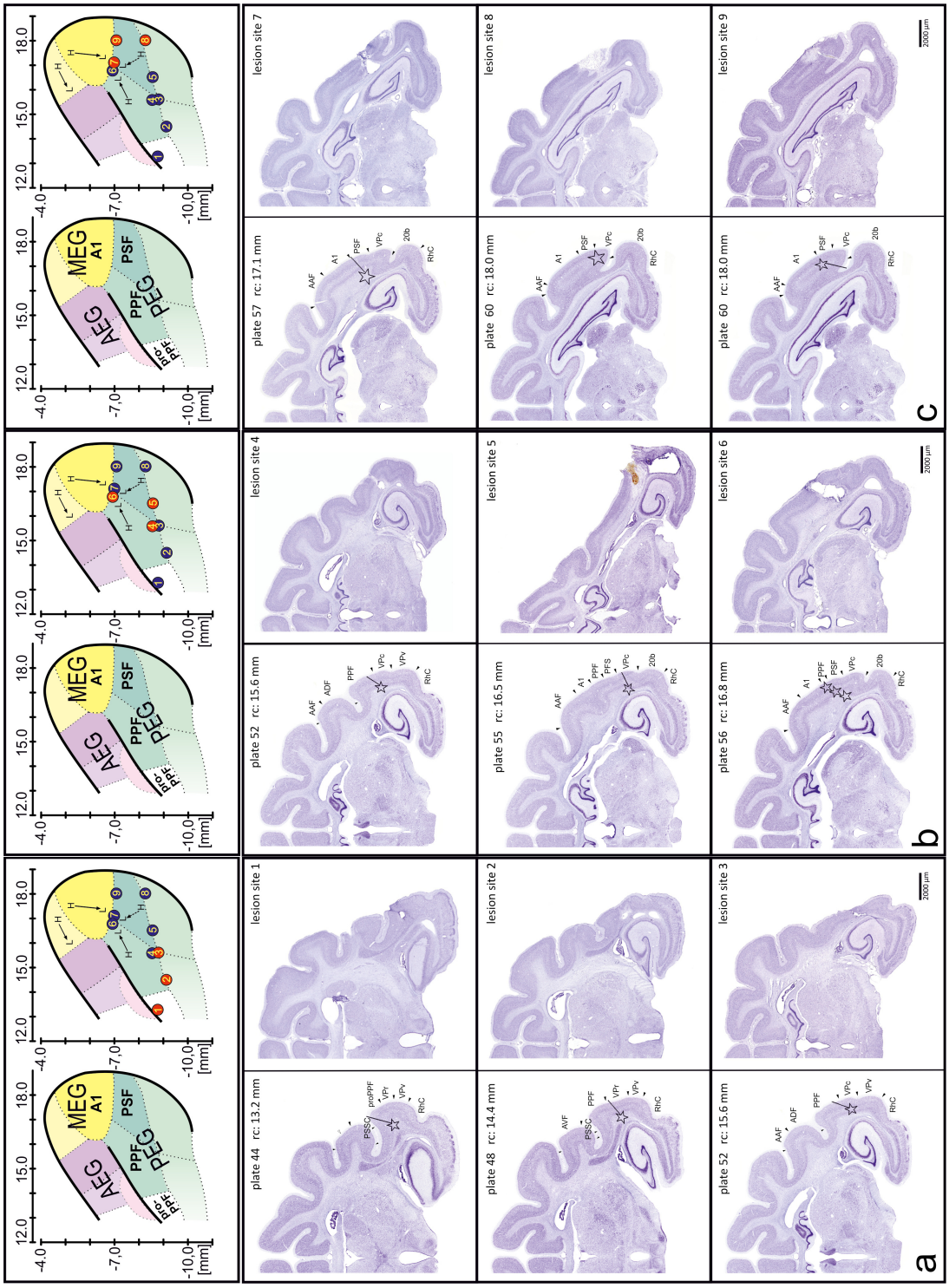

Figure 4.1: continues in next page...

Histological confirmation of recording areas. Panels a, b and c display the location of 9 example lesion sites characterized physiologically. Each panel displays, on the top, the cortical areas layout (left) and the projection of lesion sites on the cortical surface (right; red: lesion sites shown in lower panels). Arrows display the tonotopic gradient from high to low frequencies. Recordings and lesions were made in both hemispheres, but for simplicity are shown as projections onto the left hemisphere. Photographs in lower panels display 9 example lesion sites in multiple animals (right) and its matching Nissl-stained coronal sections from a ferret brain atlas created by S. Radtke-Schuller. Stars indicate the locations of the lesions made at recording sites. Our marks delineated the dorsal border of dPEG with A1 (lesion sites 6,7 and 9) and the lower border of dPEG with areas VPr (explored in Chapter 5) and VPc (lesion sites 2, 3, 4, 5 and 8). One lesion site was located in pro-PPF, an area presumed to be a parabelt field (studied in Chapter 5).

4.2.2 Passive tuning properties of dPEG neurons

Most neurons in dPEG presented robust responses to tones and TORCs presented passively to the awake, quiescent ferrets. We measured several tuning properties in responses to tones and TORCs in dPEG neurons (N=918/1130) and compared it with 2,317/2,532 neurons in A1 that were responsive to auditory stimuli (modulated from spontaneous firing rate, $p<0.05$, jack-knifed t-test). Consistent with a previous neurophysiological study (Bizley et al., 2005), we didn't find significant differences in tuning properties between PPF and PSF. Distribution of A1 and dPEG best frequencies largely overlapped, demonstrating an equivalent representation of frequency between these two areas (figure 4.2 A), but frequency tuning bandwidth of tone responses was slightly, yet significantly broader in dPEG with respect to A1 (1.41 and 0.95 octaves, respectively; figure 4.2 B; $p<0.01$, jack-knifed t-test). Tone response latencies were significantly longer in dPEG (25 ms) than in

A1 (15 ms, $p<0.0001$ jack-knifed t-test).

We also compared response properties during presentation of broadband rippled noise (TORCs), commonly used to compute STRFs. We found that dPEG neurons are less likely to phase lock to these stimuli, lowering the likelihood of computing STRFs (figure 4.2 E). We measured phase locking to TORCs as the signal-to-noise ratio (SNR) of the time-varying response to TORCs. SNR values $>$ 0.3 usually allows to estimate interpretable STRFs. We found that, compared to A1, the proportion of dPEG neurons that had SNRs > 0.3 was significantly lower than in A1 (25% vs. 58%; $p<0.001$, jack-knifed t-test). From the subset of dPEG neurons that had SNR values > 0.3, STRFs were likely to be more complex and less compact. To measure how compact STRFs are, we calculated a STRF sparseness index as the ratio of the peak magnitude of the STRF to the standard deviation of all STRF components. Since STRF components in A1 were less variable, A1 STRF sparseness indexes were significantly higher than in dPEG ($p<0.001$, jack-knifed t-test), indicating that dPEG STRFs were less concentrated than A1 STRFs, which are commonly high on a restricted spectrotemporal range.

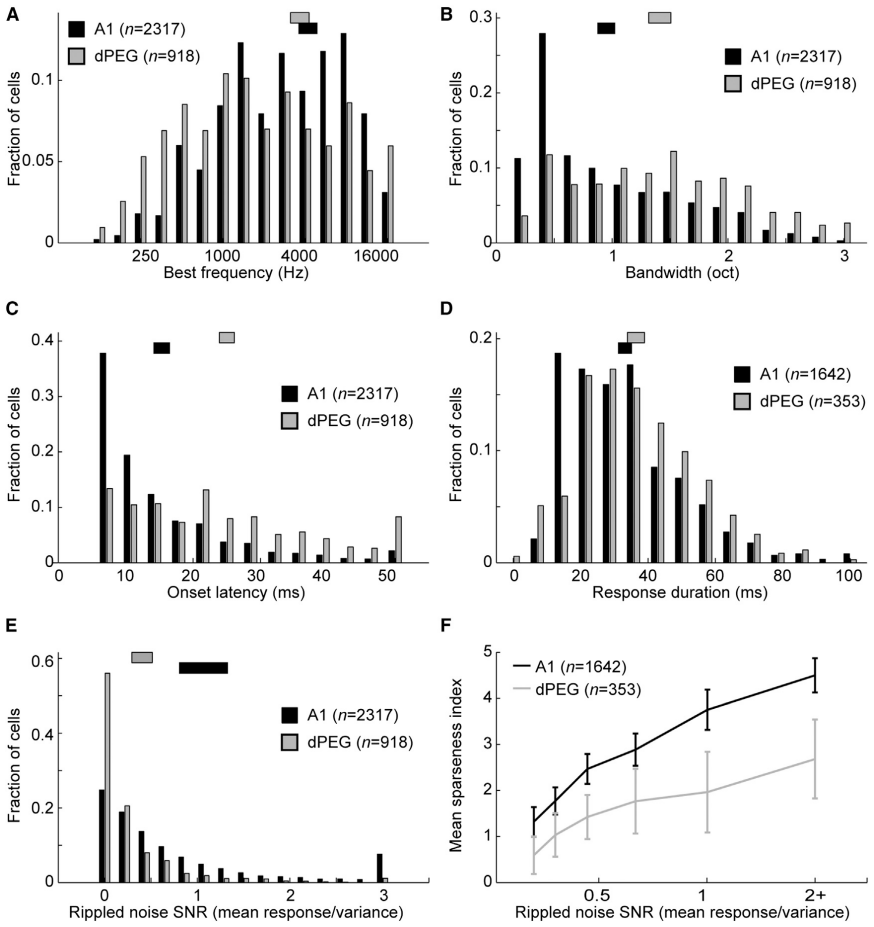

Figure 4.2: **Passive tuning properties of A1 and dPEG neurons.** Histograms plots the fraction of neurons of A1 (black) and dPEG (gray) at the specified values in horizontal axis. Bars at the top indicate 1 SEM around the mean. Plots A, B, C and E include all neurons with measurable auditory evoked responses (A1: N=2,317/2,532, dPEG: N=918/1,130, $p < 0.05$, jack-knifed t-test). Plots D and F only include neurons with significant phase-locking to TORCs, as measured in E (A1: N=1,466, dPEG: N=280, SNR > 0.3). **A:** Best frequency, measured from responses to tones. Mean A1 = 4,330 Hz, mean dPEG = 3,773 Hz, $p > 0.1$, jack-knifed t-test. **B:** Frequency tuning bandwidth measured from responses to tones as octaves at half-height of tuning curve. Mean A1 = 0.95 oct, mean dPEG = 1.41 oct, $p < 0.01$. C: Tone response onset latency. Mean A1 = 25 ms, mean dPEG = 35 ms, $p < 0.0001$. **D:** Duration of sustained response to TORCs. Mean A1 = 33 ms, dPEG = 36 ms, $p > 0.01$. **E:** Signal-to-noise ratio (SNR) of responses to TORCs, measured as trial-to-trial phase locking. Mean A1 = 1.07, mean dPEG = 0.4, $p < 0.01$. **F:** STRF sparseness index, measured as the ratio of peak magnitude to standard deviation of STRF. Since low SNRs can decrease sparseness index values, we plotted mean sparseness indexed binned by SNR. Mean A1 = 2.98, mean dPEG = 1.41, $p < 0.0001$.

4.2.3 Behavior-dependent target enhancement in dPEG responses

The low reliability of dPEG responses to TORCs, together with their low STRF sparseness values made it difficult to compute interpretable STRFs from dPEG responses. Because of this, instead of measuring rapid task-related plasticity of STRFs like has been done in previous A1 studies (Atiani et al., 2009; David et al., 2012; Fritz et al., 2003, 2005), we measured task-dependent changes in the firing rates in response to reference and target sounds.

We compared single-unit spiking activity of 283 A1 neurons and 260 dPEG neurons tested during performance of a conditioned avoidance tone detection task (Fritz et al., 2003, 2010; Heffner & Heffner, 1995) as well as in passive presentation of task stimuli before (pre-passive) and after (post-passive) behavior. 42% (110/260) of dPEG neurons displayed significant ($p < 0.05$, jack-knifed t-test) changes in their PSTH responses to either reference or target. Figure 4.3 shows raster plots and PSTHs of 3 example dPEG single-units where reference (TORC) responses are shown in blue and target (tone) responses in red (mean ± SEM). Neurons in dPEG that showed significant task-dependent response changes varied considerably in their selectivity (figures 4.3 and 4.5), but with a general tendency to increase the contrast between responses to reference and target stimuli, for example, by increasing target responses (figure 4.3 A and C), suppressing reference responses (figure 4.3 B) or both (figure 4.3 A).

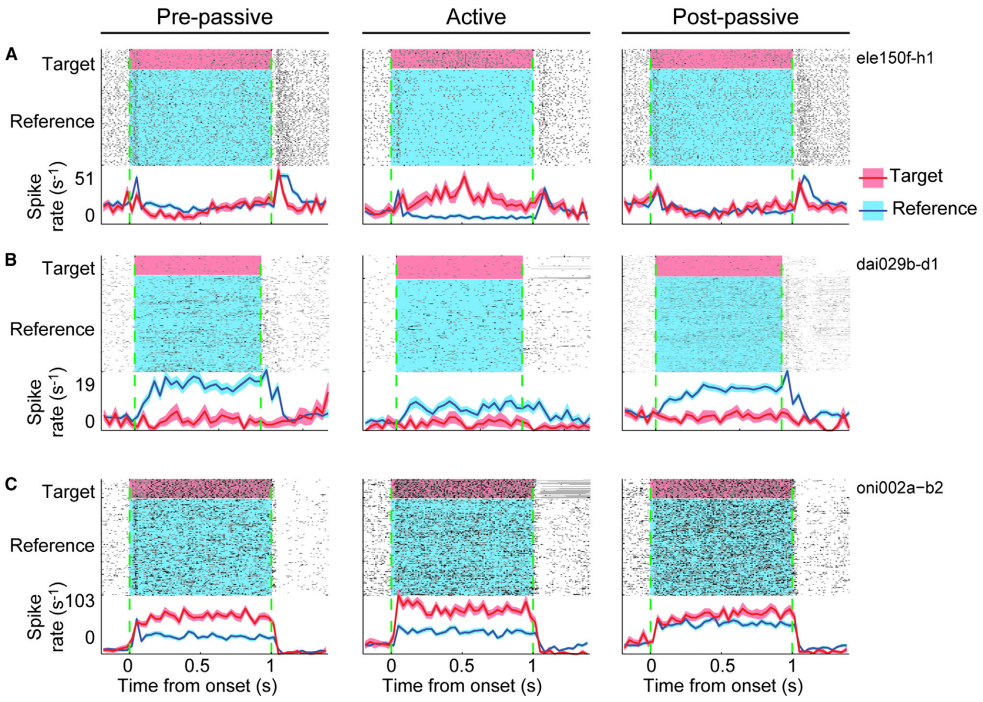

Figure 4.3: **dPEG single-unit responses before, during and after performance of the tone detection task.** Responses to 1 s reference (TORC) stimuli (blue) and 1s target (tone, red) responses (mean ± SEM) are shown before (left column, pre-passive), during (middle column, active) and after (right column, post-passive) performance of the tone detection task. PSTH were computed with a resolution of 50 Hz. Green dashed lines indicate sound onset and offset times. Gray horizontal lines after targets correspond to miss trials in which the ferret failed to stop licking after the target sound and the shock artifacts were removed. **A:** dPEG neuron that in the passive condition responded with transient onset and offset responses, but during behavior reduced reference onset and offset responses and showed a sustained target response. **B:** neuron that responded preferentially to reference sound during the passive presentation of sounds. Response to references was suppressed during behavior. **C:** Neuron that, in the passive condition, presented robust responses to reference and target sounds. During behavior, the target response increased while the reference response was slightly suppressed.

4.2.4 Comparison of target enhancement across the auditory processing hierarchy

In order to understand how the different levels of the processing hierarchy are influenced by attention we compared data from dPEG (N=110) neurons with A1 (N=155) and dlFC (N=266) responses. Population PSTHs were computed by subtracting the spontaneous firing rate to each neuron PSTH, and then normalizing each neuron response by its maximum firing rate and sign. Sign normalization was used to account for a 47% of dlFC neurons that show inhibitory responses upon presence of target sounds.

We found progressively larger behavior-driven changes along the A1, dPEG and dlFC processing chain. In A1 the average target response did not change significantly during behavior, but reference responses were slightly reduced (Figure 4.4 A). The average dPEG responses displayed stronger behavior-driven modulations, with a sustained increase in target response along with suppression of reference response (Figure 4.4 B). The dlFC population response displayed even greater enhancement of target responses during behavior, and showed almost no modulations from baseline firing rate in the responses to reference nor target sounds in the passive condition (Figure 4.4 C).

Similar task-dependent response modulation patterns can be observed in individual neuron responses in the scatter plots of figure 4.5. Firing rate modulations

from spontaneous activity (not normalized in this case) in A1, dPEG and dlFC reflect that the enhancement of response contrast between target and reference sound classes is achieved by suppressing responses to background (reference) sounds and/or increasing responses to foreground (target) stimuli. This is especially clear in the case of dPEG neurons, where a majority of reference responses (left, blue) lie below the diagonal unity line, indicating that passive responses to references were suppressed during behavior and concomitantly, target responses (right, red) show a tendency towards increased responses during behavior. Neurons in dlFC display very weak passive responses to both reference and target sound classes, but compelling increases in target responses during the active state.

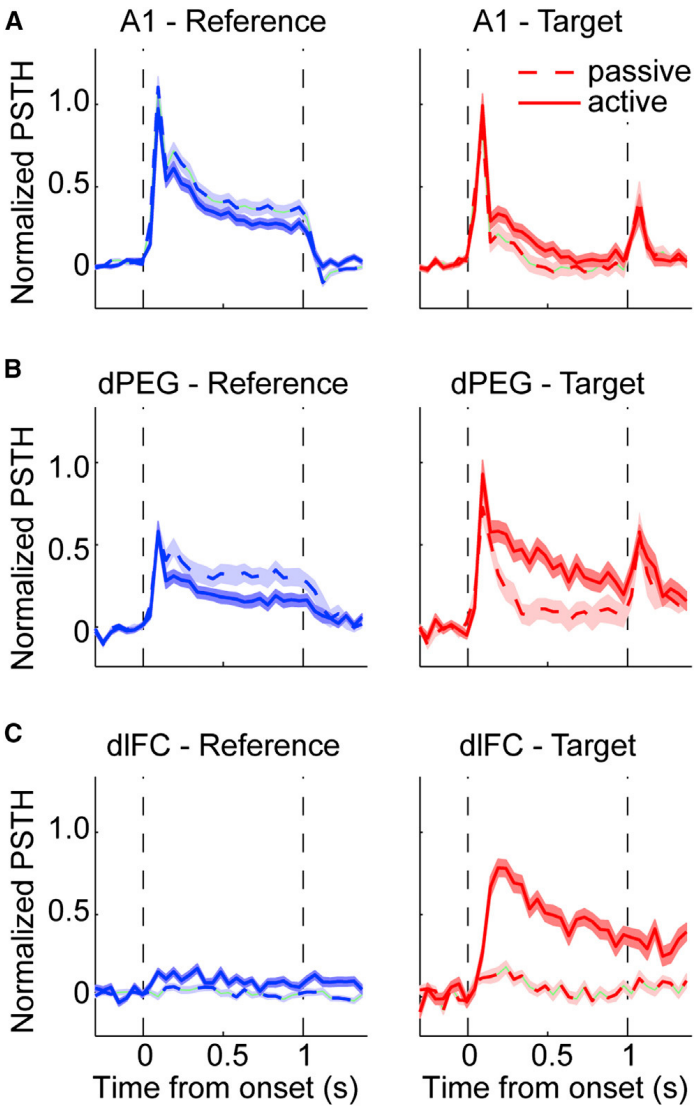

Figure 4.4: **Comparison of task-dependent changes in PSTH responses between A1, dPEG and dlFC.** Left column panels show the normalized PSTH response to reference (blue) stimuli in passive (dashed lines) and active behavior (solid line). Right panels display normalized PSTH responses to target tones in passive (dashed lines) and active behavior (solid line). **A:** A1 PSTH responses (N = 155 neurons significantly modulated during behavior, $p < 0.05$ jack-knifed t-test). The average reference response decreases slightly in these neurons, while average target response did not change significantly during behavior. **B:** dPEG PSTH responses (N = 110 neurons significantly modulated during behavior, $p < 0.05$ jack-knifed t-test). These neurons display a slightly larger suppression of reference responses and an increased average target response. **C:** dlFC PSTH responses (N = 266 neurons significantly modulated during behavior, $p < 0.05$ jack-knifed t-test). Neurons in dlFC consistently responded only to targets during behavior.

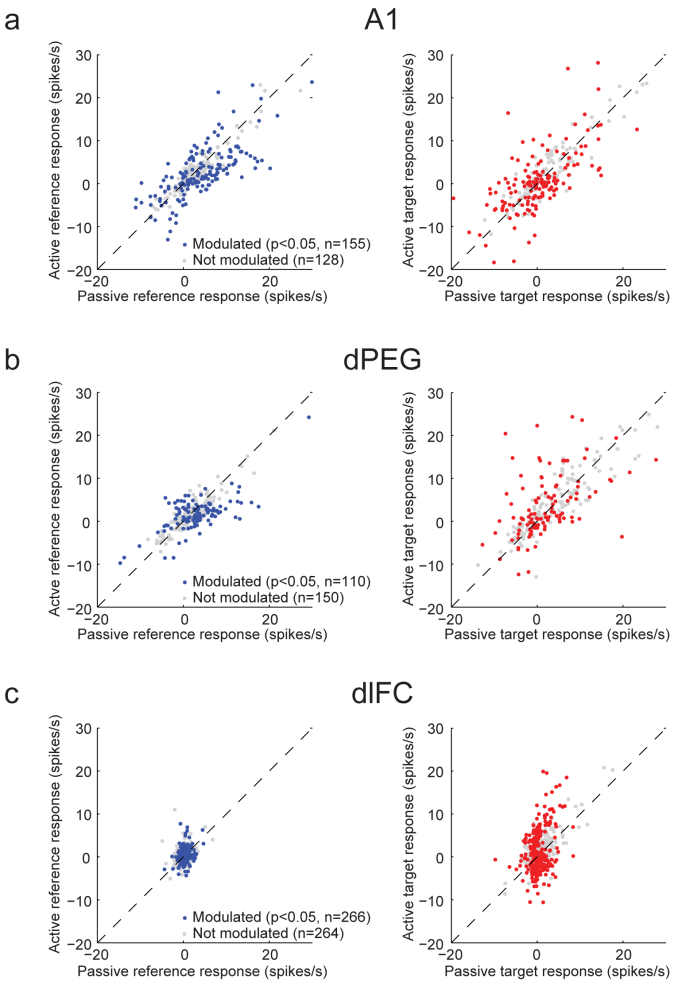

Figure 4.5: **Changes in raw firing rate during behavior in A1, dPEG and dlFC.** Left column plots display the firing rate (spontaneous activity subtracted) for each neuron in the passive and active states in response to reference stimuli. Right column shows passive and active firing rates for each neuron in response to target tones. Blue or red dots indicate neurons with significant modulation of either reference or target response during behavior. Gray dots correspond to neurons that did not change their responses during behavior. **A:** A1 neurons had a slight decrease in their responses to reference stimuli, but did not significantly change their responses to target tones during behavior, as most dots lie in the unity line. **B:** dPEG responses to reference stimuli are clustered below the diagonal, indicating that the majority of dPEG neurons decreased their responses to reference. Target responses (right, red) show a greater tendency to lie above the diagonal, indicating an overall increase in target responses during behavior. **C:** dlFC responses to references are clustered around zero, indicating almost no response modulation either in the passive and active states. Target responses are also clustered around zero in the passive condition, but display large enhanced or suppressed responses during behavior.

Neural responses observed during behavior suggest that dPEG enhances the discriminability of task-relevant sounds by increasing the contrast between responses to reference and target stimuli by either increasing target responses or suppressing reference responses.

In order to quantify changes for individual neurons, we plotted the difference in reference and target responses between the passive (in the abscissa) and active (ordinate) conditions in figure 4.6, left column. If a neuron does not change its target preference during behavior it should lie on the unity slope. A1 neurons display little change in target preference in behavior. In the other hand, most dPEG neurons lie above the diagonal, indicating that the population changes its responses to enhance target representation relative to reference. This target preference enhancement is further increased in dlFC neurons.

The distribution of distances from the unity slope (i.e. the behavior-dependent change in target preference, measured as a target enhancement index: [active r(target) – r(reference)] – [passive r(target) – r(reference)], figure 4.6 right column) in the three areas, indicate that target enhancement gets increasingly larger from A1 to dlFC, as can be seen in the progressively shifted distributions. Since the target enhancement index is computed from normalized firing rates, indices are expressed as fraction of maximum firing rate. In A1, the relative preference for target tones increased 11.9% in the active state, while dPEG exhibited a two-fold increase in target selectivity (21.5%), which was significantly larger than in A1 ($p < 0.01$, jack-knifed t-test).

The shift in target preference for dlFC neurons was of 69.8%, significantly larger than in dPEG ($p < 0.001$, jack-knifed t-test).

4.2.5 Influence of target frequency and neuronal best frequency on plasticity

Since A1 and dPEG are two tonotopic auditory areas that display robust frequency tuning, and the fact that task plasticity in A1 STRFs was shown to depend of the difference between target tone frequency and neuronal best frequency (Fritz et al., 2003), we sought to explore whether contrast enhancement between target and reference responses was dependent on neuronal auditory tuning.

Since we varied the target tone frequency at each experiment, we could measure the dependence of the difference between target frequency and best frequency by plotting the behavior-induced changes in target preference as a function of the difference between each neuron's best frequency and the target frequency tested in the task (figure 4.7 A and B). We found that in both, A1 and dPEG, the target preference change was slightly larger for neurons with best frequencies near the target. We found, however, that in A1 this trend was not significant ($r = -0.08$), but dPEG showed a significant negative correlation ($r = -0.23$, $p < 0.05$, jack-knifed t-test). By grouping target enhancement indexes (behavior-dependent target preference change) by difference between neuron's best frequency and task target

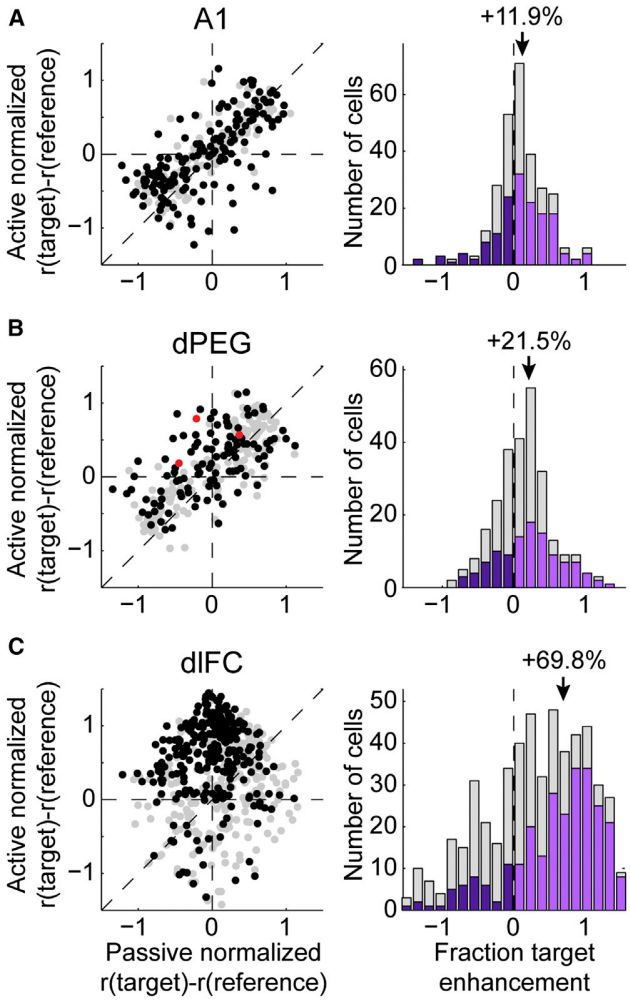

Figure 4.6: **Behavior-driven target preference changes in A1, dPEG and dlFC.** Left compares the average target preference (target minus reference response) for each neuron during passive (abscissa) and active (ordinate) conditions. Units that showed significant behavior-driven changes are plotted in black ($p < 0.05$, jack-knifed t-test). Right panels plots histograms of the change in the relative target preference caused by behavior (i.e. active target preference passive target preference). Dark/light purple bars correspond to neurons that underwent significant decrease/increase in target preference. The average change in target preference in A1 (panel A) was 11.9%, dPEG (panel B) = 21.5% and dlFC (panel C) = 69.8%. Red dots in panel B correspond to the example single-units shown in figure 4.3.

frequency (figure 4.7 C) we found that target enhancement in both A1 and dPEG were particularly large for neurons with best frequencies less than one-quarter of an octave from the target tone frequency. To understand how reference and target responses contribute to the relative target enhancement we compared average changes in responses to reference/target sound categories in relation to the target and best frequencies difference (figure 4.7 D). We found that in A1, only neurons with best frequencies less than 0.15 octaves away from target frequency showed significant increases in target responses ($p < 0.05$, jack-knifed t-test). In the other hand, dPEG showed significant target enhancements in a larger pool of neurons formed by all neurons tuned less than 0.8 octaves from target frequency ($p < 0.01$ for both < 0.15 and < 0.8 octave groups, jack-knifed t-test). This suggests that A1 and dPEG neurons enhance target responses more for target frequencies near the neuron's best frequency, but dPEG target enhancements are less restricted to the neuron's best frequency than A1. Figure 4.7 E shows that reference response suppression contributes to behavior-driven target enhancement, but it does not depend on the neuron's tuning.

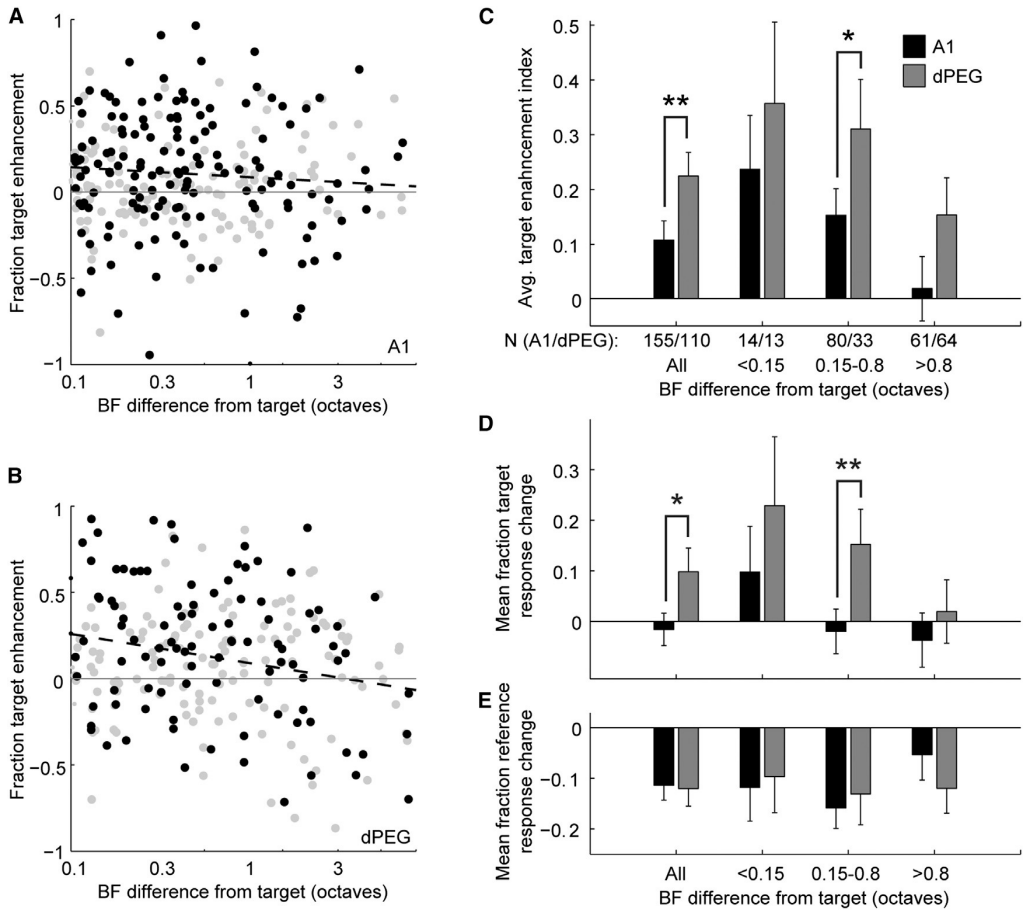

Figure 4.7: **Influence of neuronal tuning in behavior-related plasticity.** **A:** Behavior-related change in target preference for each A1 single-unit (ordinate axis) plotted as a function of the difference between target tone frequency and neuron's best frequency (abscissa). Black dots correspond to units that underwent significant response changes during behavior (N=155/283). Dashed line displays a weak (not significant) tendency for higher target enhancements for neurons with tuning near the target frequency ($r = -0.08$, $p > 0.05$ jack-knifed t-test). **B:** Scatter plot of target preference changes for dPEG neurons, plotted as in A (N=110/260 significantly modulated neurons, $r = -0.23$, $p < 0.05$, jack-knifed t-test). **C:** Average target enhancement index of A1 and dPEG neurons grouped to three ranges of differences between best frequency and target frequency. In A1 and dPEG, target enhancements were slightly larger for neurons with best frequencies near to target frequency (<0.15 octave difference). Target enhancement was significantly larger in dPEG than A1 neurons for differences >0.15 octaves (*= $p < 0.05$, **=$p < 0.01$, jack-knifed t-test). Continues in next page...

D: Average target response fraction change for A1 and dPEG neurons, plotted as in C. A1 neurons increased their target responses significantly only in the group of neurons with best frequencies < 0.15 octaves away from the target frequency. In the other hand, increases in target responses were greater in dPEG also in the range of neurons with best frequencies $0.15 - 0.8$ octaves from target frequency, which suggests that a larger pool of neurons contribute to target enhancement in dPEG than in A1. **E:** Average fraction change in reference responses for A1 and dPEG neurons. Reference responses were decreased during behavior regardless of the neuronal tuning and its difference with the target tone frequency.

4.2.6 Tuning changes driven by task-related plasticity

Since dPEG neurons display poor phase-phase locking to rippled noises (TORCs) we were unable to measure spectrotemporal tuning changes during behavior. We tested a subset of dPEG neurons (N=55) with a slightly modified version of the tone detection task, in which the reference broadband TORCs were replaced with narrow band noise bursts (1/8 – 1/2 octave bandpassed noise) centered at diverse frequencies spanning $4 - 5$ octaves.

Data collected using this stimulus showed a similar pattern of target enhancement as when TORCs were used as references. Using this task paradigm, we were able to estimate the frequency tuning of dPEG neurons by pooling responses to the reference bandpassed noise. We noticed that the relative enhancement of target responses results from a general decrease in responses that affect less the range of task-relevant frequencies in a neuron's receptive field, which is consistent with findings from previous studies (Atiani et al., 2009; Otazu et al., 2009). As can be seen in figure 4.8, tuning is shifted towards the target frequency by suppressing responses across the receptive field, but suppressing less the responses at the range of the task-relevant frequency. References away from the target frequency were significantly more suppressed than references near the target tone (figure 4.8 C and D, $p < 0.01$, jack-knifed t-test). This suggests that during active detection of a task-relevant frequency, dPEG neurons relatively enhance the response to that fequency by globally suppressing its responses, but sparing the frequency region near the tar-

get. This might be the same mechanism that accounts for STRF enhancement at the target frequency reported in A1 studies (Atiani et al., 2009; David et al., 2012; Fritz et al., 2003, 2005).

4.3 Discussion

We recorded in two tonotopically organized auditory fields in the dPEG that lie ventrally adjacent to the primary auditory cortex. A recent study of cortico-cortical connectivity in ferret auditory cortex described that dPEG is strongly connected in a frequency specific way with A1, suggesting that dPEG fields constitute a second stage in cortical processing after A1 (Bizley et al., 2015). Additionally, it has been preliminarily reported that dPEG fields receive thalamic input from the ventral division of the MGB (similarly to core auditory fields), but also from the non-lemniscal dorsal and medial MGB subdivisions (Bizley et al., 2015, 2005). This neuroanatomical evidence, together with the passive tuning properties described in this and previous studies (Bizley et al., 2005) strongly suggests that dPEG can be considered a belt or secondary auditory area in the ferret auditory cortex.

In this study we expanded on previous findings demonstrating that A1 neurons can undergo rapid spectral and temporal adjustments of their tuning properties to enhance the representation of task-relevant sounds by recording from belt auditory areas in awake ferrets performing on the same auditory task originally used to

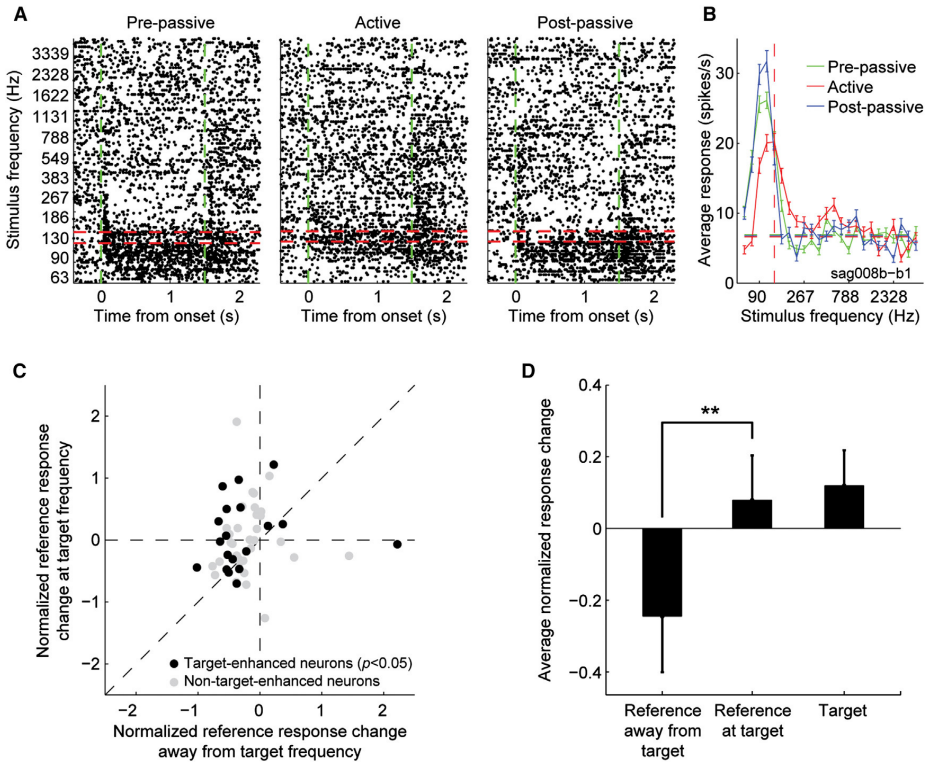

Figure 4.8: **Selective suppression of responses reshape tuning curves of dPEG during behavior. A:** Raster plots of reference responses for an example unit in the pre-passive, active behavior and post-passive conditions. Red horizontal lines indicate the noise band centered at the target frequency (1/4 octave bandpassed noise). Responses were overall suppressed during behavior, but suppression was weaker at the band centered to the target frequency. **B:** Tuning curves for the pre-passive, active and post-passive conditions, measured from the average firing rate of the single-unit shown in A, during the duration of noises (from sound onset to sound offset). There was a general suppression in firing rate that shifted the peak of the tuning curve measured in the active condition towards the target tone frequency (marked with a vertical dashed line). Horizontal dashed line indicates the spontaneous firing rate. **C:** Comparison of average response change of reference responses for each neuron at target frequency (ordinate axis) versus average change of reference responses at frequencies away from the target frequency (abscissa) showing a significant enhancement at the target frequency ($p < 0.02$, jack-knifed t-test). Note that most dots lie above the diagonal line, indicating that reference responses at the target frequency were enhanced relative to references away from target frequency. Black dots are neurons that showed significant behavior-related response changes (N=19/55, $p < 0.05$, jack-knifed t-test). **D:** Average response change from the 19 modulated neurons in C. Error bars indicate 1 SEM, ** = $p < 0.01$, jack-knifed t-test).

describe rapid task-dependent plasticity of STRFs in A1 (Fritz et al., 2003). We compared dPEG behavior-dependent response modulations with those of A1 and dlFC, and we conclude that dPEG is an intermediate stage in the auditory cortical processing hierarchy between primary auditory cortex and higher-order areas belonging to the attentional network.

Our main finding is that dPEG enhances task-relevant responses in the active attentive state by selectively increasing its responses to target stimuli (foreground) while concomitantly suppressing responses to distractor references (background). We found that the magnitude of this enhancement in greater than what is found in A1 neural responses, but less than in dlFC responses. This pattern of distractor suppression and selective target representation enhancement, suggests that top-down control circuits might influence antecedent areas in the sensory hierarchy by progressively suppressing background information and enhancing the extraction of task-relevant stimulus features (Ahissar et al., 2009).

Similar hierarchies of attentional modulation of cortical sensory responses have been reported in the visual system, where attentional enhancement of task-relevant stimuli becomes greater (Buffalo et al., 2010; Kastner & Pinsk, 2004; Maunsell & Cook, 2002; Maunsell & Treue, 2006) and earlier (Buffalo et al., 2010) in the visual cortical processing chain, which suggests that top-down biases of sensory representations occur first in higher-order sensory areas and later in earlier stages. Differential effects of attention have been reported as well in the processing hierarchy of the so-

matosensory system, with increasing proportions of responses in higher-order areas covarying with tactile perception judgments (de Lafuente & Romo, 2006).

In the auditory system, a few studies have reported on the influence of attention on non-primary auditory areas. The general finding is that higher-order auditory areas change their receptive fields to a greater extent or with a different quality than A1 in order to better encode the attended stimuli (Diamond & Weinberger, 1984; Mesgarani & Chang, 2012; Niwa et al., 2013; Polley et al., 2006; Tsunada et al., 2011). Belt areas might then encode more complex receptive fields in passive states, but also have more plastic representations that can be largely sculpted by top-down influences in order to extract sound features that become relevant in a given behavioral context. A compelling correlate of attentional enhancement of feature extraction was recently reported in a human study, where speech reconstructed from non-primary auditory cortex responses in a multi-talker context faithfully resembled the salient spectrotemporal features of the attended speech, as if the subjects were listening to that speaker alone (Mesgarani & Chang, 2012). Our results are consistent with such results, since we observed a suppression of the responses to distractor sounds and a relative enhancement in the task-relevant sounds.

Since our results provide a direct comparison of responses at three stages of the auditory processing hierarchy tested in identical behavioral conditions, our findings suggests that the auditory system might have a similar functional hierarchical organization to that of the visual and somatosensory systems, in which the primary areas

provide literal information about sensory inputs and then, in following stages, irrelevant background information is gradually suppressed while behaviorally-relevant information is preserved on its way to higher-order executive centers. However, it is still not well understood how auditory representations are transformed in this hierarchy from veridical to abstract meaning. Neurons in dPEG were similar to dlFC in that the salient stimuli evoked greater responses in the active state, but were as well similar to A1 neurons in that there were robust responses to sounds in the passive state. These dual properties are consistent with a role of dPEG as an area of converging bottom-up and top-down influences, functionally intermediate between A1 and dlFC. Because of the difficulty of computing robust receptive field estimations from non-primary auditory area responses, it is not well understood yet what sound features are encoded in belt auditory areas. Our data, however, suggests that task-relevant stimuli representations begin to emerge in the auditory ascending pathway responses.

Chapter 5: Task-related plasticity in tertiary auditory cortex of the ferret

5.1 Introduction

The auditory cortex of ferrets (*Mustela putorius furo*) is composed of several acoustically sensitive adjoining areas in the ectosylvian gyrus of the temporal lobe (Bizley et al., 2005). As in other species (Figure 1.4 and 5.1), these areas are classified as primary (or core) or non-primary (or belt and parabelt) depending on the pattern on their input projections from auditory thalamus and their cortico-cortical connectivity.

Areas A1 and AAF in the Medial Ectosylvian Gyrus (MEG) receive innervation primarily from the ventral MGB, and are, thus, considered primary (or core) auditory areas. Both, A1 and AAF are tonotopically organized, displaying greater responses to low frequencies ventrally and to high frequencies dorsally. Ventral to MEG, the Posterior Ectosylvian Gyrus (PEG) contains several non-primary cortical areas. The posterior pseudosylvian field (PPF) and posterior suprasylvian field (PSF) are two moderately tonotopically organized fields in the PEG which are

thought to be analogues to primate belt areas (Chapter 4 and Atiani et al., 2014; Bizley et al., 2005). PPF has been found to under represent low frequencies, while PSF is dominated by cells representing high and low frequencies, with sparse units tuned to intermediate frequencies (Bizley et al., 2005). We have grouped these fields under the name dorsal PEG (dPEG) because of their similarities in neurophysiological response properties, and to distinguish them from ventral areas in the PEG (Atiani et al., 2014).

The dPEG fields display some tonotopic organization, with better responses to low frequencies near the dorsal border which adjoins the low frequency area of A1, and also sharing a low frequency area between PPF and PSF. The dPEG fields show better responses to high frequencies away from both low frequency borders, that is, PPF displays a antero-ventral to postero-dorsal high to low frequency gradient, while PSF a postero-ventral to antero-dorsal high to low frquency tonotopy (see figure 5.1).

The Anterior Ectosylvian Gyrus (AEG) lies rostro-ventral to the MEG, and is separated caudally from the dPEG by the pseudosylvian sulcus (PSS). The AEG contains two auditory-responsive fields, the anterior dorsal field (ADF) and the anterior ventral field (AVF). Not much is known about these fields, but its neurons display poor (or no) frequency tuning and little or no tonotopical organization (Bizley et al., 2005).

The most ventral regions of the PEG are, to date, the least studied portion of the ferret auditory cortex. This ventral area can be divided into three ventral posterior (VP) fields, rostral, ventral and caudal VP (VPr, VPv and VPc, respectively). Additionally, rostral and ventral to area PPF and dorsal to VPr, a transition area between PPF and PSSC (the cortex of the PSS) called pro-PPF has been described (Atiani et al., 2014). In the PSS, between PEG and AEG, the Pseudo-Sylvian Sulcal Cortex (PSSC) is an area that shows responsiveness to acoustical stimulation and also receives somatosensory and visual inputs (Ramsay & Meredith, 2004).

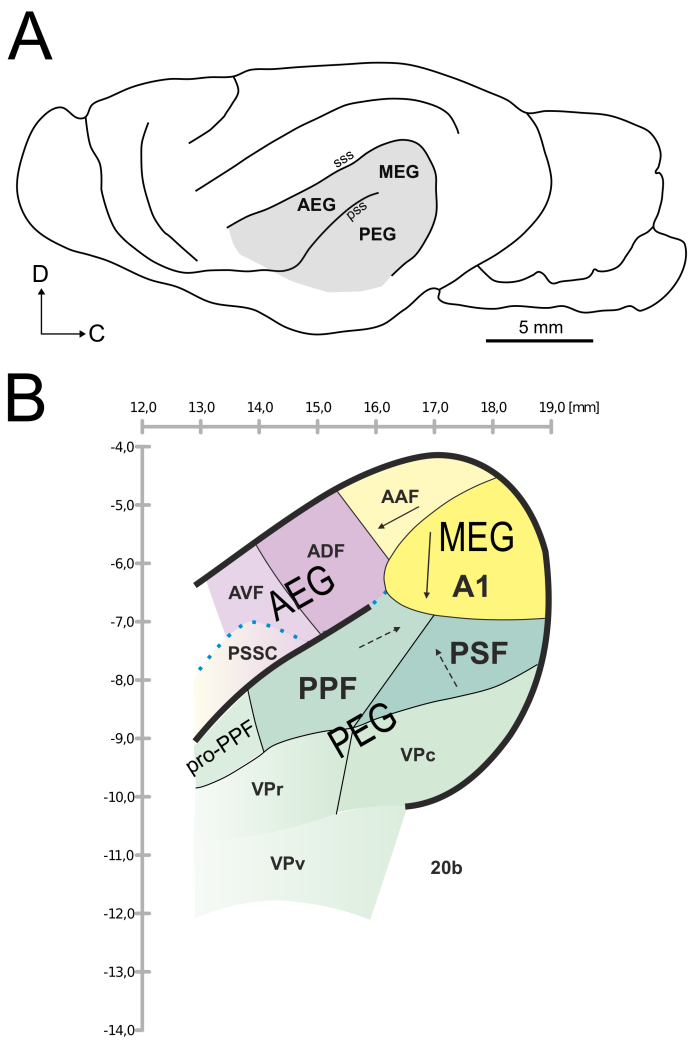

Figure 5.1: **The auditory cortex of the ferret. A:** Location of the auditory cortex in the Ectosylvian Gyrus (shaded gray). **B:** Auditory fields of the MEG (yellow), AEG (violet) and PEG (green). Arrows describe the tonotopy from high to low frequencies; solid arrows indicate clear tonotopy, dashed arrows indicate weak tonotopy. Pseudo-Sylvian Sulcal Cortex (PSSC) is displayed lateralized for clarity. B: Adapted from Atiani et al. (2014)

A recent study (Bizley et al., 2015) described for the first time the cortico-cortical connectivity of the auditory fields of the ferret (Figure 5.2). This study revealed that core areas A1 and AAF are reciprocally connected with PPF and PSF areas of the PEG in a frequency specific manner, which would explain the tonotopy observed in the dPEG. Conversely, connections from core areas to the ADF in AEG were scattered, which is consistent with its non-tonotopical organization. Virtually no connections were found between core areas and non-tonotopic areas VP, AVF and PSSC (Bizley et al., 2015). Anterograde and retrograde injections in the dPEG revealed reciprocal connections with VP, AEG and MEG. The AEG area ADF is connected with the core areas AAF and A1 in the MEG, and with areas PSF, PPF in dPEG. In contrast, AVF is connected with virtually all auditory cortex areas including AAF and A1 in the MEG, and with PSF, PPF and VP in the PEG and also with the PSSC. Bizley et al. (2015) connectivity evidence of strong connectivity of core areas with non-primary areas PPF, PSF and ADF suggests that these areas constitute a secondary stage in the auditory information flow from core areas in the MEG, A1 and AAF. Thus, dPEG areas PPF and PSF, along with AEG area ADF may be analogous to primate belt areas. Also, the lack of connectivity of core areas with VP areas, AVF and PSSC, coupled with the prominent connectivity of VP, AVF and PSSC with belt areas dPEG and ADF, suggests that these higher auditory fields (VP, AVF and PSSC) may form a third stage in the auditory cortical hierarchy of the ferret, and might be considered to be analogous to parabelt areas described in primates.

Interestingly, Bizley et al. (2015) also found that A1 is more strongly connected with posterior fields in the PEG than areas in the AEG, while AAF presents stronger connectivity with the anterior field ADF. This suggests that there might be two major parallel streams in the information flow in the ferret auditory cortex, an anterior stream starting from AAF and continuing along the AEG, and a posterior stream starting in A1 projecting into the PEG. Clearly there is some interaction and connectivity between the two streams, but it is possible that these two major streams may resemble the dorsal and ventral ('where' and 'what') streams proposed in the auditory systems of cats (Lomber & Malhotra, 2008), primates (Tian et al., 2001) and humans (Alain et al., 2001; Arnott et al., 2004; Maeder et al., 2001).

To date, the connectivity of ferret auditory cortex with auditory-related areas beyond the ectosylvian gyrus has not been thoroughly studied. Bizley et al. (2006) described reciprocal connections between auditory fields and visual, parietal and frontal cortices. They found that primary fields A1 and AAF are connected with adjacent fields and other sensory cortices (visual and somatosensory) with a higher tendency of targeting primary areas, while AEG and PEG fields tended to send and receive more projections from higher, rather than primary, sensory and multisensory areas. Interestingly, they described reciprocal connectivity between non-primary fields in PEG/AEG and the frontal lobe, specifically between the PEG and the anterior sigmoid gyrus and between the AEG and anterior and posterior sigmoid gyri. They reported, as well, direct connections from MEG to the frontal lobe, specifically in the ventral orbital gyrus and dorsal anterior sigmoid gyrus, but de-

scribe these direct connections as more sparse than those seen between non-primary areas and frontal areas.

Ventral areas of ferret auditory cortex, specifically the PSSC, have been shown as well to receive inputs from primary sensory cortices of the visual and somatosensory modalities (areas V1 and SI respectively); with inputs from somatosensory cortex being clustered at the anterior bank of the PSSC and visual inputs from V1

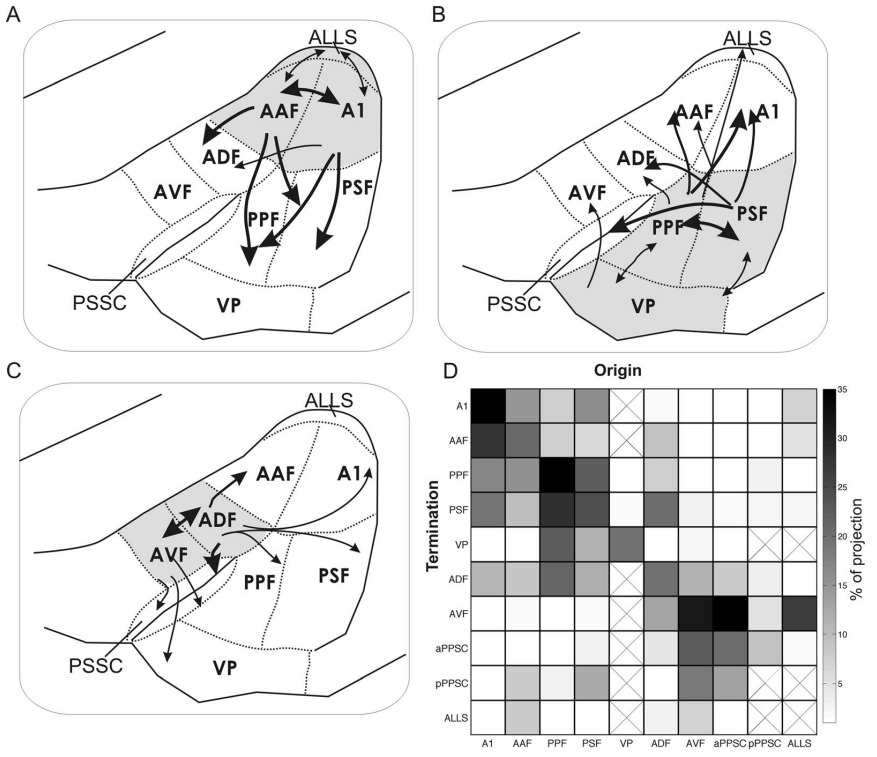

Figure 5.2: **Cortico-cortical connectivity in the auditory cortex of the ferret** revealed through the injection of anterograde and retrograde tracers in MEG (panel **A**), PEG (panel **B**) and AEG (panel **C**). **D:** Summary of projections observed, 'X' indicate areas that were not targeted with injections. Note that in this study PSSC was divided into its anterior (aPSSC) and posterior (pPSSC) banks, and VPr, VPc and VPv were consolidated into area VP. From Bizley et al. (2015).

in the posterior bank of the PSSC (Ramsay & Meredith, 2004). This suggests a role of the PSSC in multisensory integration.

More recently, Radtke-Schuller et al. (2011) further studied the connectivity of frontal cortices with auditory areas. By injecting anterograde and retrograde tracers in dorso-lateral frontal cortex (dlFC), specifically in the proreal gyrus and anterior sigmoid gyrus, they described reciprocal connectivity between these dlFC areas and non-primary auditory fields. Interestingly, no direct connections were found between dlFC and primary fields A1 and AAF, and the connections found between dlFC and belt/parabelt areas were more numerous in the ventral-anterior fields of the PEG (VPr, pro-PPF) and, specially, in the PSSC in its anterior and posterior banks and in the depth of the sulcus. These findings are consistent with results in primates (Hackett et al., 1998a; Romanski et al., 1999b) and cats (Clascá et al., 2000; Lee & Winer, 2008) that indicate that auditory-frontal bidirectional connectivity occurs mainly in belt and parabelt areas and are sparse or absent in core auditory areas.

This interconnection of the auditory cortex with higher centers in the frontal cortex might be the substrate for the attention-dependent changes that have been described in the auditory system (discussed in Chapter 1). To investigate the influence of dlFC in auditory responses in A1, Fritz et al. (2010) performed simultaneous recordings in dlFC and A1 in ferrets performing auditory discrimination tasks. They reported a decrease in the inter-areal coherence in the local field potentials (LFP) in the frequency range between 10 and 20 Hz. This desynchronization in frontal-

auditory activity was found to be greater for A1 sites with best frequencies close to the tone target used in the task. They hypothesized this decorrelation in the field potential could indicate a release in an inhibitory control of dlFC over A1 at the target frequency. The current anatomical evidence on ferret auditory and frontal connectivity, while still preliminary, suggests that higher auditory areas might be affected by activity in the frontal lobe.

This study aimed at clarifying how higher-order auditory cortex represents sounds and how these representations change when a sound class becomes behaviorally relevant. We hypothesize that higher-order auditory cortex lies at a pivotal stage in the transformation of auditory representations from purely acoustical -at lower auditory levels- to purely abstract sound meaning at higher centers, such as the frontal cortex. This hypothesis is partly motivated by the general finding from anatomy that belt and parabelt auditory areas are more connected to higher auditory-related areas than core auditory fields.

In this study, we recorded in ventral areas of the PEG of ferrets, specifically, in areas VPr, PSSC and pro-PPF, which have been shown to be directly connected with dlFC (Radtke-Schuller et al., 2011). For clarity, we have grouped these areas together as ventral-anterior PEG (vaPEG). In some experiments, simultaneous recordings in dlFC and vaPEG were performed in order to assess inter-areal functional connectivity. The present results strongly suggest that VPr, pro-PPF and PSSC areas constitute a higher processing stage than A1 and dPEG, and that as such,

neurons in vaPEG exhibit longer latencies, broader frequency tuning bandwidths and overall weaker auditory responsiveness during passive presentation of sounds. Nonetheless, vaPEG neurons can also display compelling behavioral-meaning or goal directed responses during active auditory behavioral tasks, similarly to what has been seen in dlFC (Fritz et al., 2010). We also note vaPEG neuronal responses to non-auditory, task-related information (reward timing, expectations) during task performance, which were very similar to responses previously described in dlFC.

5.2 Results

In order to study how responses to relevant sounds evolve along the auditory cortex stages, we recorded from areas VPr, pro-PPF and PSSC (grouped under the name vaPEG, ventral anterior Posterior Ectosylvian Gyrus) and compared its responses with data previously recorded from A1, dPEG and dlFC. Cortico-cortical connectivity (Bizley et al., 2015) suggests that areas in vaPEG correspond to tertiary (parabelt) stages in the auditory cortex after A1, the primary auditory cortex and dPEG belt fields PPF and PSF. Neurons in vaPEG were tested in passive listening conditions (n=418, 4 animals) and during active behavior (n=475), 4 animals).

5.2.1 Anatomy

In order to locate vaPEG, we first mapped out the earlier areas in MEG and dPEG. In each hemisphere we performed neurophysiological recordings in A1, and then in dPEG in order to find the tonotopic gradient as a roadmap (already described for A1 and dPEG fields by (Bizley et al., 2005). We determined that vaPEG was located ventral to the high frequency area of PPF, and transition from PPF to vaPEG was typically marked by an abrupt change in neuronal responses during passive presentation of tones. While cells in ventral-rostral PPF responded to high-frequency tones, in vaPEG some cells showed poor or no responses to any tones, whereas other cells that were responsive to tones often showed very broad and flat tuning over $5 - 8$ octaves (in the range 100 Hz 25 kHz). Sometimes, neurons in vaPEG showed broad frequency responses towards low frequencies.

After several months of recording in locations presumed to be vaPEG, we placed iron deposits and electrolytic lesions to confirm the relative location of the recordings post-mortem (Figure 5.3. The relative locations of electrode penetrations on the brain surface were also recorded so we could later co-register and align the location of the recording sites in vaPEG relative to the histological markings. We found that the majority of the recordings were performed in areas VPr, PSSC, proPPF and PPF, and this allowed us to re-label cell locations accordingly.

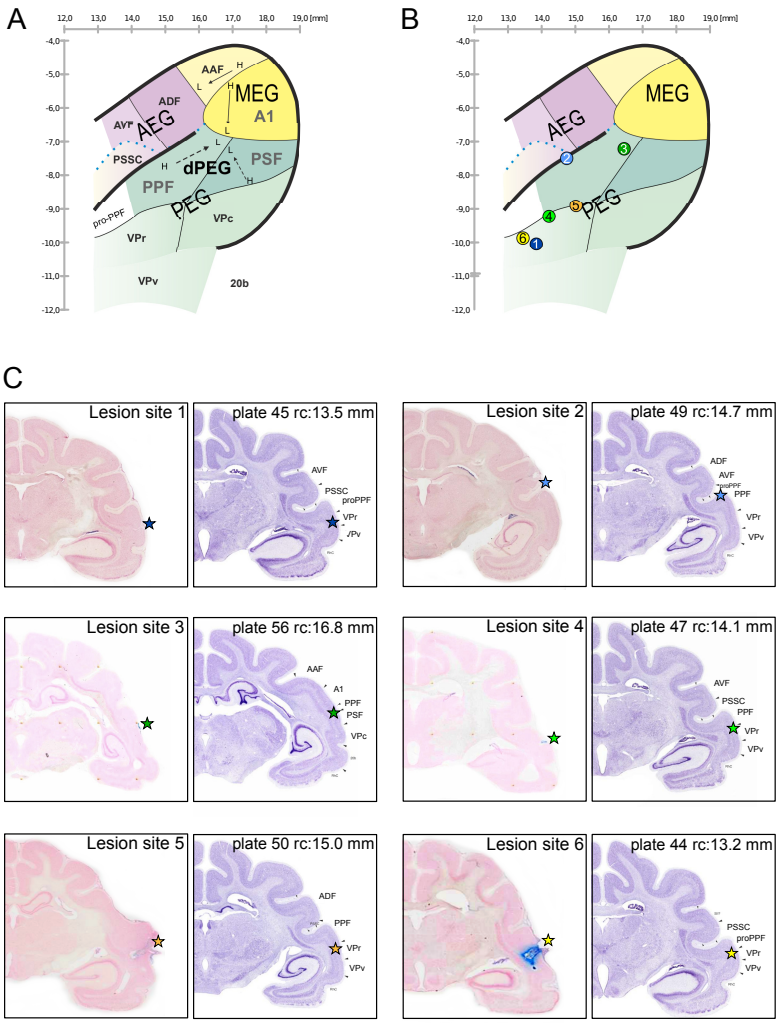

Figure 5.3: **Location of markings placed in the vicinity of recording locations in 3 animals, 6 hemispheres. A:** Fields constituting the auditory cortex of the ferret. **B:** Summary of the locations of the markings on the surface of the brain, numbers and colors correspond to those in C. **C:** Lesion/marking sites (left) and corresponding atlas plates (Ferret brain atlas kindly provided by Dr. Sussane Radtke-Schuller). Left panels display the slice with the markings stained with Prussian blue in order to label ferrous deposits. Not all iron deposit procedures were successful: lesion sites 1 and 2 show no iron staining, but clear electrolytic lesions. Right panels display the atlas plate corresponding to the location of the lesion or marking. Markings were done in six hemispheres (3 ferrets) whose auditory cortex was neurophysiologically mapped (left hemispheres n = 3 and right hemispheres n = 3). Each row corresponds to one ferret. Left half correspond to the left hemisphere. In order to facilitate comparison between lesion sites and atlas plates, right hemisphere photographs were flipped.

5.2.2 Passive auditory tuning properties

We tested vaPEG neurons passive tuning properties by presenting awake ferrets with tone pips (100 ms) of random frequencies spanning 6-8 octaves and 3 s TORCs (see methods in Chapter 2). When compared to A1 and dPEG neurons (Figure 5.4 and 5.5), we found that neurons in vaPEG displayed, overall, weaker responses to tones and TORCs, and no clear tonotopic organization. Continuing with the trend seen from A1 to dPEG (Chapter 4), vaPEG neurons display even more extreme values in most of the parameters measured. Similarly to A1 and dPEG, the distribution of best frequencies (BFs) largely overlapped, but with a significant tendency towards more representation of low frequencies (Kruskal-Wallis non-parametric analysis of variance [ANOVA], $p < 0.05$), since there was a number of cells that displayed broad tuning to low frequencies (Figure 5.4, A). Neurons in vaPEG had significantly broader tuning than those in dPEG and A1 (Figure 5.4, B), with an average bandwidth of 1.82 ± 0.056 octaves ($p < 0.001$ Kruskal-Wallis ANOVA, Bonferroni correction).

Tone response latencies were also significantly longer in vaPEG neurons than in A1 and dPEG, with a mean latency of 35 ± 1.7 ms (compare to 15 ± 0.5 and 25 ± 0.7 ms in A1 and dPEG, respectively, figure 5.4 C). Latency differences between A1, dPEG and vaPEG were significant (Kruskal-Wallis ANOVA, $p < 0.001$, Bonferroni correction).

Responses to TORCs showed longer sustained responses (Figure 5.4, D) and, similarly to what was found in dPEG neurons, followed the envelope of TORCs less reliably than A1, as measured with the SNR metric (Figure 5.4, E). The proportion of vaPEG neurons that had an SNR > 0.2 was 25.8% (n=108/418), which is less to what was found in A1 (65.18%, n=1651/2533) and dPEG (31.59%, n=357/1130). We also measured the STRF sparseness as a ratio of peak STRF magnitude to the mean amplitude over all spectrotemporal bins to assess the sharpness of the computed STRFs (Figure 5.4, F). TORC response durations, TORC SNR and sparseness ratio were significantly different from those from A1 and dPEG neurons (Kruskal-Wallis ANOVA, Bonferroni correction, $p < 0.05$). Higher sparseness index values are related with sharply tuned STRFs in which a clear peak can be isolated from the background. Most vaPEG neurons displayed highly complex STRF patterns, with no clear spectrotemporal peak, which is consistent with the lower values of STRF sparseness in this area compared to A1 and dPEG neurons. These low SNR and STRF sparseness index values made very difficult to compute interpretable STRFs from vaPEG neurons. A small number of vaPEG neurons displayed relatively high SNR values, but uninterpretable STRFs. Figure 5.5 summarizes the data displayed in figure 5.4, comparing basic tuning properties among A1, dPEG and vaPEG (mean + SEM). The relative broader tuning and increased latencies in responses to tones in vaPEG neurons, as well as the difficulty for computing lineal STRFs from these neurons are consistent with our hypothesis that vaPEG is part of a higher cortical processing stage than A1 (core) and dPEG (belt).

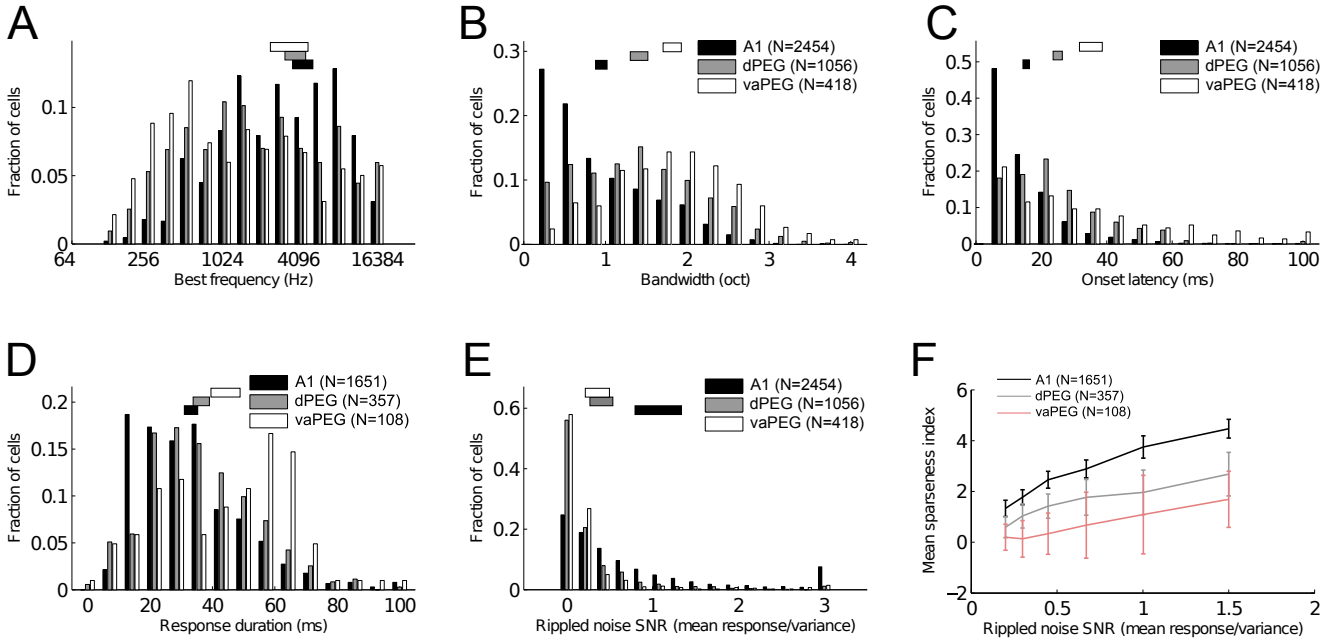

Figure 5.4: **Basic tuning properties in areas A1, dPEG and vaPEG.** Tuning parameters were measured from responses to tones (A, B and C) and to TORCs and resultant STRFs (D, E and F). Bars at the top of every histogram indicate mean1 SEM in the corresponding color (A1: black, dPEG: gray, vaPEG: white). **A:** Distribution of neurons best frequency. Neurons with measurable auditory responses were included (A1: n=2454/2533, dPEG: n=1056/1263, vaPEG: n=418/742; $p < 0.05$, jackknifed t-test). **B:** Bandwidth of frequency tuning measured as octaves at half-height of tuning curves. **C:** Response latency measured from the PSTH in response to all tones presented in passive tuning assessment. Latency was considered as the time at the first bin significantly modulated from baseline after tone onset ($p < 0.05$, jackknifed t-test). **D:** Sustained response duration measured from the PSTH in response to TORCs. Only neurons with phase-locking (SNR) > 0.2 were considered (A1: n=1651/2533, dPEG: n=357/1130, vaPEG: n=108/418). **E:** Signal-to-noise ratio (SNR) measured as the trial-to-trial phase locking to TORC stimuli. All neurons with measurable auditory responses were included (A1: n=2454/2533, dPEG: n=1056/1263, vaPEG: n=418/742; $p < 0.05$, jackknifed t-test). **F:** STRF sparseness index, measured as the ratio between peak magnitude and mean magnitude from STRF estimations. Only neurons with SNR values > 0.2 were included. Since low phase-locking values can affect the sparseness index, we display the sparseness index binned by SNR values.

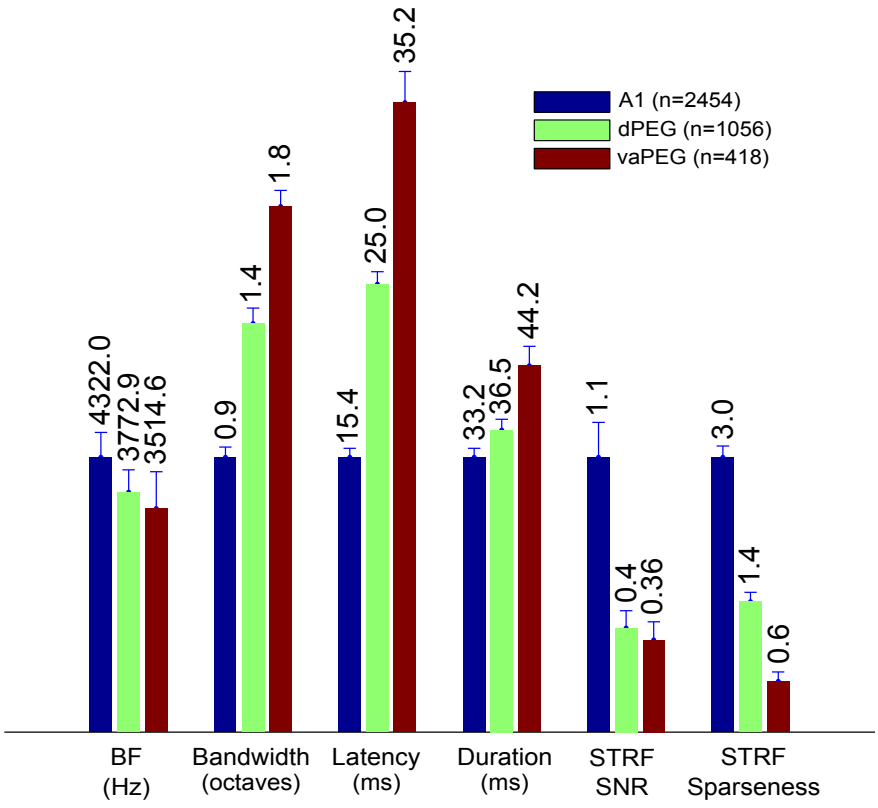

Figure 5.5: **Summary comparing basic tuning properties in areas A1, dPEG and vaPEG.**

5.2.3 Behavioral performance

Before implant surgery, ferrets were trained in both tasks in a test sound-proof booth that allowed them to move freely without head or body restraint. After reaching an acceptable behavioral performance (discrimination rate ≤ 0.65 and both hit rate and safe rate ≤ 0.8) consistently for 2 or more consecutive training sessions, the animals received surgery to implant a headpost on the skull. After surgery, animals re-learned the auditory task in the head-restrained condition (instead of walking

away from it in the freely moving condition). It took $1-2$ weeks for all animals to reach again an acceptable performance level in the head-fixed holder, where they received tail-shock rather than tongue-shock for incorrect responses.

Figure 5.6 displays the average licking behavior across 185 recording sessions (counted as tongue contacts with the water spout) in the tone detection task and 159 sessions in the click-rate discrimination task. Blue color indicates licks during reference sounds and red color illustrate lick responses during target sounds. Panel A only includes trials in which the animals successfully refrained from licking during the shock window (Hit trials); panel B displays only average lick patterns in trials in which the animals continued licking during the shock window (Miss trials). In panel A it's clear that the ferrets decrease their licking upon presentation of target sounds and completely avoid licking in the 0.4 s shock window, while maintaining a relatively constant licking rate during the presentation of reference sounds. In the click-rate detection task there was no difference between licking profile to the reference and target sound classes during the initial TORC portion of the stimuli, confirming that TORCs in this task have a neutral behavioral value and because they are the same stimuli preceding both slow and fast click trains, they carry virtually no information about upcoming reference or target sound identity.

Panel B displays the average licking behavior only in miss trials. The conditioned avoidance task has the design disadvantage that it can confound true miss trials — where the ferret genuinely confuses the target stimulus with the reference

stimulus — to misses arising from errors in response timing. Since animals were deprived of water in order for them to be thirsty enough to be motivated to perform avidly in the tasks, they usually tried to lick as much as possible. Because of that, many times ferrets tried to lick as soon as the shock window was over, so timing errors such as licking right before the shock window offset could get counted as miss trials despite the fact that many times the ferrets correctly perceived the target as such and decreased their licking during and immediately after the target. Because of that, both plots in panel B suggest that most of the time the ferrets correctly decreased their licking during the target stimuli presentation, and did not fail in detecting the targets, but returned to lick too soon. This is especially clear in the left plot (tone detection task), where there is a clear peak in the licking probability right before the end of the shock window.

5.2.4 Modulation of vaPEG neural responses during behavior

Despite the fact that vaPEG neurons displayed weak and sluggish responses to task sounds in the passive condition, the general finding in the present study was that vaPEG neurons greatly enhance their responses to target sounds during performance of auditory tasks. 343 neurons were tested in the tone detection task, and 367 were tested in the click-rate detection task. Of these, 234 had significant changes in their responses during performance of the tone detection task, and 206 in the click rate discrimination task (68% and 56% respectively, $p < 0.05$ Wilcoxon signed rank

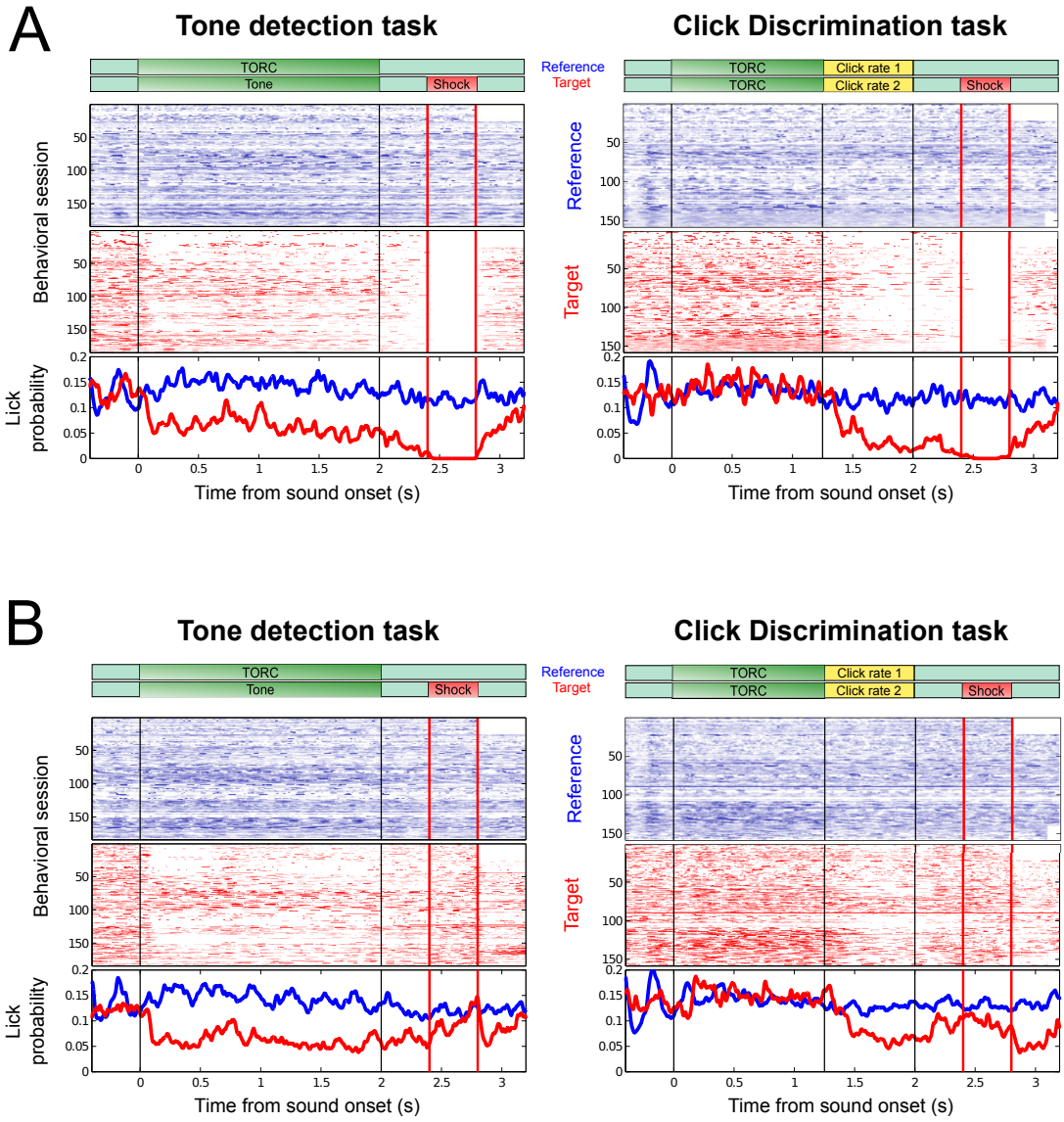

Figure 5.6: **Behavioral performance in tone detection (left) and click-rate discrimination (right) tasks.** Plots at the top of each panel display the average lick probability for each behavioral session (185 sessions tone detection, 159 sessions click-rate discrimination). Blue color indicates the licking during presentation of reference sounds. Red color indicates licking during target sounds. Plots in panel **A** displays the average licking behavior across trials where the animals correctly detected the target sounds and were successful at avoiding licking during the shock window. Panel **B** displays the average licking behavior during miss trials, where the ferrets lick during the shock window.

test, Bonferroni correction). 235 cells were tested in both auditory tasks, of those, 125 had significant effects in both tone detection and click rate discrimination tasks (53%).

We recorded vaPEG neural responses in the active behavioral condition during performance of both tasks, and passively before and after the active condition, when they were presented with an identical sequence of task stimuli. We measured behavioral effects in vaPEG neurons responses by comparing their firing rates (PSTHs) in responses to reference and target stimuli between the passive and active conditions.

Neurons in vaPEG displayed a variety of effects during performance of both auditory tasks, with a general tendency to enhance their responses to target sounds in the active condition. Figure 5.7 displays 5 single-units, two in presence of the tone detection task (panel A), and three during the click-rate discrimination task (panel B). In each panel, a raster plot at the top displays the spike events for each task stimuli (blue shaded area: reference stimuli, red area: target stimuli), and the mean firing rate (PSTH) is shown at the bottom.

As single-units in the top 3 rows, many neurons in vaPEG displayed weak responses to task stimuli in the passive condition before behavior (pre-passive), but greatly increased their firing rates in response to the target during behavior. The neuron in the first row (avo053b-d2) increased its target response reaching a peak firing rate at 250 ms and decaying after. In the post-passive epoch, this neuron dis-

played a persistent increased response during the first target presentations (visible at the top row in the post-passive target raster). The neuron in the second row (avo061a-c2) displayed a sustained increase in its firing rate during the duration of the target during behavior. This increased firing rate persisted even after the target offset, and decayed during the shock window. This sustained activity greatly resembles some behavioral effects seen in dlFC neurons (Fritz et al., 2010) and differs from the general findings in dPEG and A1 PSTH responses (Atiani et al., 2014, Chapter 4). Some neurons such as the one at the first row of panel B (lemon065b-b1) showed no responses during task stimuli, but responded in the silence period after the target, which suggest that some of these neurons might be coding more for aspects of the task structure and timing than acoustical features of the stimuli. The two neurons at the bottom of panel B (avo063a-c2 and avo055a-b2) followed both reference and target clicks in the pre-passive condition, but suppressed their firing rate in response to reference clicks while maintaining their responses to target clicks during behavior. These responses can greatly enhance the contrast between the representations of reference and target clicks during performance of the click rate discrimination task.

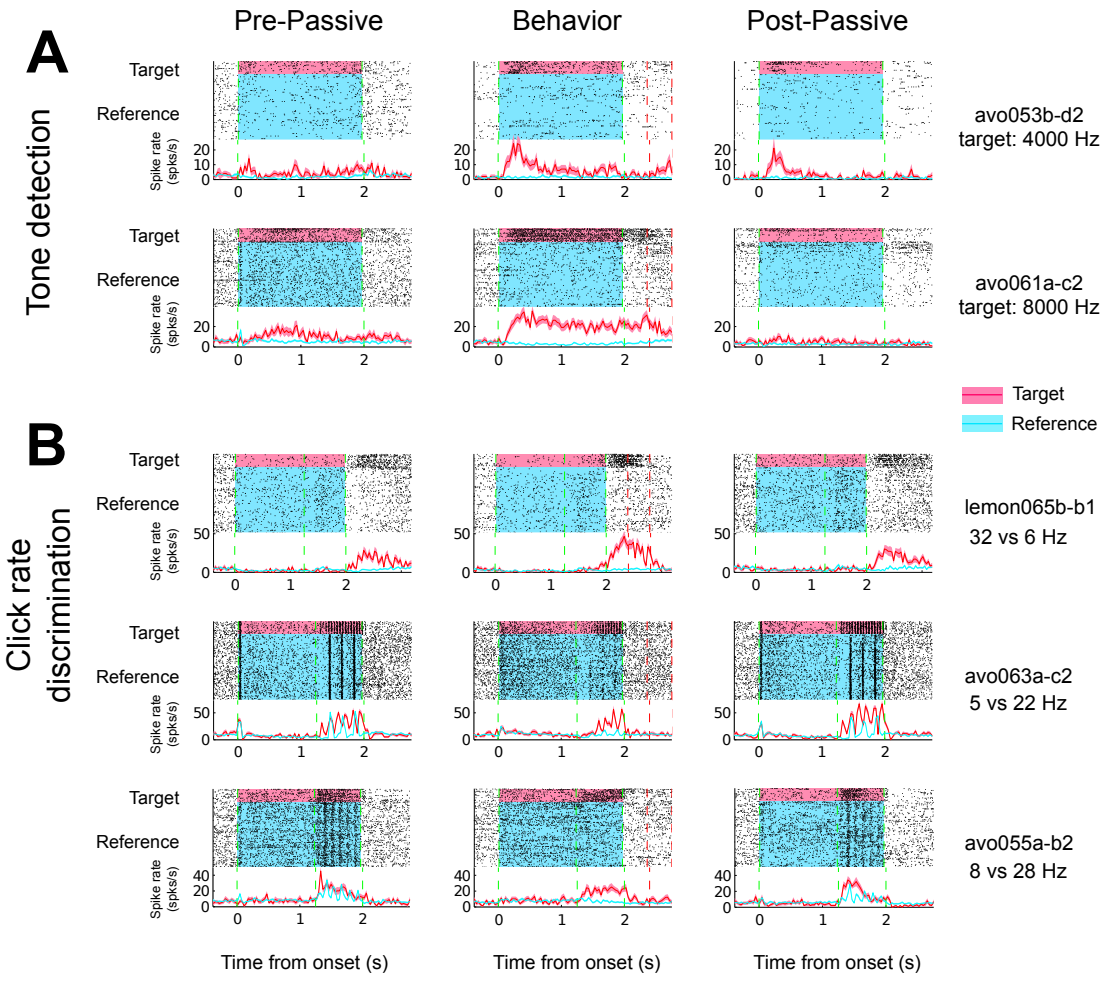

Figure 5.7: **Single-unit responses to reference and target stimuli.** **A:** Raster plots and PSTHs of vaPEG neurons before (pre-passive), during (behavior) and after (post-passive) performance of the tone detection task. Top unit had a short response after a long latency (∼250 ms). Unit at the bottom had a sustained response that lasted until the end of the shock window (800 ms after target offset). **B:** Raster plots and PSTHs of three units before, during and after performance of the click-rate discrimination task. Unit at the top row did not respond to task stimuli, but increased its firing rate in the silence period after target, especially during behavior. The units at the bottom suppressed their responses to reference clicks while maintaining a higher firing rate in response to targets.

The mean response of the population follows the same trend (Figure 5.8). All single units that had a significant change in their responses during behavior to reference or target stimuli were normalized and averaged. We first subtracted the baseline firing rate (measured as the spiking rate in the 0.4 s silence period before each task stimulus) and then divided the PSTHs by the maximum firing rate measured across the population. The resulting normalized PSTHs show general suppressive response to TORCs in the passive state that declines during behavior. Target tones and clicks were significantly enhanced during behavior ($p < 0.05$, t-test, Bonferroni correction). Interestingly, target enhancement in vaPEG is generally sustained and lasts beyond the duration of the target sounds. TORC responses in the click rate discrimination were not significantly different between reference and target within the passive or active states, confirming that TORCs in this task provide no information about stimulus identity. Nonetheless, the generally suppressed responses to TORCs in the passive condition are reduced during behavior, where TORC responses increase to firing rates closer to baseline, and show a slight build up.

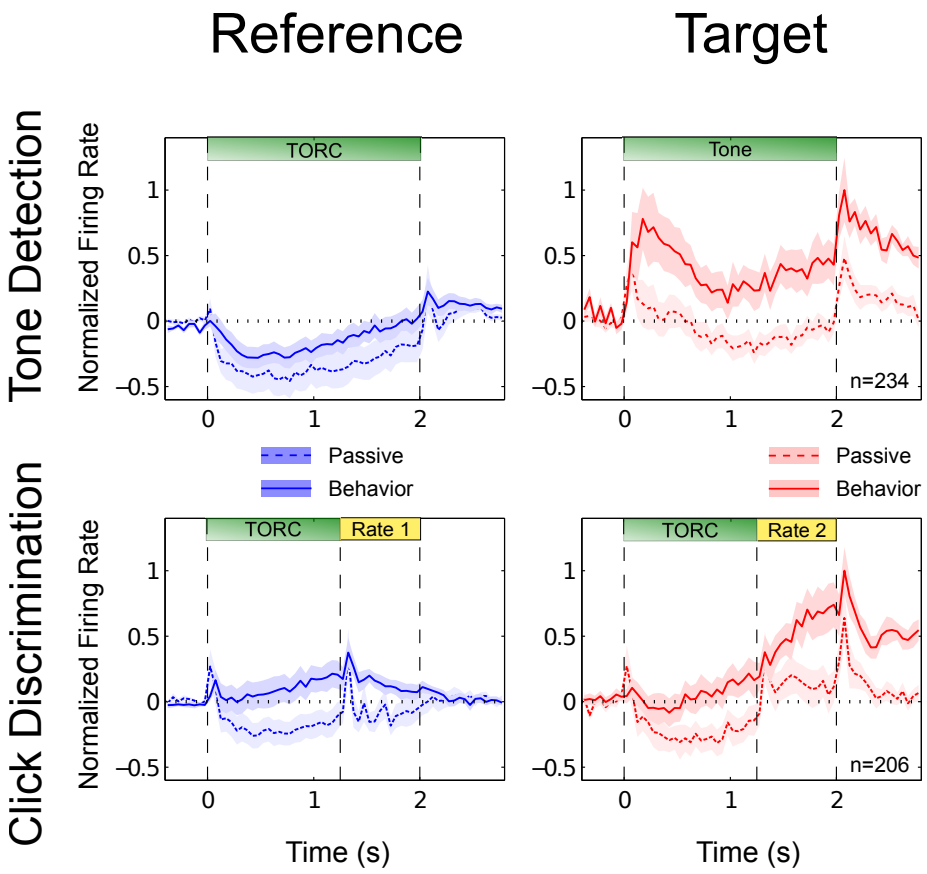

Figure 5.8: **Average behavior-dependent change in firing rate in vaPEG neurons.** Average responses recorded in the vaPEG of four ferrets in the tone detection (top row) and click-rate discrimination (bottom row) tasks comparing responses to reference (blue) and target (red) stimuli before behavior (passive, dashed lines) and during performance of the tasks (behavior, continuous lines). Behavior-dependent changes provided a higher contrast between reference and target responses. PSTHs in the active (behavior) condition were measured from neural activity collected only during correct performance of the task ('Hit' trials).

In order to better understand how individual vaPEG neurons change their responses to reference and target sounds, and how they might contribute to a better discrimination between these sound classes, we compared firing rates in the passive condition versus responses during behavior in scatter plots (Figure 5.9. Firing rates are presented with the spontaneous rate subtracted. Neurons that do not change their passive responses during behavior should lie at the unity slope, while behavior-dependent enhancement should be located above the diagonal. In both, tone detection (panel A) and click-rate discrimination (panel B) tasks, there is a relative enhancement to references and targets, but the majority of target responses tend to increase during behavior. Reference responses that were suppressed in the passive condition were enhanced during behavior, as can be seen in the lower left quadrants, where most points lie above the diagonal. Most reference responses that were not suppressed in the passive presentation of both tasks (positive values on the abscissa) were clustered on the diagonal, reflecting little or no change during behavior, but with a slight tendency of having more units decreasing their responses to references during behavior.

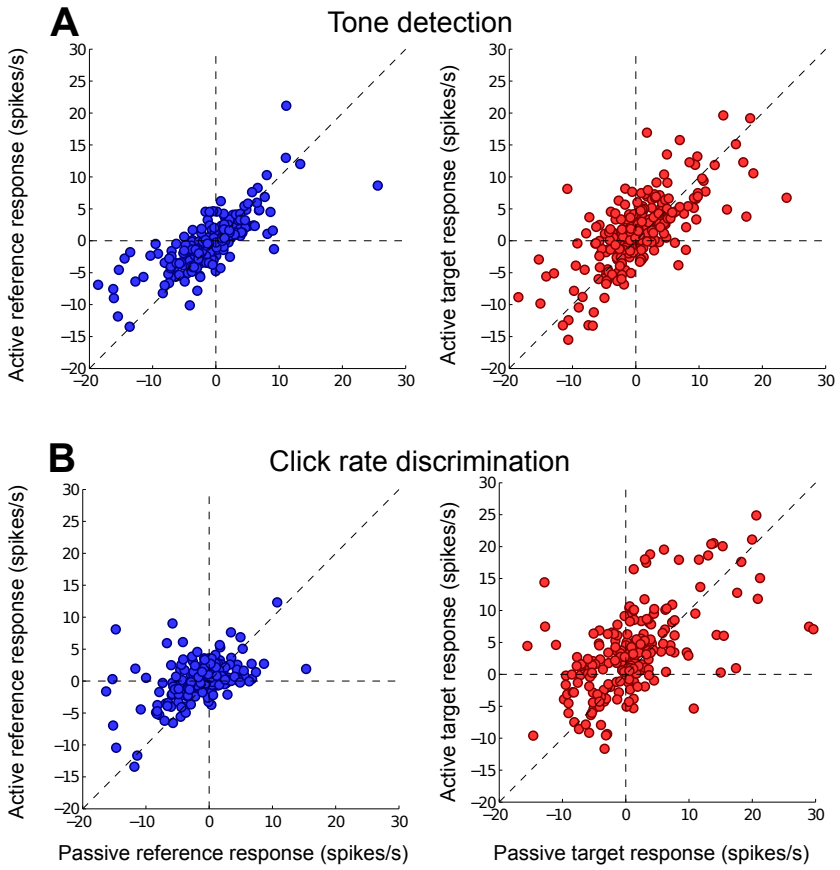

Figure 5.9: **Behavior-dependent changes in raw firing rates** in response to reference (blue) and target (red) stimuli. **A:** Scatter plots of passive vs. active (behavior) firing rates for units tested in the tone detection task that had significant changes during behavior (n=234, $p < 0.05$, Wilcoxon signed rank test, Bonferroni correction). Firing rates were measured in a time window $0 - 2$ s from sound onset. **B:** Passive vs. active responses for units tested in the click rate discrimination task (n=206, $p < 0.05$, Wilcoxon signed rank test, Bonferroni correction). Firing rates were measured in a time window $0 - 0.75$ s from click train onset after TORCs.

In order to better understand how coding of vaPEG neurons might be affected by engagement in auditory tasks, we measured changes in pair-wise noise correlations. Often neighboring neurons covary in their stimulus-unrelated spiking, and reductions in these correlations have been found in the transition from passive to active engagement on visual (Cohen & Maunsell, 2009; Mitchell et al., 2009), and auditory tasks (Downer et al., 2015; Jeanne et al., 2013). A reduction in noise correlations might increase the signal-to-noise ratio in coding relevant stimuli. For this, the average firing rate $100 - 2000$ ms after stimulus onset was correlated between pairs of simultaneously recorded units in the passive and active states. Figure 5.10 displays how a population of 392 pairs of vaPEG neurons in the passive, active and post-passive conditions of the tone detection task change their noise correlations. Consistent with previous findings in A1 (Downer et al., 2015), we found that noise correlations are significantly reduced during the attentive active state (Wilcoxon signed-rank test, p=0.001).

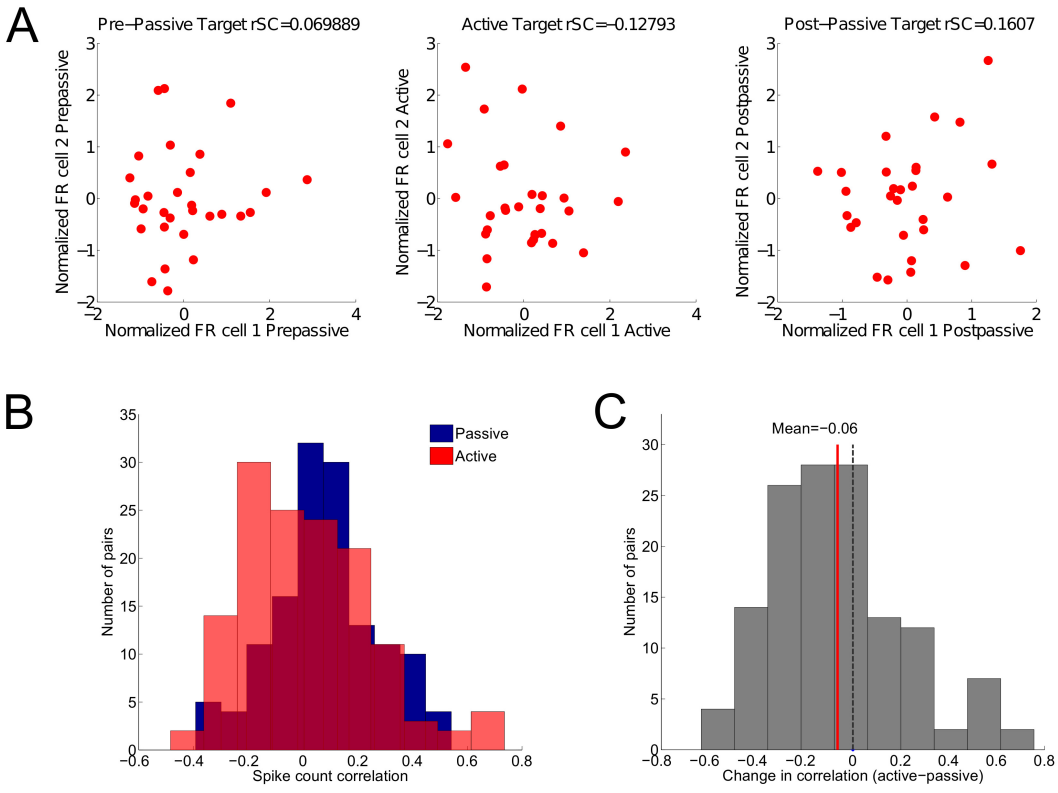

Figure 5.10: **Neuron pairs in vaPEG reduce their noise correlations in the active state. A:** joint firing response distribution of an example pair of vaPEG neurons. Each dot represents the joint mean firing rate in response to one presentation of a target sound. Noise correlations (rSC), while modest, are reduced during active performance of the task, and increase back in a passive presentation of the task after behavior. **B:** Distributions of passive and active rSC from 392 neighboring neuron pairs. The rSC distribution in the active state is significantly shifted towards lower values (Wilcoxon signed-rank test, p=0.001). **C:** Histogram of the difference in correlation (active minus passive), the mean change in rSC was −0.06.

5.2.5 Comparison of vaPEG behavior-dependent changes with other areas in the auditory processing hierarchy

In order to put vaPEG responses in the context of other areas of the auditory processing hierarchy previously characterized by our lab, we retrieved and reanalyzed data from A1, dPEG and dlFC originally collected for previous publications (Atiani et al., 2014; David et al., 2012; Fritz et al., 2003, 2010) along with more recent data collected from these areas. These data corresponds to neural responses that were significantly modulated during the tone detection task (A1 N=133, dPEG N=330, dlFC N=230; $p < 0.05$, Wilcoxon signed rank test with Bonferroni correction). We hypothesized that, similar to our findings in dPEG (see Chapter 4 and Atiani et al. (2014)) where increasing behavior-dependent changes were seen along the A1, dPEG and dlFC processing chain, vaPEG would present changes greater than A1 and dPEG, but lower than those in dlFC.

As seen in figure 5.9, not all neurons with significant behavior-dependent effects increase their response to targets during behavior. Because of that, and since there was a considerable population percentage (47%) of cells in dlPFC that showed suppressive responses (Fritz et al., 2010), the PSTH responses in each area were ordered by their relative enhancement of target response (Figure 5.11). This was done by first subtracting pre-passive response from active firing rate to calculate the behavior-dependent change for reference and targets, and then subtracting reference change from target change. The resulting firing rates were averaged on a time win-

dow from sound onset to 0.2 s before offset (i.e. from 0 to 1.8 s in vaPEG and from 0 to 0.8 s in all other areas), resulting in a measure of the mean contrast between reference and target sound classes (Figure 5.11, heatmaps in left panels). Since we first subtracted spontaneous firing rates from the responses used in this analysis, positive values indicate increases of spiking activity above baseline, while negative values mean a suppression in the response below spontaneous activity. This could account for cells that enhance the contrast between both sound classes by decreasing their responses to reference sounds. This analysis resulted in a separation of each area population into a group that enhanced their relative response to targets and another that reduced or maintained their representation of targets.

To assess significant changes in the average PSTH in each area population, a paired t-test with Bonferroni correction for multiple comparisons was performed for each time bin. We considered a significant behavior-dependent change in the PSTH response when at least 3 contiguous time bins (each 50 ms long) were significantly different between conditions. In all areas, a majority of the neurons that changed their responses with behavior, enhanced their relative responses to targets. We found that 53% of A1 and 54.4% of dPEG neurons significantly increased their firing rate in response to target during behavior, and dPEG also enhanced target relative contrast by suppressing their responses to reference TORCs in the active condition. A subset of neurons in A1 and dPEG (47 and 45.5%, respectively) also showed significant reductions in their responses to target tones during behavior.

While A1 and dPEG were similar in that their responses had a clear onset peak, vaPEG and dlFC neurons displayed more sustained responses to targets that, interestingly, lasted for a considerable amount of time after sound offset ($\sim 0.8 - 1$ s) in the active condition. Both, vaPEG and dlFC neurons, significantly enhanced their responses to targets during the active condition. The subset of vaPEG neurons that did not enhance target responses (47% of vaPEG neurons, lower PSTH panels, figure 5.11) showed strong suppressive responses to TORC references, which were relatively reduced during behavior by increasing firing rate closer to baseline levels.

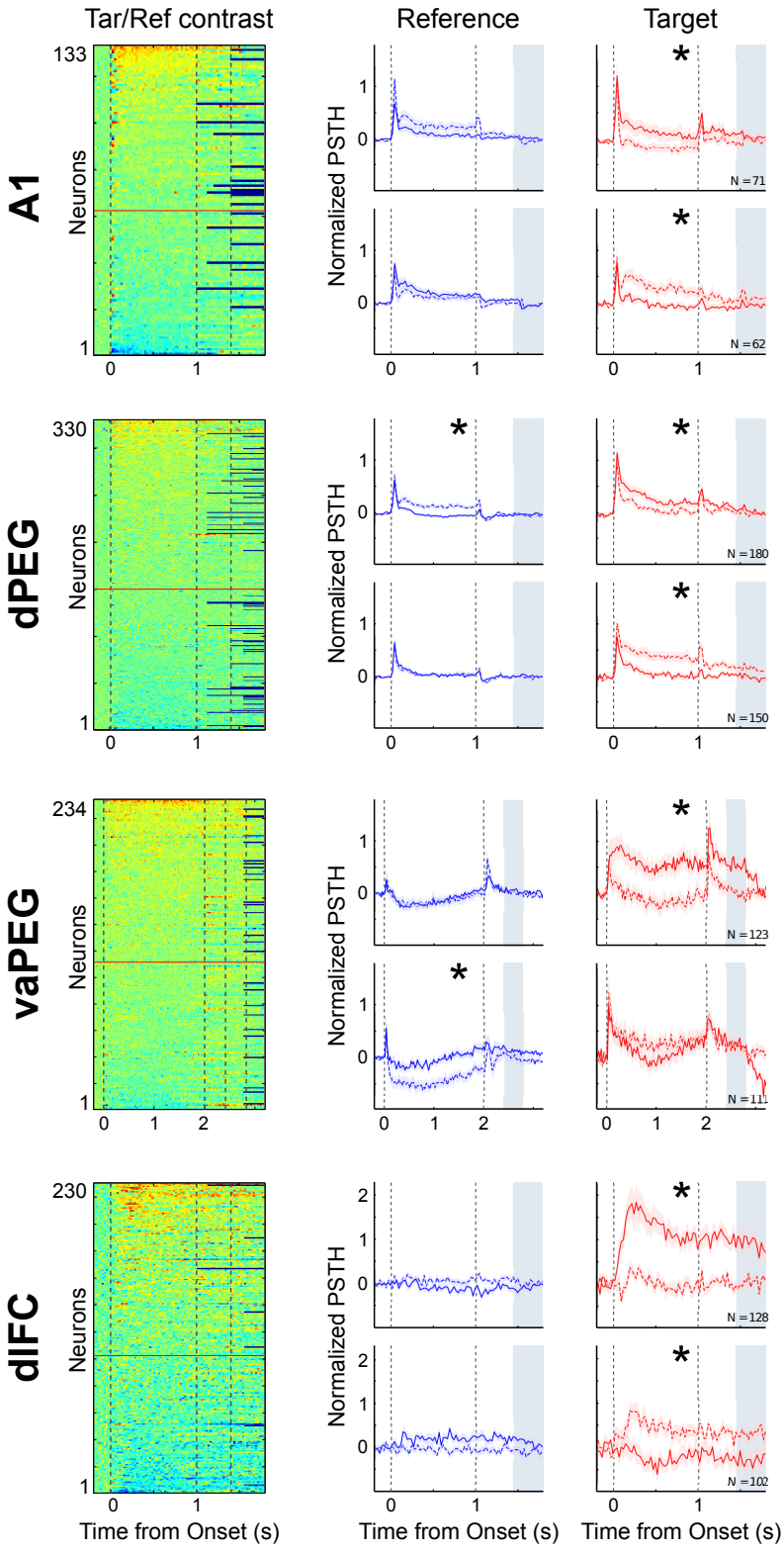

Figure 5.11: **Comparison of behavior-dependent changes in vaPEG with areas A1, dPEG and dlFC.** Continues in next page...

Comparison of behavior-dependent changes in vaPEG with areas A1, dPEG and dlFC. Only tone detection task data is shown. **Left** heatmaps show the contrast between target (tones) and reference (TORCs) response changes computed from firing rates with baseline subtracted ([target active – target passive] – [reference active – reference passive]). Target/Reference contrast response were sorted so that neurons that displayed an average relative enhancement of target response (by increasing target responses and/or decreasing reference responses during behavior) are plotted at the top of the heatmaps and all other cells were left at the bottom. The division between both groups is marked in the heatmaps with a red line. Dashed vertical lines mark, from left to right, times of sound onset and offset and shock onset and offset. **Right** plots correspond to normalized PSTH responses to reference (blue) and target (red) in passive (dashed lines) and active behavior (continuous line) conditions. In each area, top PSTHs correspond to the mean firing rate ± SEM of the units that had an average positive target/reference contrast; bottom PSTHs correspond to units that displayed no change or average decrease in target relative responses. Shock window duration is marked with a gray shades and vertical dashed lines mark times of sound onset and offset. Asterisks mark PSTHs that had at least 3 consecutive time bins with significant differences between passive/active conditions ($p < 0.05$, t-test, Bonferroni correction).

The magnitude of target responses during behavior were greater in vaPEG from those in A1 and dPEG, but less than dlFC behavior-dependent changes. To quantify the overall magnitude of these changes in target responses, we present the distribution of absolute changes in each area in figure 5.12. Rectification of behavior-dependent changes in target responses was necessary to account for neurons that diminished their responses to targets during behavior. Values represent the changes (active minus passive firing rates) from responses with spontaneous activity subtracted and normalized by the maximum firing rate obtained at each area population. vaPEG normalized absolute target change was significantly greater than dPEG, and while it was lower than dlFC, this difference was not significant ($p < 0.05$, Kruskal-Wallis ANOVA with Bonferroni correction for multiple comparisons).

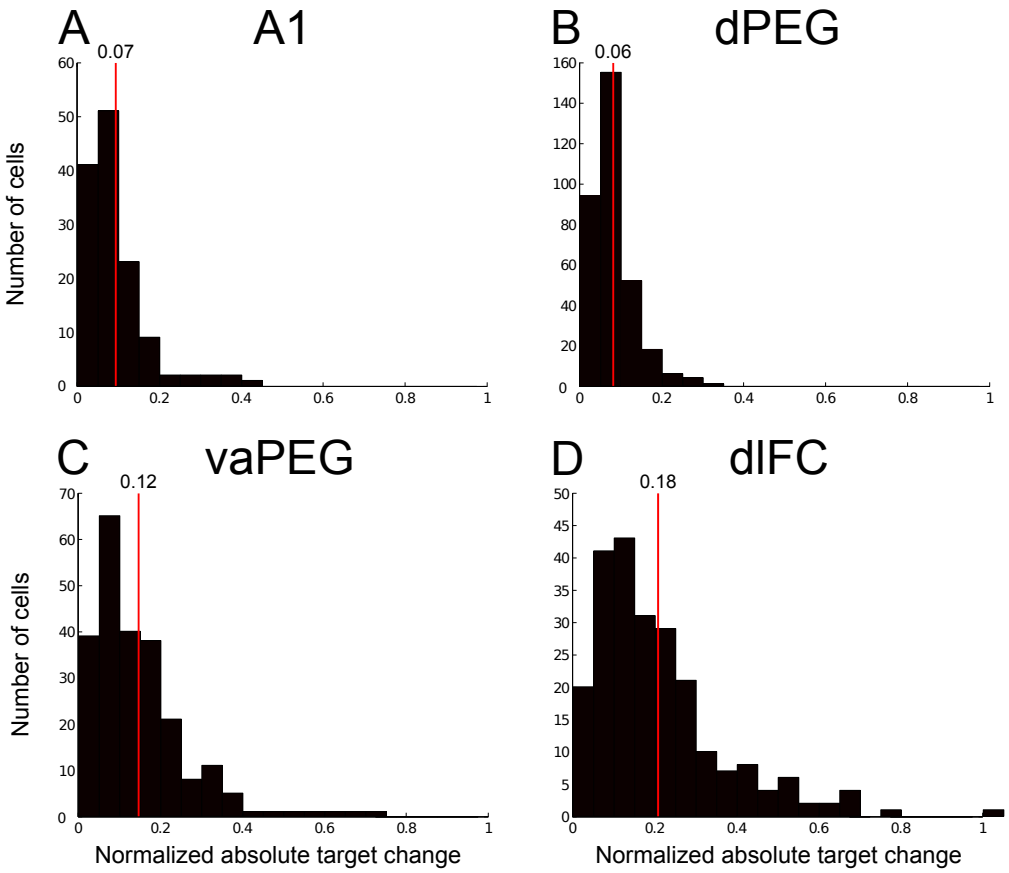

Figure 5.12: **Absolute behavior-dependent change of target responses in areas A1, dPEG, vaPEG and dlFC.** Significantly modulated neurons in each area could increase or decrease their responses to targets during performance of the tone detection task. Changes in firing rate (active minus passive) were rectified (absolute value) for simplicity. Firing rates were subtracted baseline spontaneous rate and normalized by maximum value across each population. Red lines indicate mean value. **A:** Data from 133 significantly modulated neurons in A1 ($p < 0.05$, Wilcoxon signed rank test, Bonferroni correction), mean ± SEM = 0.07 ± 0.0054. **B:** Data from 330 significantly modulated neurons in dPEG ($p < 0.05$, Wilcoxon signed rank test, Bonferroni correction), mean ± SEM = 0.06 ± 0.0039. **C:** Data from 234 significantly modulated neurons in vaPEG ($p < 0.05$, Wilcoxon signed rank test, Bonferroni correction), mean ± SEM = 0.12 ± 0.0071. **D:** Data from 230 significantly modulated neurons in dlFC ($p < 0.05$, Wilcoxon signed rank test, Bonferroni correction), mean ± SEM = 0.18 ± 0.0248.

Figure 5.11 displays a qualitative difference in the population responses between vaPEG and its preceeding auditory areas A1 and dPEG; a sustained behavior-driven response that lasts until the end of the shock period. This sustained response during the post-target silent period is similar to what is seen in dlFC population. In order to compare these post-target responses in ferret A1, belt, parabelt and dlFC, we analyzed a time period of 700 ms starting 100 ms after target offset up to 800 ms after target offset. The first 400 ms after the target is a silent period that is not penalized, and provides time for the animal to decide on its behavioral response. After the decision period, a 400 ms lick-penalized time window follows, where the animal can receive a 100 ms shock if fails to refrain from licking. We compared neural responses collected in this post-target time period in passive vs. active conditions, as well as with a 700 ms time period before target offset (during target presentation) in the active behavior condition.

Figure 5.13 displays two panels per area; left panel display the distribution of active and passive responses and their differences from normalized firing rates with baseline subtracted. A1 did not show significant responses in this post-target time period in passive nor active behavior conditions ($p > 0.05$ one-sample t-test) and no significant differences between passive and active (oblique histogram, $p > 0.05$, paired t-test). dPEG had modest, but significant passive and active responses in the post-target period (marked with 3 stars close to the axes, $p < 0.001$ one-sample t-test), but no significant changes between passive and behavior conditions (oblique histogram, $p > 0.05$, paired t-test). vaPEG had significantly higher responses from

spontaneous rate in the passive condition in the silent post-target time epoch ($p < 0.001$ one-sample t-test) and its responses were significantly enhanced during behavior ($p < 0.001$ paired t-test). dlFC did not present passive responses in the post-target period ($p=0.06$, one-sample t-test), but significant increases during behavior ($p < 0.01$, paired t-test).

In order to test if these increases were behavior-driven or depended on prior passive responses we correlated passive and active responses in the post-target time period (left panels, figure 5.13). We found that in dlFC firing rates increases after target were solely dependent on active performance of the task, since passive responses were not correlated with active increases in firing rates (Pearson's correlation coefficient $r=0.096$, $p=0.28$). In the other hand, vaPEG active responses in the post-target epoch were significantly correlated with responses in the previous passive condition, suggesting that existing responses in the passive condition were later enhanced during behavior, as this can be verified by the greater proportion of dots lying below the diagonal unity line. A1 and dPEG active responses in the post-target period were significantly correlated with passive responses, since these responses did not show significant behavior-dependent modulations.

In order to test whether these sustained post-target increased responses were correlated with behavior-dependent firing rate changes during target presentation, we compared post-target firing rate with a time window 700 ms before target offset, that is while the targets are being presented (right panels in figure 5.13). We found

that dlFC and vaPEG tend to maintain sustained increases in firing rate during behavior into the post-target silent period: firing rates were not significantly different during and after the target (paired t-test: vaPEG p=0.58, dlFC p=0.87) and were strongly correlated (vaPEG r=0.36, p=0; dlFC r=0.65, p=0). Scatter plots show clear clustering of firing rates in the upper-right quadrant (vaPEG: 59%, dlFC: 62.2% of neurons), which indicate that firing rates were kept above spontaneous activity during and after the target. In contrast, A1 and dPEG firing rates tended to be more clustered around zero (spontaneous rate). Post-target responses were significantly different from during-target responses in dPEG ($p < 0.001$, paired t-test), which suggests that responses returned to firing rates closer to baseline after target offset.

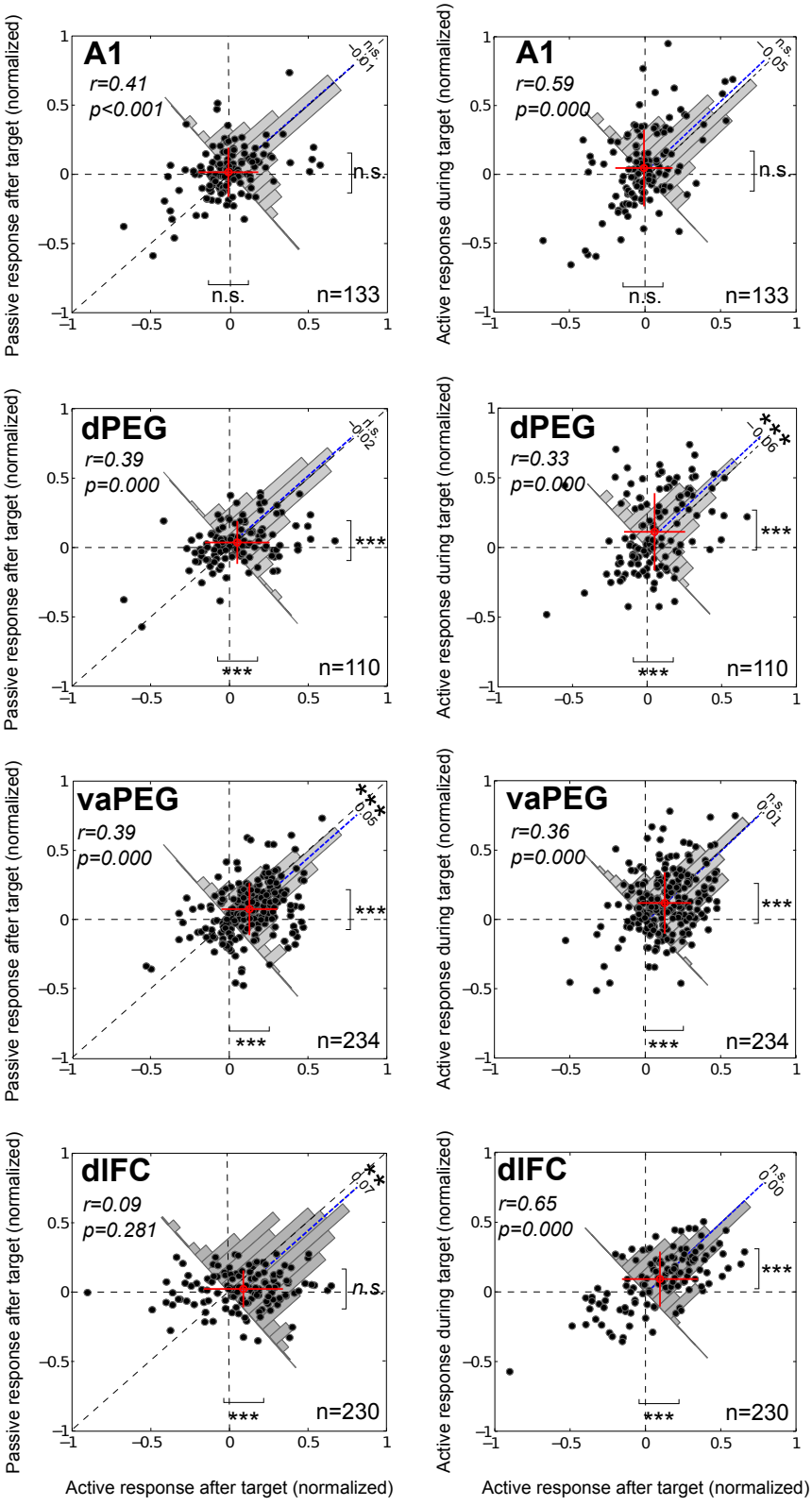

Figure 5.13: **Analysis of firing rate after target offset.** Continues in next page...

Analysis of firing rate after target offset. dlFC and vaPEG displayed sustained behavior-dependent increases in firing rate that outlasted the duration of targets and were maintained in the silent period after targets. For comparison, data from A1, dPEG, vaPEG and dlFC units that were significantly modulated during engagement in the task detection task is shown ($p < 0.05$, Wilcoxon signed rank test, Bonferroni correction). **Left** columns compare the unit responses (normalized firing rates, baseline subtracted) in the passive condition and active behavior in the silent period after target. The oblique histogram shows the distribution of behavior-dependent changes in responses (active passive) in the post-target period. Mean change is shown above the histogram as well as with a blue dashed line. **Right** scatter plots compare normalized responses $100-800$ ms after and 700 ms before target offset during active behavior, to analyze whether behavior-dependent increased post-target responses are correlated with sustained firing rates during the target stimuli. Oblique histograms display the distribution of after-target minus during-target responses.Significance of population responses relative to spontaneous activity are shown next to brackets near the bottom and right axes (n.s.: not significant, *: $p < 0.05$, **: $p < 0.01$, ***: $p < 0.001$; t-test). Red marks in scatter plots indicates the mean change value from normalized firing rates $\pm$ standard deviation.

5.2.6 Functional connectivity between dlFC and vaPEG

The striking behavior-dependent changes observed in vaPEG responses, as well as preliminary anatomical information gathered by our lab revealing that reciprocal connectivity between dlFC and auditory cortex might be exclusive to ventral and rostral areas of the PEG (Radtke-Schuller et al., 2011), raised the question whether functional connectivity between dlFC and vaPEG might differ from what was reported previously in A1/dlFC (Fritz et al., 2010). Fritz et al. (2010) presented evidence showing that, during performance of the tone detection task, there is a decrease in the A1/dlFC interareal coherence in the beta-band range (10-20 Hz, Figure 5.14 A).

We simultaneously recorded LFP signals from areas vaPEG and dlFC during passive presentation and active engagement in the tone detection task in one ferret. We computed the mean spectral coherence across all possible vaPEG/dlFC LFP signal pairs that were simultaneously recorded (304 pairs, figure 5.14 B). We found significant increases ($p < 0.05$, paired t-test with Bonferroni correction) in the delta-theta (< 6 Hz) and beta-band range coherence ($12 - 20$ Hz). The low frequency increase in coherence was also present in the A1/dlFC study, it was common to both reference and target responses and its biological basis is obscured by possible motor artifacts caused by the ferret licking. The increase in beta band was exclusive to LFP responses to target stimuli and during active engagement of the task (figure 5.14, B). This result is very different to the one reported in A1/dlFC

coherence (figure 5.14 A, plots provided by the authors), where synchrony was lowered in the beta band in the active condition and for both stimulus classes. In the vaPEG/dlFC case, no clear behavior-dependent coherence changes were measured in LFP responses to reference sounds. Also, A1/dlFC coherence was shown to gradually return back to pre-passive levels (in a period of ∼100 s), as indicated by a smaller reduction in the beta band coherence when only the first 10 trials were analyzed. We also analyzed vaPEG/dlFC coherence in the first 10 trials, but found no differences with the coherence results calculated from all trials (data not shown). This suggests that vaPEG/dlFC activity is synchronized with faster dynamics than A1 and dlFC, probably due to more direct connectivity.

Coherence provides a bilateral functional connectivity estimation, but no directionality information. In order to find out causal influences in the top-down (dlFC to vaPEG) and bottom-up (vaPEG to dlFC) directions, we performed spectral Granger causality analysis on the same LFP signals (figure 5.15). Granger causality is a statistical analysis that allows to estimate, in either time or frequency domains, the causal influence of past values of a signal in the future of a second signal (Seth et al., 2015). Our Granger causality analysis in the bottom-up direction presented peaks in delta-theta bands and in the beta range, the bottom-up causality during the active condition only revealed a decreased causality in the beta band range in reference responses. In the top-down direction, causality in the passive state was much lower than the bottom-up causality. In the active condition we found increases in causality in the delta-theta and beta band ranges in responses to

both sound classes, and a clear peak at ∼15 Hz in the dlFC/vaPEG causality in target responses. This peak at the beta band range coincides with the coherence peak we found between vaPEG and dlFC LFPs, and since the greatest change we found in causality in this frequency range was found in the top-down direction, it becomes a plausible explanation that most of the activity synchronization we found between vaPEG and dlFC might be caused by top-down influence of dlFC onto vaPEG.

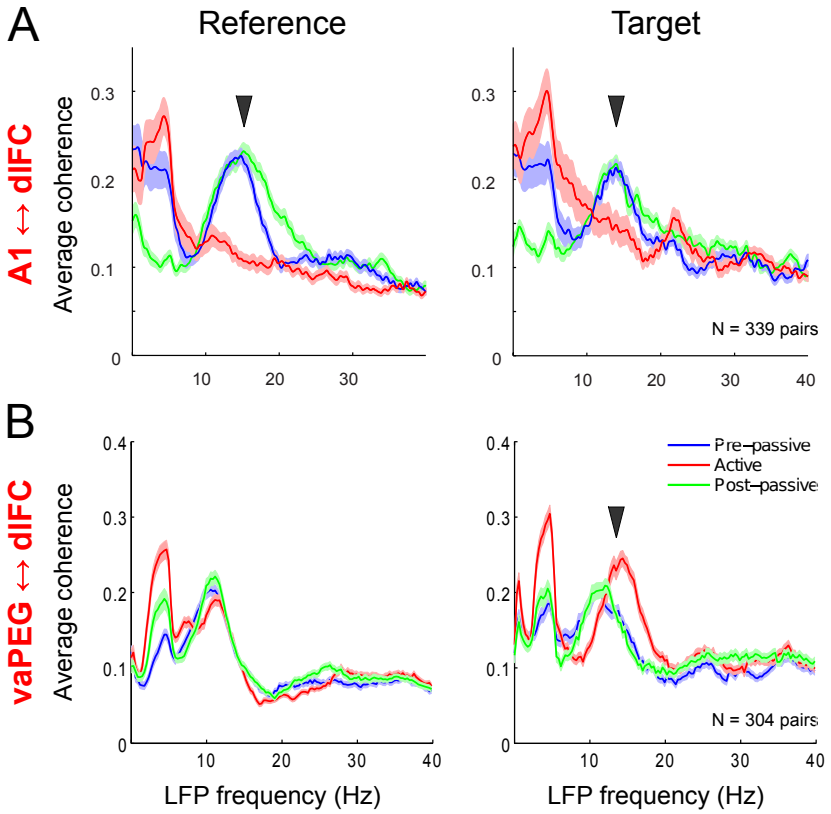

Figure 5.14: **LFP spectral coherence between auditory areas and dlFC. A:** A1/dlFC coherence measured from 339 pairs of simultaneously recorded LFP signals in the tone detection task. Active behavior caused a decrease in the beta band range ($\sim 10-20$ Hz) in both reference and target responses (marked with arrow heads). Plots provided by Stephen David and Jonathan Fritz. **B:** vaPEG/dlFC coherence measured from 304 pairs of LFP signals simultaneously recorded in the task detection task. Task engagement caused a significant increase ($p < 0.05$, paired t-test with Bonferroni correction) in the coherence in the beta band range, exclusively in target responses. In both areas, the increase in coherence at frequencies < 6 Hz might be caused by motor artifacts due to licking.

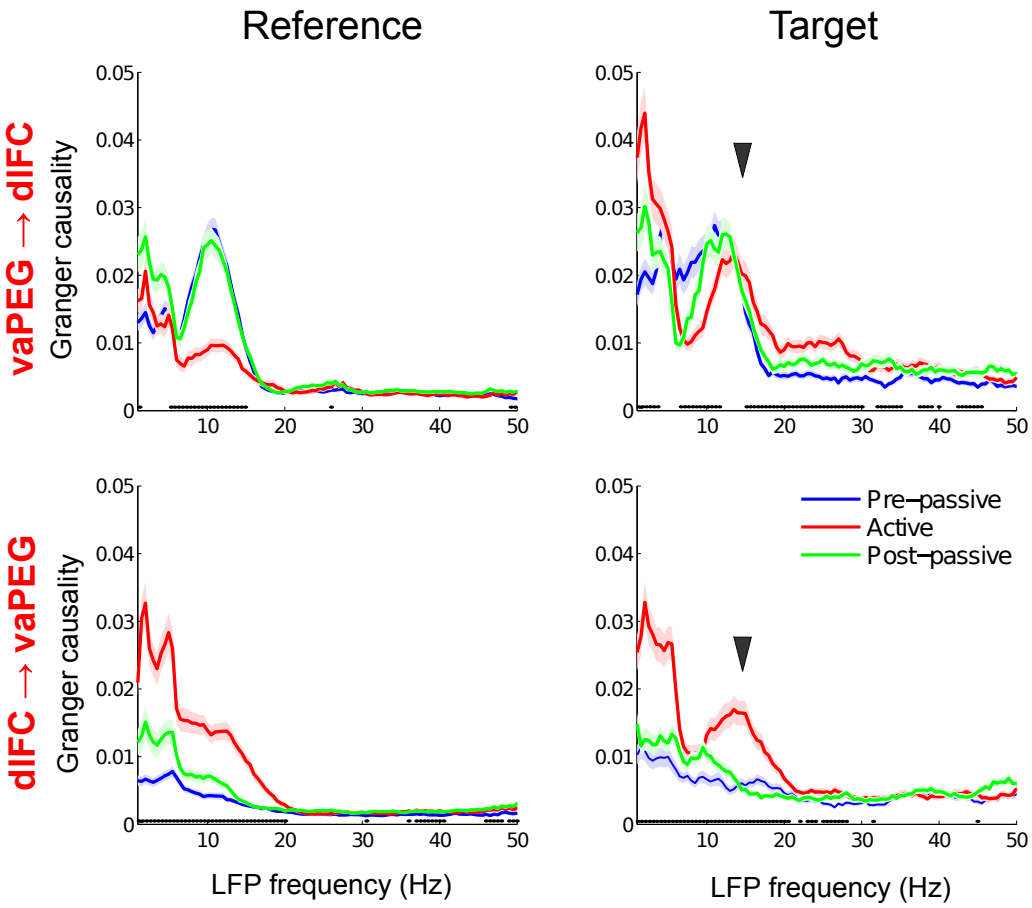

Figure 5.15: **Spectral Granger causality between vaPEG and dlFC.** Mean Granger causality ± SEM in pre-passive (blue), active behavior (red) and post-passive (green) conditions. Bottom black dots mark significant prepassive/active differences ($p < 0.05$, paired t-test with Bonferroni correction). **Top:** Granger causality in the bottom-up direction (vaPEG to dlFC) in LFP responses to references (left) and targets (right). Active behavior caused a significant decrease in causality in the alpha-beta band ($8 - 15$ Hz) range. **Bottom:** Granger causality in the top-down direction (dlFC to vaPEG). Active behavior increased top-down causality in frequencies < 18 Hz in reference and target responses. Arrow heads marks were placed at 15 Hz, where the maximum behavior-dependent change in coherence was found; the peak at 15 Hz in top-down causality measured in the active condition might underlie the increased behavior-driven coherence found in target responses.

5.2.7 Influence of task context on vaPEG responses

As can be seen in figure 5.8, vaPEG neurons showed an increased contrast between reference and target click responses during active engagement in the click-rate discrimination task. Nonetheless, we found that in the passive condition there was a significant contrast between reference and target click trains as well. To test whether this differential response to reference and target click trains in the passive stage of the click-rate discrimination task was due to different response affinity to the acoustical features of the reference and target click rates or to an influence of the task temporal structure, we compared task-sound normalized responses along with responses to isolated click trains presented out of the task context.

In every experiment we presented 1 s long click trains at several rates randomly chosen ($4 - 60$ Hz) to assess click tuning before presenting the passive and active stages of the click-rate discrimination task. We pooled the unit responses to isolated click trains that matched (or were closest to) the click rates used as references and targets in the task. We found no significant differences between the responses to isolated click trains with rates equal to reference or target (Figure 5.16, panel C). Interestingly, the same click train rates presented in the passive task context (0.75 s click trains preceded with a 1.25 s TORC) produce responses to target clicks that were significantly greater than reference click responses ($p < 0.05$, paired t-test with Bonferroni correction for multiple comparisons). These responses were later even greater during the active behavior state (figure 5.8, B and figure 5.16, C).

We performed the same analysis in some A1 and dPEG recordings gathered in our lab in the click-rate discrimination task to be able to see if these passive increased responses occur at earlier auditory cortical stages or if these are exclusive to vaPEG neurons (figure 5.16, A and B). We found no significant differences between reference and target responses in the passive stage of the task in A1 and dPEG ($p > 0.05$, paired t-test, Bonferroni correction). We only found a significant contrast between reference and target click rates in dPEG responses during the active state.

We also compared A1, dPEG and vaPEG responses to the tone detection task sounds, to see if a similar increased contrast between reference TORC and target tone passive responses occur along the hierarchy of auditory cortical areas (figure 5.17). In this comparison we confronted reference TORC and target tone responses from the tone detection task along with passive responses to tones and TORCs presented alone. Tones (0.1 s) of random frequencies were routinely presented to assess tone tuning, we selected responses to tones of the same frequency used in the task. TORCs (3 s) were also routinely presented to attempt to compute STRFs. Unfortunately, the short duration of tones used for tuning do not allow us to compare sustained responses to tones out of task context with those measured during the task. Nonetheless, we were able to find an increased contrast between passive responses to task stimuli, which was further increased in the active state.

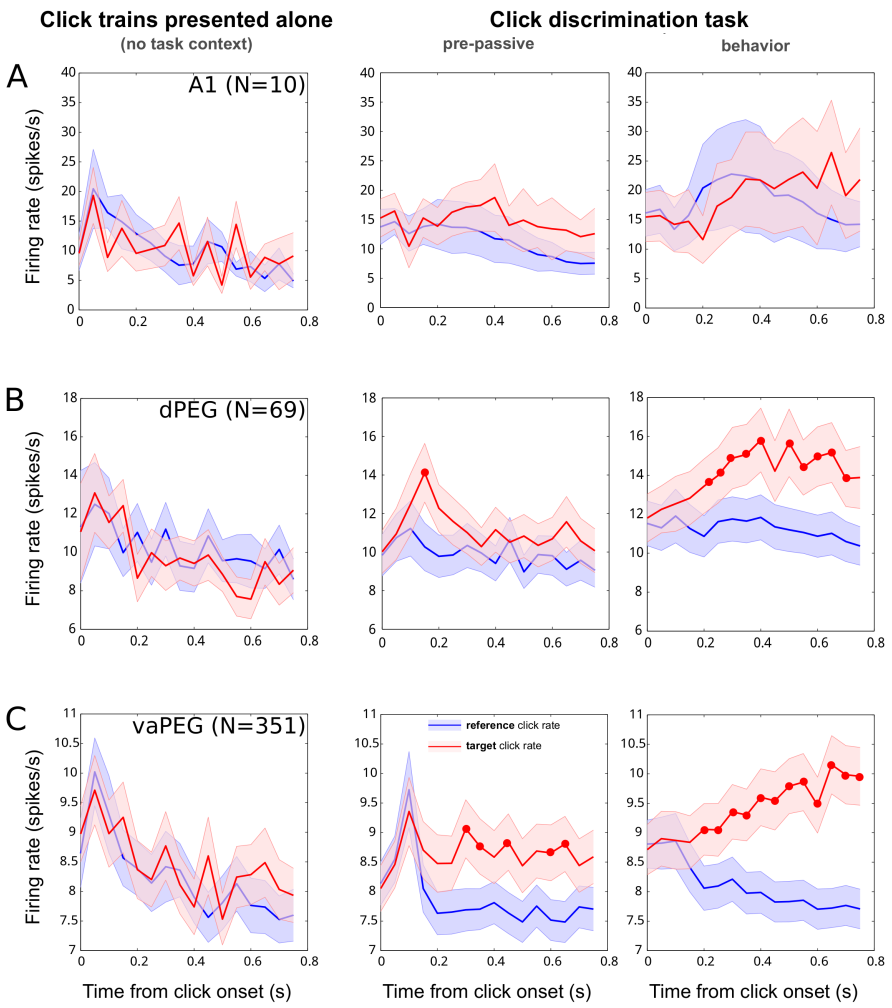

Figure 5.16: **Comparison of responses to click rates in and out of click rate discrimination task. A:** Responses of 10 A1 single units tested in the click rate discrimination task. Middle and right panels correspond to the passive and active responses to reference (blue) and target (red) click trains. Left panel correspond to responses to click trains of same rates used in the passive and active stages of the task, but presented isolated among click trains of several rates. No significant differences between reference and target click rates were found (p¿0.05, paired t-test with Bonferroni correction). **B:** Responses of 69 dPEG single units presented in the same way as in A. Only one bin was significantly different in the passive condition of the task, while a majority of bins (10) were enhanced in target click responses in the active condition ($p < 0.05$ paired t-test, Bonferroni correction). **C:** Responses of 351 vaPEG neurons in response to reference and target click rates, presented as panels A and B. Significant differences between reference and target click responses were found in passive and active conditions ($p < 0.05$ paired t-test, Bonferroni correction).

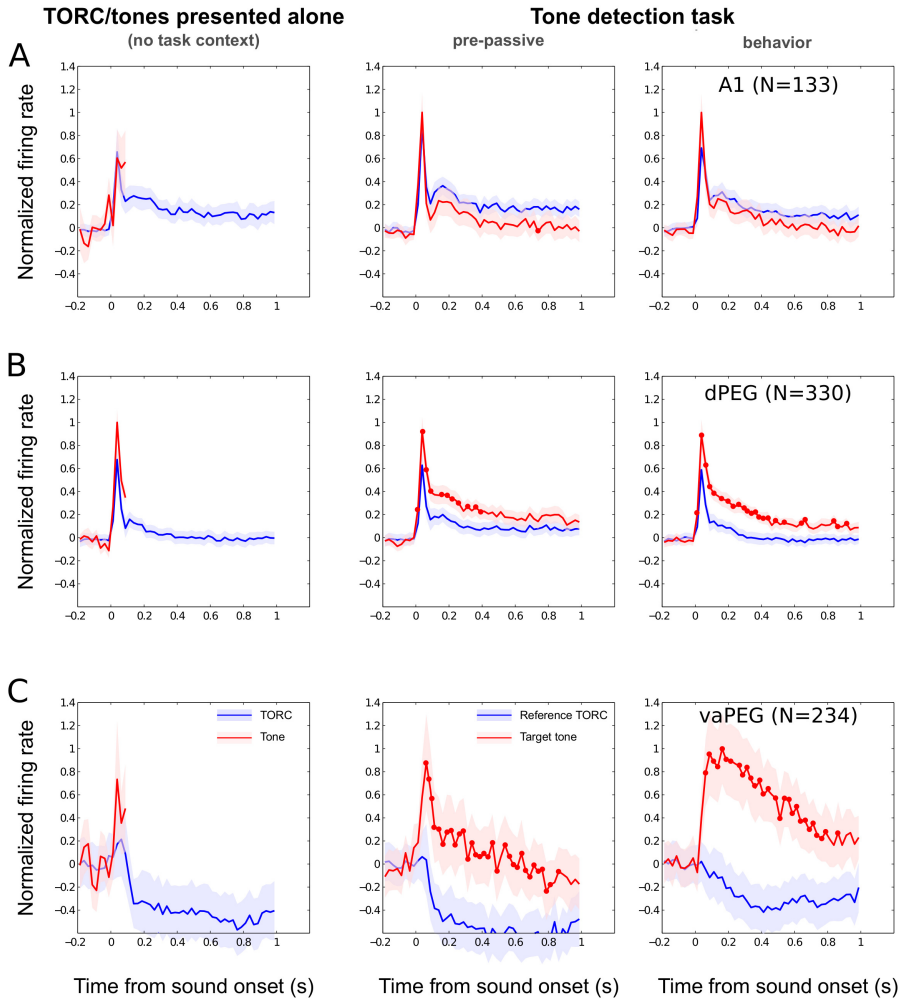

Figure 5.17: **Comparison of responses to TORCs and tones in and out of the tone detection task.** TORC (3 s) and tone (0.1 s) responses out of the task context were taken from responses to stimuli presented at the beginning of each recording session for assessing cell tuning properties. **A:** Responses to TORCs and tones in A1 neurons out of task context (left), passive task condition (middle) and active behavior condition (right). No significant changes were found between reference and target responses. **B:** Responses to TORCs and tones in dPEG neurons presented in the same was as in A. Significantly different time bins are marked with red dots ($p < 0.05$, paired t-test with Bonferroni correction). **C:** Responses to TORCs and tones in vaPEG neurons presented in the same way as in A and B. Significantly different time bins are marked with red dots ($p < 0.05$, paired t-test with Bonferroni correction).

5.3 Discussion and Conclusions

In this study we aimed at expanding previous findings in our lab on task-related plasticity in auditory cortex responses. We recorded from several cortical areas in the ferret ectosylvian gyrus that may correspond to a parabelt auditory area.

By using the same behavioral task previously used by our lab to describe rapid task-related plasticity in A1 (Chapter 3, Atiani et al., 2009; David et al., 2012; Fritz et al., 2003, 2005), dPEG (Chapter 4, Atiani et al., 2014) and dlFC (Fritz et al., 2010), we were able to compare plasticity in these four stages in the auditory processing hierarchy. Our main result in this study is that task-related plasticity in vaPEG occur with magnitudes that are intermediate to dPEG and dlFC. Specifically, neurons in vaPEG display responses that seem weaker than those in A1 and dPEG for passive, irrelevant sounds, but show strong responses to task-relevant sounds, similar to the behaviorally-gated responses reported in dlFC. We also note that, similarly to dlFC, behavior-dependent changes in target representations in vaPEG can be sustained and maintained until the end of the shock time window, suggesting that these neurons can signal non-acoustical features of task sounds, such as trial length timing, expectations and reward.

5.3.1 Does vaPEG correspond to a parabelt auditory area?

The experimental results we observed in terms of passive responses, attentional modulation of responses, and functional connectivity, all support the hypothesis that vaPEG might correspond to a tertiary stage in the auditory processing hierarchy in the ferret.

A recent report in neuroanatomical connectivity of auditory cortical fields (Bizley et al., 2015), despite focusing more on MEG, dPEG and AEG connectivity and having some differences with our auditory field denominations, support the idea that the areas we have included under the term vaPEG (VPr, PSSC and pro-PPF) constitute a higher processing stage in the ascending information flow, since these areas receive their ascending inputs mainly from belt areas and not from core areas. These findings are consistent with neuroanatomical evidence from primates and cats, where parabelt areas receive little (or no) direct inputs from core areas, but provide feedback projections to core areas (Hackett, 2011; Hackett et al., 1998a; Lee & Winer, 2008; Winer & Lee, 2007). Also, unpublished evidence gathered in our lab (Radtke-Schuller et al., 2011) suggesting greater density of auditory/dlFC connectivity in ventral areas around the PSSC and VPr, is in agreement with results in primates and cats showing that connectivity with extra-auditory higher-order areas (such as in the parietal and frontal lobes) are more numerous in belt and parabelt auditory areas (Hackett, 2011; Romanski et al., 1999b; Winer & Lee, 2007). Despite the anatomical evidence suggesting that vaPEG could be an analog to primate and

cat parabelt areas, complete studies of vaPEG thalamocortical connections are still lacking and are greatly needed to clarify the auditory cortical areas in the ferret and establish comparisons with other species. Additional neuroanatomical studies are also needed in order to more fully understand the connectivity of ferret auditory cortex with parietal and frontal areas.

We also found distinctive passive tuning features that suggest that vaPEG constitutes a higher-order processing stage, such as increased response latencies, increased tuning bandwidths and complex response properties that generally preclude computing linear STRFs using reverse correlation. In the scarce opportunities when we could compute STRFs from vaPEG neurons with signal-to-noise ratios > 0.2, the resulting STRFs were complex and hard to interpret, and usually changed completely in consecutive receptive field measurements. This didn't allow us to evaluate plasticity of receptive fields, so we focused our plasticity measurements on firing rate changes, as we did in dPEG (Chapter 4, Atiani et al., 2014).

5.3.2 Passive tuning properties of vaPEG neurons

The broad tuning properties we found in vaPEG made it difficult to find any topographical arrangement of responses. In our initial experiments, we usually started recording from A1 neurons in order to find tonotopy, and then continued recording ventrally onto dPEG. Our positional references in the surface of the brain

were based on the tonotopic arrangement already described in A1 and dPEG fields. Ventral to generally broad high-frequency areas in PPF, we usually found neurons with even broader tuning properties, which in some occasions tended to show greater responses to low frequencies. Instead of constituting a reversal point to a ventral tonotopic area, these low frequency neurons were sparse and often surrounded by neurons that showed weak responses (sometimes faint inhibition) with very broad tuning curves (more than $5-6$ octaves). Because of the ventral position of our recordings, and the impossibility of recording more ventrally due to the location of the ear canal and the extent of the bone cement implants, we were not able to explore further ventral in VPr and VPv, but given the scarcity of tuned neurons we found in vaPEG, we would suppose that ventral areas of the PEG are non-tonotopic, a finding that has been suggested as well by other authors (Bizley et al., 2015, 2005).

In previous studies in A1 and dPEG, plasticity has been studied in terms of the best frequencies and their relation to target frequencies (Atiani et al., 2014; Fritz et al., 2003). These studies found that neurons show greater response enhancements to tones that are within or close to their receptive fields, and usually suppress their responses to non-tuned stimuli. Given that vaPEG neurons rarely display clear tuning, we were not able to correlate tuning with magnitude of behavior-dependent response changes, as many times, neurons that displayed no clear stimulus preference in the experiment initial tuning assessment, were strongly modulated during the active behavior state, similarly to dlFC neurons (Fritz et al., 2010).

5.3.3 Enhancement of target responses in the auditory hierarchy

We found that not all neurons that had significant behavior-dependent changes enhanced the relative response to targets. Instead, $44-47\%$ of neurons in each area we compared did not enhance their relative responses to target, and sometimes even decreased their representation of target sounds during the active state.

In a previous study done by our lab (Chapter 4 and Atiani et al., 2014) we took the absolute value of all changed responses to account for a significant number of dlFC neurons that exhibit negative responses. This allowed us to easily compare dlFC behavior-dependent changes in target responses with A1 and dPEG. In this study, instead, we separated the neuron populations by their relative behavior-dependent contrast in target/reference responses. We found that more than 50% of neurons enhanced target responses during behavior; in A1 and dPEG this was achieved by incrementing target responses and suppressing reference responses. In vaPEG, 53% of the neurons displayed robust enhancements of target responses and little or no changes in reference responses. The remaining 47% of vaPEG neurons did not change significantly their target responses, but reduced the suppressive responses that presented during the passive state. This suggests that, similarly to dPEG and A1, vaPEG might enhance the contrast between reference and target responses by using two different mechanisms, but in vaPEG case these mechanisms might be segregated into different neural populations (see figure 5.11).

One qualitative difference we found between vaPEG and its preceding auditory processing areas A1 and dPEG, was a strong similarity with dlFC sustained responses. These responses were maintained during the salient time period after the target offset (400 ms) and lasted until the end of the shock time window (400 ms, 800 ms total). It is unlikely that these correspond to auditory sensory responses, since they occurred in a silent period where the animals were required to refrain from licking to report the detection of the target. We found that these post-target responses in vaPEG and dlFC were not significantly different from firing rates immediately before target offset (during the target), which suggest that the information coded during the target was maintained until the end of the trial. The relative weak responses to sounds presented passively, along with unclear tuning properties and these sustained responses that lasted until the end of target trials, suggest that vaPEG, as well as dlFC, code for non-acoustical features of the target stimuli, such as their meaning or timing. An obvious question arising from this result is how these responses vary when the animal failed to detect the target sound. We did find slightly smaller responses in miss-only trials relative to PSTHs computed from hit-only trials (data not shown), but these results are obscured by the inability to separate miss trials due to perceptual errors (i.e. failure to detect the target) from timing errors (i.e. failure to refrain from licking for 400 ms) in the conditioned avoidance task paradigm. In future studies, a two alternative forced choice task paradigm might allow us to separate real perceptual errors from hits and better assess how auditory/dlFC single units encode perceptual judgements.

5.3.4 Differential functional connectivity of dlFC and auditory areas

In simultaneous recordings from auditory areas and dlFC we measured synchronization of LFP activity by calculating the spectral coherence. Our results in vaPEG/dlFC functional connectivity are significantly different from A1/dlFC results previously reported (Fritz et al., 2010). A1/dlFC coherence showed a desynchronization of LFP activity in the beta band, which was selective to A1 sites that responded to the target frequency. This suppression of beta-coherence was hypothesized to correspond to a selective decrease of inhibitory inputs from dlFC onto the A1 tonotopic areas close to target frequency, and was present in reference and target LFP responses. In the vaPEG/dlFC coherence analysis we found a behavior-dependent increase in beta coherence, which was selective for target stimuli. Similar to Fritz et al. (2010), we analyzed the first 10 trials separately to see if there was a partial recovery on coherence in the post-passive presentation of the task stimuli, but we found that results were not different to those obtained by using all trials, where post-passive coherence was not different from pre-passive (result not shown). This, along selective target coherence changes, suggests a swift synchronization of activity between vaPEG and dlFC, in contrast with a tonic and slower functional connectivity change between A1 and dlFC. This might be explained by a differential anatomical connectivity of the auditory fields with the frontal lobe, where belt and parabelt could be more directly communicated with frontal areas, while core areas are separated by at least one or two synapses. In the ferret this is also suggested by preliminary neuronanatomy data (Radtke-Schuller et al., 2011), but this remains to

be studied in greater detail.

Our Granger causality analysis in vaPEG/dlFC LFP responses suggests that the increased coherence we observed in the beta band in active target responses might be mainly due to dlFC influences over vaPEG LFP activity, since target responses Granger causal influence was not different between passive and active conditions in the bottom-up direction, but had a clear peak in the beta band in the top-down direction. This result is similar to a recent paper where top-down influences among primate visual areas were found separately in the beta range, while bottom-up influences were carried in theta and gamma bands (Bastos et al., 2014). While these are interesting results, these were measured from data collected in only one animal, and more data is necessary to confirm this differential influence of dlFC on auditory areas.

5.3.5 Possible influence of task context on vaPEG responses

Neurons in vaPEG show substantial behavior-driven target response enhancements in the active state. But we also found that in the passive condition vaPEG neurons display a significant response contrast between reference and target sound classes. We were able to test in the click rate discrimination task if this response difference between reference and target click responses was due to a difference in response magnitude to the click rates used as reference and target by pooling responses

to clicks trains of matched rates, presented alone and out of the task context. We did not find significant differences between responses to isolated click trains, which suggest that the differences we saw in the passive condition of the click rate discrimination task is caused by the evocation of the task structure or context. In contrast, when we performed the same comparison in A1 and dPEG recordings we found no differences between responses to clicks in or out of the task context. This comparison among areas revealed that along the auditory processing hierarchy, there is an increasing contrast between reference and target click train responses in the passive condition of the task, a contrast that is further increased in the active condition. We performed the same comparison in the tone detection task and found a similar tendency of increased contrast between sound classes in the passive task along the hierarchy.

This finding raises several important questions about long-term representation of task-relevant sounds in the auditory system, since all the data we analyzed was collected from heavily trained animals. It is possible that memories about learned sounds are stored at higher-order sensory areas and these memories become activated when the stimuli become relevant. It might be possible that sounds with no behavior-associated training, while evoking strong responses at early stages like A1, evoke progressively weaker responses along the processing chain of higher-order areas. In contrast, sounds that have been associated with behavioral meaning become progressively better represented in higher-order areas. A good way to prove or rule this out would be to collect responses to the same stimulus set from task-nave

animals, and ultimately, studying how these initially irrelevant sounds are encoded before, during and after learning.

5.3.6 Conclusions

The fields at vaPEG, a parabelt area in the ferret auditory cortex, exhibit weak and sluggish responses to passive sounds, but compelling enhancement of its responses to relevant sound in the attentive active state. The responses we found in vaPEG are a hybrid between the higher-order dPEG responses we described in Chapter 4 and dlFC task-gated responses (Fritz et al., 2010), in that they display passive auditory responsiveness, but strong goal-directed response modulations. This is further emphasized by the fact that many responses were maintained during the silent time period after target sounds until the end of the trial, signaling non-acoustical features of task-relevant sounds in a similar way as dlFC neurons.

These findings put vaPEG as an intermediate step of the chain of cortical stages from A1 and dPEG towards frontal areas, where coding of auditory stimuli are transformed from more literal acoustical feature analysis towards a more abstract representation of the task-related meaning of sounds. Along this processing hierarchy, regions in the auditory cortex become less veridical in their encoding of sounds in favor of gradually representing their behavioral relevance in the task at hand.

Chapter 6: Concluding remarks and future directions

6.1 Concluding remarks

It is widely accepted in the field of sensory neuroscience that top-down influences can alter early sensory representations (Gilbert & Sigman, 2007). In this dissertation work, I present three studies demonstrating the influence of top-down attention at four levels of the auditory processing hierarchy (core, belt, parabelt and dlFC). These results present evidence that in the auditory system, attention can cause rapid task-related plasticity at every processing stage, but the magnitude and quality of these influences vary along the ascending pathway in a way that suggests that auditory representations in the brain are transformed in a continuum from veridical information about stimulus physical properties to a purely abstract representation of stimulus task-related meaning.

Throughout this dissertation, it is argued that the effects observed are the result of top-down attentional processes influencing auditory cortical responses, but we did not separate possible responses caused by either attention- or desicion-related top-down influences. We argue our effects were caused by selective top-down attention because we found response changes that selectively enhanced target neural

representations by either enhancing target responses and/or suppressing reference responses. This is different to what would be expected to see if effects were caused by sustained attention or vigilance, where representation of reference and target stimuli would have been modulated with a similar polarity (both enhanced or suppressed). Since animals are very motivated to perform correctly to obtain enough water from performing the task, and hence, try to achieve the best possible task performance, we think that the task-related changes in neural responses we observed in auditory cortex were the result of selective (and not global) attention, because the performance animals would achieve by globally attending to every stimuli (global or divided attention) would have been lower than what can be achieved by selectively attending to a restricted range of sound features (Matlin, 2012).

The effects we observed in auditory cortical responses could also be related to top-down signals of decisions or motor responses. Our go/no-go conditioned avoidance behavioral paradigm doesn't allow to easily separate attention- from decision-related responses, since animals were challenged with only one choice: to report target detection by refraining from licking water from the spout. In this setting, "miss" responses could be associated with real perceptual errors, failure to attend stimuli or failure to wait enough time before resume licking. It is even possible to find, in very thirsty animals receiving mild punishments, miss responses where animals prefer to lick during all stimuli presentation, despite being punished. In order to be able to separate influence by decision from attention, a multiple-choice behavioral paradigm that allow to parametrically change task difficulty would be

needed. Also, in our task design we sought to keep a regular level of motivation by adjusting punishment and reward. Since we didn't systematically study the influence of reward (water flow rate) of punishment (shock voltage) in neural responses, we cannot rule out a role of reward/punishment expectations in our results (Maunsell, 2004).

In chapter 3 we studied the influence of attention on the different laminae of the primary auditory cortex (A1). We found plasticity at all depths of A1, but we found that plasticity was greatest in the supragranular layers. We confirmed this finding measuring three different electrophysiological signals (multi-unit activity, high-gamma local field potential and current-source density) as well as in STRFs computed from these signals. We concluded that the higher magnitude of rapid task-related plasticity in supragranular layers might be the result of inter-columnar influences that takes place in layers II and III.

Chapters 4 (Atiani et al., 2009) and 5 explore rapid task-related plasticity in two non-primary auditory areas in the Posterior Ectosylvian Gyrus of the ferret. By recording neural responses from awake animals performing the same task used to describe plasticity in A1 and dlFC (Fritz et al., 2003, 2010) we were able to compare dPEG and vaPEG task-related plasticity with A1 and dlFC, a total of four levels of the auditory cortical hierarchy. The main finding is that attention can modulate auditory responses in A1 (core), dPEG (belt) and vaPEG (parabelt), but the magnitude of these response changes is greater towards higher-order stages (A1 <dPEG

<vaPEG). The present results are consistent with results observed in other sensory modalities (de Lafuente & Romo, 2006; Kastner & Pinsk, 2004; Maunsell & Cook, 2002; Maunsell & Treue, 2006), and in the auditory cortex of humans (Petkov et al., 2004), where higher influence of attention was observed in higher order sensory areas.

We observed a gradual transformation of passive and behavior-dependent responses along the hierarchy. Earlier A1 and dPEG neurons displayed robust responses to sound passively presented, tuned responses and reliable responses to rippled noise that allowed for the computation of STRFs. Higher-order vaPEG displayed overall weaker passive auditory responses, broader receptive fields and sluggish temporal properties that didn't make it possible to compute STRFs in most neurons. Auditory-related area dlFC showed some infrequent passive responses but, as was previously observed by Fritz et al. (2010), these might be related to persistent attentional effects from previous behaviors tested earlier in the same recording session.

Behavior modulated responses at each of the four levels of the auditory cortical hierarchy that we studied. As mentioned before, task-related responses progressively increased from early to higher-order areas. However, we found that vaPEG responses were qualitatively different from A1 and dPEG responses. A1 and dPEG neurons exhibited a task-dependent increase in their sustained responses during the duration of task sounds. Given that both A1 and dPEG neurons display tuned passive responses, and their plasticity is dependent on the neuron's tuning and the target

tone frequency, it is reasonable to argue that A1 and dPEG responses during behavior are emphasizing the acoustic features of task sounds in relation to their own prior passive filter properties. On the other hand, while vaPEG neurons often have weak passive responses, they display strong task-dependent modulations in their responses to target sounds. Similar to neurons in dlFC, many vaPEG cells displayed sustained response increases that lasted until the end of the trial, returning back to baseline response levels by the end of the shock time period. This is a qualitative change in the responses we collected along the auditory cortical processing (see figure 6.1); the post-target responses we described in Chapter 5 are unlikely to be caused entirely by sensory off-responses, since they span a silent time interval of about 800 ms, and in our analysis, we did not include the off-response in the initial 100 ms after target offset. This result strongly suggests that the information that vaPEG encodes is not purely auditory, and that vaPEG may be partly encoding the behavioral meaning of task-relevant sounds, acting as an intermediate hybrid between A1 and higher auditory-related areas.

6.2 Future directions

Although we have made some progress in understanding the transformation of responses from A1 to higher-order auditory areas, there are still many outstanding questions.

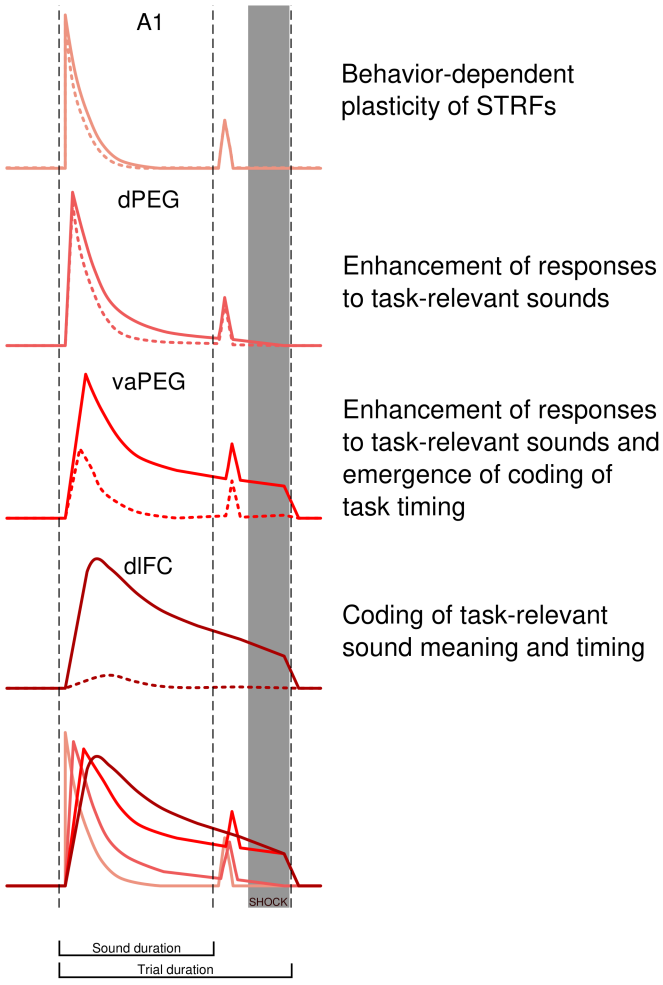

Figure 6.1: **The progression of task-related responses along the auditory processing hierarchy.** A1, dPEG and vaPEG display passive responses to sounds that are enhanced during the active attentive state. Higher-order auditory cortex (vaPEG) share response properties with dlFC that suggest the emergence of coding for non-acoustical task features, such as timing and sound meaning.

6.2.1 Neuroanatomical connectivity of ferret auditory cortex

The behavioral neurophysiological results shown in this dissertation make it clear how critical it is to further explore and understand the underlying neu-

roanatomical connectivity. To date, not much is known about the thalamocortical connectivity of the auditory fields in the ferret. This would allow us to determine what thalamic inputs arrive to higher-order auditory fields. Also, a better understanding of the connectivity between auditory areas and the attentional cortical circuits becomes necessary. A previous connectivity study showed that ventral areas in the auditory cortex of ferrets (specifically the PSSC) receive afferent inputs from visual and somatosensory areas (Ramsay & Meredith, 2004). Multisensory inputs and connectivity with dlFC (Radtke-Schuller et al., 2011) suggests that ventral areas in the PEG could be involved in the integration of auditory information with information coming from other sensory modalities as well as memory and internal representations of behavioral goals and expectations.

6.2.2 Role of other auditory fields in ferret auditory cortex

While we have described a hierarchy of attentional effects along three areas in the auditory cortex of the ferret, we have not yet explored the function of the anterior fields in the AEG. Bizley et al. (2015) described that A1 is more strongly connected with posterior fields in the PEG than areas in the AEG, while AAF presents stronger connectivity with the anterior field ADF. This suggests that there might be two major parallel streams in the information flow in the ferret auditory cortex, an anterior stream starting from AAF and continuing along the AEG, and a posterior stream starting in A1 projecting into the PEG. It is possible, despite

a significant interconnection between anterior and posterior areas, that these two major streams may resemble the dorsal and ventral ('where' and 'what') streams proposed in the auditory systems of cats and primates (Lomber & Malhotra, 2008; Tian et al., 2001) and humans (Alain et al., 2001; Maeder et al., 2001). Such functional processing streams may have different roles in auditory perception.

6.2.3 Top-down influence in behavior and early auditory representations

The convergence of sensory feed-forward information, as well as the more direct connectivity with the frontal lobe might allow higher-order auditory areas (such as parabelt) to be a pivotal processing stage for the binding of representations of features belonging to an auditory source into an auditory object. One of the key questions raised by our results is how influential the top-down projections from dlFC are in shaping the responses in vaPEG. Manipulation of frontal cortical activity by using cooling or optogenetic techniques could be useful in answering this question. Also, it would be very interesting to examine the importance of each of these stages in the auditory cortical hierarchy in behavioral performance. Would the inactivation of vaPEG impair target detection? Would selective activation of frequency-specific areas in tonotopic auditory areas (A1 or dPEG) bias the decisions of the animal during performance of an auditory task?

Also, it's not yet completely clear by what mechanisms A1 neurons can change their filter properties. Our study of the laminar profile of rapid task-related plasticity (Chapter 3) showed that STRF plasticity occurs in all cortical layers and is greater in supragranular laminae. But it's not yet understood how top-down influences arrive to A1. Are higher-order auditory fields necessary for task-related STRF plasticity? Winkowski et al. (2013) showed that pairing of electrical stimulation in orbitofrontal cortex can influence responses in A1, but it is not yet clear if these top-down influences are the result of direct synaptic contact from frontal cortex onto A1, or are conveyed to A1 from higher-order auditory areas.

6.2.4 Neural correlates of perceptual jugements

The responses we reported in dlFC and vaPEG suggest that responses at higher-order stages in the auditory processing hierarchy are strongly shaped by the cognitive context and behavioral relevance of incoming sounds.

One unanswered question arising from our studies is whether there are any differences in neural responses collected during correct and incorrect behavioral responses. A trial-by-trial analysis of responses has been elusive, in part because of flaws in our task design.This calls for an improvement in task design. Despite the fact that our data displays a slight difference in firing rates between hit and miss responses (not shown), we cannot clearly distinguish between miss trials that are

the result of real failure in target recognition or good target recognition but failure in the timing of the behavioral response. This is a disadvantage of our conditioned avoidance behavioral paradigm, where animals have to refrain from licking for a total of 400 ms after the target offset to avoid punishment. If animals correctly recognize the target stimulus, and stop licking for an initial period, but come back to the spout too soon, and thus fail to wait long enough they resume licking, they will get punished despite correctly detecting and reporting the presence of the target sound by decreased licking before the shock window. One plausible alternative to study the influence of perceptual judgments on auditory responses would be to move from our current go-nogo paradigm to a two-alternative forced choice task design, where hits and misses could be more clearly delineated and where incorrect responses could be more clearly correlated with perceptual errors.

6.2.5 Stream segregation in higher-order auditory areas

The strong task-related modulations we observed in vaPEG responses, and the overall greater effects in higher-order auditory cortical areas, suggest that the representations of task-relevant sounds as auditory objects might emerge in higher-order auditory levels. It might be worth targeting higher-order auditory areas in stream segregation studies. Consistent with this idea are the findings in human subjects that show that lateral auditory cortex (belt/parabelt) are activated during attentive auditory experience, while medial auditory cortex respond similarly to attended and

unattended sounds (Petkov et al., 2004). Also, Mesgarani & Chang (2012) showed that attended, but not unattended speech presented in a multitalker setting can be reconstructed from parabelt responses. In the studies described in this thesis, we have always presented reference and target stimuli separately, rather than as simultaneous, overlapping streams. It would be exciting to explore the responses in vaPEG during selective attention to one stream against a background of other acoustic streams.

6.2.6 Long-term representation of task-relevant sounds, learning and memory

We observed an increasing contrast between passive responses to reference and target sounds along the auditory hierarchy. While this might suggest that the representation of trained stimuli becomes progressively more salient along the hierarchy, it is not clear if this is due to inherent passive responsivity to sounds used on our auditory tasks or if this is an effect of training. In order to clarify this, it becomes necessary to measure responses to the same sounds in higher-order auditory areas of naive, untrained animals. If responses in naive vs. trained animals are indeed different, it would be interesting to test how these responses evolve with learning.

Bibliography

Ahissar, M., Nahum, M., Nelken, I., & Hochstein, S. (2009). Reverse hierarchies and sensory learning. Philosophical transactions of the Royal Society of London. Series B, Biological sciences, 364, 285–99.

Ahveninen, J., Huang, S., Nummenmaa, A., Belliveau, J. W., Hung, A., Jääskeläinen, I. P., Rauschecker, J. P., Rossi, S., Tiitinen, H., & Raij, T. (2013). Evidence for distinct human auditory cortex regions for sound location versus identity processing. Nature communications, 4, 2585.

Alain, C., Arnott, S. R., Hevenor, S., Graham, S., & Grady, C. L. (2001). "What" and "where" in the human auditory system. Proceedings of the National Academy of Sciences of the United States of America, 98, 12301–12306.

Anton-Erxleben, K., Stephan, V. M., & Treue, S. (2009). Attention reshapes center-surround receptive field structure in macaque cortical area MT. Cerebral Cortex, 19, 2466–2478.

Arnott, S. R., Binns, M. A., Grady, C. L., & Alain, C. (2004). Assessing the auditory dual-pathway model in humans. NeuroImage, 22, 401–408.

Atiani, S., David, S. V., Elgueda, D., Locastro, M., Radtke-Schuller, S., Shamma, S. A., & Fritz, J. B. (2014). Emergent selectivity for task-relevant stimuli in higher-order auditory cortex. Neuron, 82, 486–99.

Atiani, S., Elhilali, M., David, S. V., Fritz, J. B., & Shamma, S. A. (2009). Task difficulty and performance induce diverse adaptive patterns in gain and shape of primary auditory cortical receptive fields. Neuron, 61, 467–80.

Bakin, J. S. & Weinberger, N. M. (1990). Classical conditioning induces CS-specific receptive field plasticity in the auditory cortex of the guinea pig. Brain Research, 536, 271–286.

Barbas, H., Medalla, M., Alade, O., Suski, J., Zikopoulos, B., & Lera, P. (2005). Relationship of prefrontal connections to inhibitory systems in superior temporal areas in the rhesus monkey. Cerebral cortex, 15, 1356–70.

Bastos, A., Vezoli, J., Bosman, C., Schoffelen, J., Oostenveld, R., Dowdall, J., DeWeerd, P., Kennedy, H., & Fries, P. (2014). Visual Areas Exert Feedforward and Feedback Influences through Distinct Frequency Channels. Neuron, pp. 390–401.

Bizley, J. K., Bajo, V. M., Nodal, F. R., & King, A. J. (2006). Cortico-cortical connections of ferret auditory cortex. In Twenty-ninth Annual Midwinter Meeting of the Association for Research in Otolaryngology, p. Abstract # 703.

Bizley, J. K., Bajo, V. M., Nodal, F. R., & King, A. J. (2015). Cortico-cortical connectivity within ferret auditory cortex. Journal of Comparative Neurology, 523, 2187–2210.

Bizley, J. K. & Cohen, Y. E. (2013). The what, where and how of auditory-object perception. Nature Reviews Neuroscience, 14, 693–707.

Bizley, J. K., Nodal, F. R., Nelken, I., & King, A. J. (2005). Functional organization of ferret auditory cortex. Cerebral cortex, 15, 1637–53.

Bosman, C. A., Schoffelen, J., Brunet, N., Oostenveld, R., Bastos, A. M., Womelsdorf, T., Rubehn, B., Stieglitz, T., De Weerd, P., & Fries, P. (2012). Attentional stimulus selection through selective synchronization between monkey visual areas. Neuron, 75, 875–88.

Budinger, E. & Scheich, H. (2009). Anatomical connections suitable for the direct processing of neuronal information of different modalities via the rodent primary auditory cortex. Hearing Research, 258, 16–27.

Buffalo, E. A., Fries, P., Landman, R., Liang, H., & Desimone, R. (2010). A backward progression of attentional effects in the ventral stream. Proceedings of the National Academy of Sciences of the United States of America, 107, 361–5.

Buzsáki, G., Anastassiou, C. a., & Koch, C. (2012). The origin of extracellular fields and currents–EEG, ECoG, LFP and spikes. Nature reviews. Neuroscience, 13, 407–20.

Cant, N. B. & Benson, C. G. (2003). Parallel auditory pathways: Projection patterns of the different neuronal populations in the dorsal and ventral cochlear nuclei. Brain Research Bulletin, 60, 457–474.

Clascá, F., Llamas, A., & Reinoso-Suárez, F. (2000). Cortical connections of the insular and adjacent parieto-temporal fields in the cat. Cerebral Cortex, 10, 371–399.

Cohen, M. R. & Maunsell, J. H. R. (2009). Attention improves performance primarily by reducing interneuronal correlations. Nature neuroscience, 12, 1594–1600.

Constantinople, C. M. & Bruno, R. M. (2013). Deep cortical layers are activated directly by thalamus. Science, 340, 1591–4.

Coomes Peterson, D. & Schofield, B. R. (2007). Projections from auditory cortex contact ascending pathways that originate in the superior olive and inferior colliculus. Hearing research, 232, 67–77.

David, S. V., Fritz, J. B., & Shamma, S. A. (2012). Task reward structure shapes rapid receptive field plasticity in auditory cortex. Proceedings of the National Academy of Sciences of the United States of America, 109, 2144–9.

de Lafuente, V. & Romo, R. (2006). Neural correlate of subjective sensory experience gradually builds up across cortical areas. Proceedings of the National Academy of Sciences of the United States of America, 103, 14266–14271.

Delano, P. H., Elgueda, D., Hamame, C. M., & Robles, L. (2007). Selective attention to visual stimuli reduces cochlear sensitivity in chinchillas. The Journal of neuroscience, 27, 4146–53.

Desimone, R., Albright, T. D., Gross, C. G., & Bruce, C. (1984). Stimulus-selective properties of inferior temporal neurons in the macaque. The Journal of neuroscience, 4, 2051–62.

Diamond, D. M. & Weinberger, N. M. (1984). Physiological plasticity of single neurons in auditory cortex of the cat during acquisition of the pupillary conditioned response: II. Secondary field (AII). Behavioral neuroscience, 98, 189–210.

DiCarlo, J. J. & Cox, D. D. (2007). Untangling invariant object recognition. Trends in cognitive sciences, 11, 333–41.

Douglas, R. J. & Martin, K. A. (2004). Neuronal Circuits of the Neocortex. Annual Review of Neuroscience, 27, 419–451.

Downer, J. D., Niwa, M., & Sutter, M. L. (2015). Task Engagement Selectively Modulates Neural Correlations in Primary Auditory Cortex. Journal of Neuroscience, 35, 7565–7574.

Du, Y., He, Y., Arnott, S. R., Ross, B., Wu, X., Li, L., & Alain, C. (2013). Rapid Tuning of Auditory "What" and "Where" Pathways by Training. Cerebral cortex, 25, 496–506.

Durand, J. B., Nelissen, K., Joly, O., Wardak, C., Todd, J. T., Norman, J. F., Janssen, P., Vanduffel, W., & Orban, G. A. (2007). Anterior Regions of Monkey Parietal Cortex Process Visual 3D Shape. Neuron, 55, 493–505.

Elgueda, D., Delano, P. H., & Robles, L. (2011). Effects of Electrical Stimulation of Olivocochlear Fibers in Cochlear Potentials in the Chinchilla. Journal of the Association for Research in Otolaryngology : JARO, 327, 317–327.

Englitz, B., David, S. V., Sorenson, M. D., & Shamma, S. a. (2013). MANTA–an open-source, high density electrophysiology recording suite for MATLAB. Frontiers in neural circuits, 7, 69.

Ferrera, V. P., Rudolph, K. K., & Maunsell, J. H. (1994). Responses of neurons in the parietal and temporal visual pathways during a motion task. The Journal of neuroscience, 14, 6171–6186.

Fritz, J., Shamma, S., Elhilali, M., & Klein, D. (2003). Rapid task-related plasticity of spectrotemporal receptive fields in primary auditory cortex. Nature neuroscience, 6, 1216–23.

Fritz, J. B., David, S. V., Radtke-Schuller, S., Yin, P., & Shamma, S. A. (2010). Adaptive, behaviorally gated, persistent encoding of task-relevant auditory information in ferret frontal cortex. Nature Neuroscience, 13, 1011–1019.

Fritz, J. B., Elhilali, M., David, S. V., & Shamma, S. A. (2007). Does attention play a role in dynamic receptive field adaptation to changing acoustic salience in A1? Hearing research, 229, 186–203.

Fritz, J. B., Elhilali, M., & Shamma, S. A. (2005). Differential dynamic plasticity of A1 receptive fields during multiple spectral tasks. The Journal of neuroscience, 25, 7623–35.

Gilbert, C. D. & Sigman, M. (2007). Brain states: top-down influences in sensory processing. Neuron, 54, 677–96.

Guo, F., Intskirveli, I., Blake, D. T., & Metherate, R. (2013). Tone-detection training enhances spectral integration mediated by intracortical pathways in primary auditory cortex. Neurobiology of learning and memory, 101, 75–84.

Hackett, T. A. (2011). Information flow in the auditory cortical network. Hearing Research, 271, 133–146.

Hackett, T. A., de la Mothe, L. A., Camalier, C. R., Falchier, A., Lakatos, P., Kajikawa, Y., & Schroeder, C. E. (2014). Feedforward and feedback projections of caudal belt and parabelt areas of auditory cortex: Refining the hierarchical model. Frontiers in Neuroscience, 8, 72.

Hackett, T. A., Stepniewska, I., & Kaas, J. H. (1998a). Subdivisions of auditory cortex and ipsilateral cortical connections of the parabelt auditory cortex in macaque monkeys. Journal of Comparative Neurology, 394, 475–495.

Hackett, T. A., Stepniewska, I., & Kaas, J. H. (1998b). Thalamocortical connections of the parabelt auditory cortex in macaque monkeys. Journal of Comparative Neurology, 400, 271–286.

Happel, M. F. K., Jeschke, M., & Ohl, F. W. (2010). Spectral Integration in Primary Auditory Cortex Attributable to Temporally Precise Convergence of Thalamocortical and Intracortical Input. The Journal of neuroscience, 30, 11114–11127.

Heffner, H. E. & Heffner, R. S. (1995). Conditioned Avoidance. In Methods in Comparative Psychoacoustics, G. M. Klump, R. J. Dooling, R. R. Fay, & W. C. Stebbins, eds. (Basel: Birkhäuser Verlag), 1st edn., pp. 79–93.

Hernandez-Peon, R., Scherrer, H., & Jouvet, M. (1956). Modification of Electric Activity in Cochlear Nucleus during "Attention" in Unanesthetized Cats. Science, 123, 331–332.

Huang, C. L. & Winer, J. A. (2000). Auditory thalamocortical projections in the cat: Laminar and areal patterns of input. Journal of Comparative Neurology, 427, 302–331.

Hubel, D. H. & Wiesel, T. N. (1959). Receptive fields of single neurones in the cat's striate cortex. The Journal of physiology, pp. 574–591.

Hudspeth, A. J. (2000). Hearing. In Principles of Neural Science, E. R. Kandel, J. H. Schwartz, & T. M. Jessel, eds. (New York: McGraw-Hill), 4th edn., chap. 30. Hearing, pp. 590–613.

Humphries, C., Sabri, M., Lewis, K., & Liebenthal, E. (2014). Hierarchical organization of speech perception in human auditory cortex. Frontiers in Neuroscience, 8, 1–12.

Intskirveli, I. & Metherate, R. (2012). Nicotinic neuromodulation in auditory cortex requires MAPK activation in thalamocortical and intracortical circuits. Journal of Neurophysiology, 107, 2782–2793.

Jeanne, J. M., Sharpee, T. O., & Gentner, T. Q. (2013). Associative learning enhances population coding by inverting interneuronal correlation patterns. Neuron, 78, 352–363.

Kaas, J. H. & Hackett, T. A. (2000). Subdivisions of auditory cortex and processing streams in primates. Proceedings of the National Academy of Sciences of the United States of America, 97, 11793–9.

Kajikawa, Y., Frey, S., Ross, D., Falchier, A., Hackett, T. A., & Schroeder, C. E. (2015). Auditory properties in the parabelt regions of the superior temporal gyrus in the awake macaque monkey: an initial survey. The Journal of neuroscience, 35, 4140–50.

Kajikawa, Y. & Schroeder, C. E. (2011). How local is the local field potential? Neuron, 72, 847–58.

Kastner, S. & Pinsk, M. A. (2004). Visual attention as a multilevel selection process. Cognitive, Affective, & Behavioral Neuroscience, 4, 483–500.

Kaur, S., Lazar, R., & Metherate, R. (2004). Intracortical pathways determine breadth of subthreshold frequency receptive fields in primary auditory cortex. J Neurophysiol, 91, 2551–2567.

Kawai, H., Lazar, R., & Metherate, R. (2007). Nicotinic control of axon excitability regulates thalamocortical transmission. Nature neuroscience, 10, 1168–1175.

Kern, A., Heid, C., Steeb, W. H., Stoop, N., & Stoop, R. (2008). Biophysical parameters modification could overcome essential hearing gaps. PLoS Computational Biology, 4.

Kim, J. G. & Kastner, S. (2013). Attention flexibly alters tuning for object categories. Trends in Cognitive Sciences, 17, 368–370.

King, A. J. & Nelken, I. (2009). Unraveling the principles of auditory cortical processing: can we learn from the visual system? Nature neuroscience, 12, 698–701.

Klein, D. J., Depireux, D. A., Simon, J. Z., & Shamma, S. A. (2000). Robust spectrotemporal reverse correlation for the auditory system: optimizing stimulus design. Journal of computational neuroscience, 9, 85–111.

Konen, C. S. & Kastner, S. (2008). Two hierarchically organized neural systems for object information in human visual cortex. Nature neuroscience, 11, 224–231.

Lee, C. C. & Winer, J. A. (2008). Connections of cat auditory cortex: III. Corticocortical system. The Journal of comparative neurology, 507, 1920–43.

Lehky, S. R. & Sereno, A. B. (2007). Comparison of shape encoding in primate dorsal and ventral visual pathways. Journal of neurophysiology, 97, 307–319.

León, A., Elgueda, D., Silva, M. A., Hamamé, C. M., & Delano, P. H. (2012). Auditory cortex basal activity modulates cochlear responses in chinchillas. PloS one, 7, e36203.

Linden, J. F. & Schreiner, C. E. (2003). Columnar transformations in auditory cortex? A comparison to visual and somatosensory cortices. Cerebral cortex, 13, 83–89.

Lomber, S. G. & Malhotra, S. (2008). Double dissociation of 'what' and 'where' processing in auditory cortex. Nature neuroscience, 11, 609–616.

Maeder, P., Meuli, R., Adriani, M., Bellmann, A., Fornari, E., Thiran, J.-P., Pittet, A., & Clarke, S. (2001). Distinct Pathways Involved in Sound Recognition and Localization: A Human fMRI Study. NeuroImage, 14, 802–16.

Malmierca, M. S. (2003). The structure and physiology of the rat auditory system: An overview. International Review of Neurobiology, 56, 147–211.

Malmierca, M. S., Merchán, M. a., Henkel, C. K., & Oliver, D. L. (2002). Direct projections from cochlear nuclear complex to auditory thalamus in the rat. The Journal of neuroscience, 22, 10891–10897.

Matlin, M. W. (2012). Perceptual Processes II: Attention and Consciousness. In Cognition. (Wiley Global Education), 8th edn., chap. 3, pp. 69–96.

Maunsell, J. H. R. (2004). Neuronal representations of cognitive state: Reward or attention? Trends in Cognitive Sciences, 8, 261–265.

Maunsell, J. H. R. & Cook, E. P. (2002). The role of attention in visual processing. Philos Trans R Soc Lond, B, Biol Sci, 357, 1063–1072.

Maunsell, J. H. R. & Treue, S. (2006). Feature-based attention in visual cortex. Trends in Neurosciences, 29, 317–322.

McMains, S. & Kastner, S. (2011). Interactions of top-down and bottom-up mechanisms in human visual cortex. The Journal of neuroscience : the official journal of the Society for Neuroscience, 31, 587–597.

Medalla, M. & Barbas, H. (2014). Specialized prefrontal "auditory fields": Organization of primate prefrontal-temporal pathways. Frontiers in Neuroscience, 8, 1–15.

Mesgarani, N. & Chang, E. F. (2012). Selective cortical representation of attended speaker in multi-talker speech perception. Nature, 485, 233–236.

Miller, E. K. & Cohen, J. D. (2001). An integrative theory of prefrontal cortex function. Annual review of neuroscience, 24, 167–202.

Mishkin, M., Ungerleider, L. G., & Macko, K. A. (1983). Object vision and spatial vision: two cortical pathways. Trends in neurosciences, 6, 414–417.

Mitchell, J. F., Sundberg, K. A., & Reynolds, J. H. (2009). Spatial Attention Decorrelates Intrinsic Activity Fluctuations in Macaque Area V4. Neuron, 63, 879–888.

Mountcastle, V. B. (1997). The columnar organization of the neocortex. Brain : a journal of neurology, 120 (Pt 4, 701–22.

Movshon, J. A., Adelson, E. H., Gizzi, M. S., & Newsome, W. T. (1985). The analysis of moving visual patterns. In Pattern Recognition Mechanisms, C. Chagas, R. Gattass, & C. Gross, eds. (New York: Springer-Verlag), pp. 117–151.

Nelson, a., Schneider, D. M., Takatoh, J., Sakurai, K., Wang, F., & Mooney, R. (2013). A Circuit for Motor Cortical Modulation of Auditory Cortical Activity. Journal of Neuroscience, 33, 14342–14353.

Ni, A. M., Ray, S., & Maunsell, J. H. R. (2012). Tuned Normalization Explains the Size of Attention Modulations. Neuron, 73, 803–813.

Niwa, M., Johnson, J. S., O'Connor, K. N., & Sutter, M. L. (2013). Differences between primary auditory cortex and auditory belt related to encoding and choice for AM sounds. The Journal of neuroscience, 33, 8378–95.

Oatman, L. C. (1971). Role of visual attention on auditory evoked potentials in unanesthetized cats. Experimental neurology, 32, 341–356.

Obleser, J., Zimmermann, J., Van Meter, J., & Rauschecker, J. P. (2007). Multiple stages of auditory speech perception reflected in event-related fMRI. Cerebral Cortex, 17, 2251–2257.

Ohl, F. W. & Scheich, H. (1996). Differential frequency conditioning enhances spectral contrast sensitivity of units in auditory cortex (field Al) of the alert Mongolian gerbil. The European journal of neuroscience, 8, 1001–17.

Okada, K., Rong, F., Venezia, J., Matchin, W., Hsieh, I.-H., Saberi, K., Serences, J. T., & Hickok, G. (2010). Hierarchical organization of human auditory cortex: evidence from acoustic invariance in the response to intelligible speech. Cerebral cortex, 20, 2486–95.

Oostenveld, R., Fries, P., Maris, E., & Schoffelen, J. M. (2011). FieldTrip: Open source software for advanced analysis of MEG, EEG, and invasive electrophysiological data. Computational Intelligence and Neuroscience, 2011.

Otazu, G. H., Tai, L.-H., Yang, Y., & Zador, A. M. (2009). Engaging in an auditory task suppresses responses in auditory cortex. Nature neuroscience, 12, 646–54.

Pallas, S. L. & Sur, M. (1993). Visual projections induced into the auditory pathway of ferrets:{II}. Corticocortical connections of primary auditory cortex. J. Comp. Neurol., 337, 317–333.

Petersen, C. C. H. & Crochet, S. (2013). Synaptic computation and sensory processing in neocortical layer 2/3. Neuron, 78, 28–48.

Petersen, S. E. & Posner, M. I. (2012). The attention system of the human brain: 20 years after. Annual review of neuroscience, 35, 73–89.

Petkov, C. I., Kang, X., Alho, K., Bertrand, O., Yund, E. W., & Woods, D. L. (2004). Attentional modulation of human auditory cortex. Nature neuroscience, 7, 658–63.

Pettersen, K. H., Devor, A., Ulbert, I., Dale, A. M., & Einevoll, G. T. (2006). Current-source density estimation based on inversion of electrostatic forward solution: Effects of finite extent of neuronal activity and conductivity discontinuities. Journal of Neuroscience Methods, 154, 116–133.

Pickles, J. O. (2012). An Introduction to the Physiology of Hearing. (Bingley: Emerald Group Publishing), 4th edn.

Plakke, B. & Romanski, L. M. (2014). Auditory connections and functions of prefrontal cortex. Frontiers in Neuroscience, 8, 1–13.

Pluta, S., Naka, A., Veit, J., Telian, G., Yao, L., Hakim, R., Taylor, D., & Adesnik, H. (2015). A direct translaminar inhibitory circuit tunes cortical output. Nature Neuroscience, 18, 1631–1640.

Polley, D. B., Steinberg, E. E., & Merzenich, M. M. (2006). Perceptual learning directs auditory cortical map reorganization through top-down influences. The Journal of neuroscience, 26, 4970–82.

Poremba, A., Malloy, M., Saunders, R. C., Carson, R. E., Herscovitch, P., & Mishkin, M. (2004). Species-specific calls evoke asymmetric activity in the monkey ' s temporal poles. Nature, 427, 448–451.

Radtke-Schuller, S., Schuller, G., Shamma, S. A., & Fritz, J. B. (2011). Does the claustrum play a role in mediating top-down influence of frontal cortex on auditory cortex? In 41st Annual Meeting of the Society for Neuroscience, p. Program # 173.11. Washington, DC.

Rainer, G., Asaad, W. F., & Miller, E. K. (1998). Memory fields of neurons in the primate prefrontal cortex. Proceedings of the National Academy of Sciences of the United States of America, 95, 15008–13.

Ramsay, A. & Meredith, M. (2004). Multiple sensory afferents to ferret pseudosylvian sulcal cortex. Neuroreport, 15, 61–65.

Rao, S. C., Rainer, G., & Miller, E. K. (1997). Integration of What and Where in the Primate Prefrontal Cortex. Science, 276, 821–824.

Rauschecker, J. P. & Tian, B. (2000). Mechanisms and streams for processing of "what" and "where" in auditory cortex. Proceedings of the National Academy of Sciences of the United States of America, 97, 11800–6.

Rauschecker, J. P., Tian, B., & Hauser, M. (1995). Processing of Complex Sounds in the Macaque Nonprimary Auditory Cortex. Science, 268, 111–114.

Recanzone, G. H. (2008). Representation of con-specific vocalizations in the core and belt areas of the auditory cortex in the alert macaque monkey. The Journal of neuroscience : the official journal of the Society for Neuroscience, 28, 13184–93.

Recanzone, G. H. & Cohen, Y. E. (2010). Serial and parallel processing in the primate auditory cortex revisited. Behavioural brain research, 206, 1–7.

Robles, L. & Ruggero, M. A. (2001). Mechanics of the mammalian cochlea. Physiological reviews, 81, 1305–1352.

Romanski, L. M., Bates, J. F., & Goldman-Rakic, P. S. (1999a). Auditory belt and parabelt projections to the prefrontal cortex in the rhesus monkey. Journal of Comparative Neurology, 403, 141–157.

Romanski, L. M., Bates, J. F., & Goldman-Rakic, P. S. (1999b). Auditory belt and parabelt projections to the prefrontal cortex in the rhesus monkey. Journal of Comparative Neurology, 403, 141–157.

Romanski, L. M., Tian, B., Fritz, J. B., Mishkin, M., Goldman-Rakic, P. S., & Rauschecker, J. P. (1999c). Dual streams of auditory afferents target multiple domains in the primate prefrontal cortex. Nature neuroscience, 2, 1131–6.

Rouiller, E. M., Simm, G. M., Villa, A. E. P., de Ribaupierre, Y., & de Ribaupierre, F. (1991). Auditory corticocortical interconnections in the cat: evidence for parallel and hierarchical arrangement of the auditory cortical areas. Experimental Brain Research, 86, 483–505.

Saalmann, Y. B., Pinsk, M. A., Wang, L., Li, X., & Kastner, S. (2012). The Pulvinar Regulates Information Transmission Between Cortical Areas Based on Attention Demands. Science, 337, 753–756.

Schneider, D. M. & Mooney, R. (2015). Motor-related signals in the auditory system for listening and learning. Current Opinion in Neurobiology, 33, 78–84.

Schofield, B. R. (2009). Projections to the inferior colliculus from layer VI cells of auditory cortex. Neuroscience, 159, 246–58.

Schofield, B. R. & Cant, N. B. (1999). Descending auditory pathways: Projections from the inferior colliculus contact superior olivary cells that project bilaterally to the cochlear nuclei. Journal of Comparative Neurology, 409, 210–223.

Sereno, A. B. & Maunsell, J. H. (1998). Shape selectivity in primate lateral intraparietal cortex. Nature, 395, 500–503.

Sereno, M. E., Trinath, T., Augath, M., & Logothetis, N. K. (2002). Three-dimensional shape representation in monkey cortex. Neuron, 33, 635–652.

Seth, A. K., Barrett, A. B., & Barnett, L. (2015). Granger Causality Analysis in Neuroscience and Neuroimaging. Journal of Neuroscience, 35, 3293–3297.

Shamma, S., Fleshman, J., Wiser, P., & Versnel, H. (1993). Organization of response areas in ferret primary auditory cortex. Journal of Neurophysiology, 69, 367–383.

Shamma, S. A., Elhilali, M., & Micheyl, C. (2011). Temporal coherence and attention in auditory scene analysis. Trends in neurosciences, 34, 114–23.

Sharpee, T. O., Atencio, C. A., & Schreiner, C. E. (2011). Hierarchical representations in the auditory cortex. Current opinion in neurobiology, 21, 761–7.

Slee, S. J. & David, S. V. (2015). Rapid Task-Related Plasticity of Spectrotemporal Receptive Fields in the Auditory Midbrain. The Journal of neuroscience, 35, 13090–13102.

Störmer, V. & Alvarez, G. (2014). Feature-Based Attention Elicits Surround Suppression in Feature Space. Current Biology, 30, 1985–1988.

Tian, B., Reser, D., Durham, A., Kustov, A., & Rauschecker, J. P. (2001). Functional specialization in rhesus monkey auditory cortex. Science, 292, 290–293.

Tsao, D. Y., Freiwald, W. A., Knutsen, T. A., Mandeville, J. B., & Tootell, R. B. H. (2003). Faces and objects in macaque cerebral cortex. Nature Neuroscience, 6, 989–995.

Tsao, D. Y., Freiwald, W. A., Tootell, R. B. H., & Livingstone, M. S. (2006). A cortical region consisting entirely of face-selective cells. Science, 311, 670–4.

Tsao, D. Y., Moeller, S., & Freiwald, W. A. (2008). Comparing face patch systems in macaques and humans. Proceedings of the National Academy of Sciences of the United States of America, 105, 19514–19519.

Tsunada, J., Lee, J. H., & Cohen, Y. E. (2011). Representation of speech categories in the primate auditory cortex. Journal of neurophysiology, 105, 2634–2646.

Ungerleider, L. G. & Haxby, J. V. (1994). 'What' and 'where' in the human brain. Current Opinion in Neurobiology, 4, 157–165.

Wallace, M. N., Kitzes, L. M., & Jones, E. G. (1991). Intrinsic inter- and intralaminar connections and their relationship to the tonotopic map in cat primary auditory cortex. Experimental Brain Research, 86, 527–544.

Wannig, A., Rodríguez, V., & Freiwald, W. A. (2007). Attention to Surfaces Modulates Motion Processing in Extrastriate Area MT. Neuron, 54, 639–651.

Wessinger, C. M., VanMeter, J., Tian, B., Van Lare, J., Pekar, J., & Rauschecker, J. P. (2001). Hierarchical organization of the human auditory cortex revealed by functional magnetic resonance imaging. Journal of cognitive neuroscience, 13, 1–7.

Wilson, F. A. W., Scalaidhe, S. P., & Goldman-Rakic, P. S. (1993). Dissociation of object and spatial processing domains in primate prefrontal cortex. Science, 260, 1955–1958.

Winer, J. A. & Lee, C. C. (2007). The distributed auditory cortex. Hearing research, 229, 3–13.

Winkowski, D. E., Bandyopadhyay, S., Shamma, S. a., & Kanold, P. O. (2013). Frontal Cortex Activation Causes Rapid Plasticity of Auditory Cortical Processing. Journal of Neuroscience, 33, 18134–18148.

Zeki, S. & Shipp, S. (1988). The functional logic of cortical connections. Nature, 355, 311–317.

Zhou, H., Schafer, R. J., & Desimone, R. (2016). Pulvinar-Cortex Interactions in Vision and Attention. Neuron, 89, 209–220.